Energy Efficient, Cooperative Communication in Low-Power Wireless Networks

Abdelrahman Abdelkader

von der Fakultät Elektrotechnik und Informationstechnik
der Technischen Universität Dresden

zur Erlangung des akademischen Grades

DOKTORINGENIEUR
(Dr.-Ing.)

genehmigte Dissertation

Vorsitzende:	Prof. Dr.-Ing. habil. Frank Ellinger
Gutachter:	Prof. Dr.-Ing. Eduard A. Jorswieck,
	Dr. Marco di Renzo
Weiteres Mitglied:	Prof. Dr. rer. nat. Stephan Mannsfeld
Tag der Einreichung:	30. 10. 2019,
Tag der Verteidigung:	22. 01. 2020

To my late father.

Acknowledgements

A PhD title is a challenging dream that requires sacrifices and dedication. Therefore, it is impossible to achieve it without a proper support system. I owe being at this stage in my PhD journey to my parents, who raised me from a young age on scientific achievements and excellence. Your pride of my success has gotten me through many difficult days throughout the past 4 years.

I would like to thank my supervisor and mentor Prof. Dr.-Ing. Eduard A. Jorswieck. Your patience was unending, and your guidance has taught me more than you can know. Also, i would like to thank Dr. Marco Zimmerling for introducing me to Glossy, on which this dissertation is based. Next, i would like to thank Dr. Johannes Richter for enriching my understanding of network coding and his cooperation through our collaborative research.

I would like to thank Dr. Marco di Renzo for accepting to be the second reviewer of my dissertation and for always providing me with valuable feedback. I am also grateful to the chair of the examination committee Prof. Dr.-Ing. habil Frank Ellinger, and the board member of the committee Prof. Dr. rer. nat. Stephan Mannsfeld.

I would like to acknowledge all my colleagues from TNT, as well as ComNets, who supported me logistically or emotionally throughout this journey, including, Vincent Latzko and Dr. Riccardo Bonetto who was very supportive during the final phase of this dissertation. I would also like to thank my family here in dresden, namely Roberto Torre and Dr.-Ing. Angel Ochoa Brezmes, who showed extreme compassion and understanding. Finally, my family in Egypt, you have set an example for me to follow; Thank you.

Dresden, January 2020 Abdelrahman Abdelkader

Abstract

The increased interest in massive deployment of wireless sensors and network densification requires more innovation in low-latency communication across multi-hop networks. Moreover, the resource constrained nature of sensor nodes calls for more energy efficient transmission protocols, in order to increase the battery life of said devices. Therefore, it is important to investigate possible technologies that would aid in improving energy efficiency and decreasing latency in wireless sensor networks (WSN) while focusing on application specific requirements. To this end, and based on state of the art Glossy, a low-power WSN flooding protocol, this dissertation introduces two energy efficient, cooperative transmission schemes for low-power communication in WSNs, with the aim of achieving performance gains in energy efficiency, latency and power consumption. These approaches apply several cooperative transmission technologies such as physical layer network coding and transmit beamforming. Moreover, mathematical tools such as convex optimization and game theory are used in order to analytically construct the proposed schemes. Then, system level simulations are performed, where the proposed schemes are evaluated based on different criteria.

First, in order to improve over all latency in the network as well as energy efficiency, MF-Glossy is proposed; a communication scheme that enables the simultaneous flooding of different packets from multiple sources to all nodes in the network. Using a communication-theoretic analysis, upper bounds on the performance of Glossy and MF-Glossy are determined. Further, simulation results show that MF-Glossy has the potential to achieve several-fold improvements in goodput and latency across a wide spectrum of network configurations at lower energy costs and comparable packet reception rates. Hardware implementation challenges are discussed as a step towards harnessing the potential of MF-Glossy in real networks, while focusing on key challenges and possible solutions.

Second, under the assumption of available channel state information (CSI) at all nodes, centralized and distributed beamforming and power control algorithms are proposed and their performance is evaluated. They are compared in terms of energy efficiency to standard Glossy. Numerical simulations demonstrate that a centralized power control scheme can achieve several-fold improvements in energy efficiency over Glossy across a wide spec-

trum of network configurations at comparable packet reception rates. Furthermore, the more realistic scenario where CSI is not available at transmitting nodes is considered. To battle CSI unavailability, cooperation is introduced on two stages. First, cooperation between receiving and transmitting nodes is proposed for the process of CSI acquisition, where the receivers provide the transmitters with quantized (e.g. imperfect) CSI. Then, cooperation within transmitting nodes is proposed for the process of multi-cast transmit beamforming. In addition to an analytical formulation of the robust multi-cast beamforming problem with imperfect CSI, its performance is evaluated, in terms of energy efficiency, through numerical simulations. It is shown that the level of cooperation, represented by the number of limited feedback bits from receivers to transmitters, greatly impacts energy efficiency. To this end, the optimization problem of finding the optimal number of feedback bits B is formulated, as a programming problem, under QoS constraints of 5% maximum outage. Numerical simulations show that there exists an optimal number of feedback bits that maximizes energy efficiency. Finally, the effect of choosing cooperating transmitters on energy efficiency is studied, where it is shown that an optimum group of cooperating transmit nodes, also known as a transmit coalition, can be formed in order to maximize energy efficiency. The investigated techniques including optimum feedback bits and transmit coalition formation can achieve a 100% increase in energy efficiency when compared to state of the art Glossy under same operation requirements in very dense networks.

In summary, the two main contributions in this dissertation provide insights on the possible performance gains that can be achieved when cooperative technologies are used in low-power wireless networks.

Zusammenfassung

Das zunehmende Interesse an einem massiven Einsatz von drahtlosen Sensoren und einer Verdichtung des Netzwerks erfordert weitere Innovation bei der Kommunikation über Multi-Hop-Netzwerke. Darüber hinaus erfordert die ressourcenbeschränkte Beschaffenheit der Sensorknoten energieeffizientere Übertragungsprotokolle, um die Akkulaufzeit der Geräte zu erhöhen. Daher ist es wichtig, mögliche Technologien zu untersuchen, die zur Verbesserung der Energieeffizienz und zur Verringerung der Latenzzeiten in niederenergetischen drahtlosen Sensornetzwerken (Wireless Sensor Networks, WSN) beitragen und sich gleichzeitig auf anwendungsspezifische Anforderungen konzentrieren.

Zu diesem Zweck und auf der Grundlage des Standes der Technik Glossy, ein energiesparendes WSN Flutungsprotokoll, stellt diese Dissertation zwei energieeffiziente, kooperative Übertragungskonzepte für die niederenergetischen Kommunikation in WSNs vor, mit dem Ziel, Verbesserungen in Energieeffizienz, Latenz und Leistungsaufnahme zu erreichen. Diese Konzepte wenden mehrere kooperative Übertragungstechnologien an, wie z.B. Netzwerkcodierung in der physikalische Schicht und Strahlformung auf Senderseite. Darüber hinaus werden mathematische Methoden wie konvexe Optimierung und Spieltheorie genutzt, um die vorgeschlagenen Konzepte analytisch zu konstruieren. Anschließend werden Simulationen auf Systemebene durchgeführt, bei denen die vorgeschlagenen Systeme nach verschiedenen Kriterien bewertet werden.

Erstens wird MF-Glossy vorgeschlagen, um die Gesamtlatenzzeit im Netzwerk sowie die Energieeffizienz zu verbessern; ein Kommunikationsschema, das die gleichzeitige Flutung verschiedener Pakete von mehreren Quellen zu allen Knoten im Netzwerk ermöglicht. Mit Hilfe einer nachrichtentheoretischen Analyse werden die oberen Grenzen der Leistungsfähigkeit von Glossy und MF-Glossy bestimmt. Darüber hinaus zeigen Simulationsergebnisse, dass MF-Glossy das Potenzial hat, über ein breites Spektrum von Netzwerkkonfigurationen bei niedrigeren Energiekosten und vergleichbaren Paketempfangsraten eine mehrfache Verbesserung von Goodput und Latenz zu erreichen. Die Herausforderungen bei der Implementierung in Hardware werden diskutiert, um das Potenzial von MF-Glossy in realen Netzwerken zu nutzen, wobei der Schwerpunkt auf den wichtigsten Herausforderungen und möglichen Lösungen liegt.

Zweitens, werden unter der Annahme der verfügbaren Kanalinformationen (Channel State Information, CSI) an allen Knoten sowohl zentralisierte als auch verteilte Strahlformungs- und Stromregelungsalgorithmen vorgeschlagen und deren Performance bewertet. Sie werden in Bezug auf ihre Energieeffizienz mit dem Standard Glossy verglichen. Numerische Simulationen zeigen, dass ein zentralisiertes Stromversorgungsschema eine mehrfache Verbesserung der Energieeffizienz gegenüber Glossy über ein breites Spektrum von Netzwerkkonfigurationen bei vergleichbaren Paketempfangsraten erreichen kann. Darüber hinaus wird das realistischere Szenario berücksichtigt, bei dem CSI an den Sendeknoten nicht verfügbar sind. Um die Nichtverfügbarkeit von CSI zu bekämpfen, wird die Zusammenarbeit auf zwei Stufen eingeführt. Als erstens die Zusammenarbeit zwischen Empfangs- und Sendeknoten für den Prozess des begrenzten CSI-Feedback. Daraufhin die Zusammenarbeit innerhalb der Sendeknoten für den Prozess der Multi-Cast-Sende-Strahlformung. Zusätzlich zu einer analytischen Formulierung des robusten Multi-Cast Sende-Strahlformung-Problems mit unvollständigen CSI wird dessen Performance bewertet. Es wird gezeigt, dass der Grad der Zusammenarbeit, dargestellt durch die Anzahl der begrenzten Rückmeldungsbits von Empfängern zu Sendern, die Energieeffizienz stark beeinflusst. Zu diesem Zweck wird das Programmierproblem zum Auffinden der optimalen Anzahl von Rückmeldungsbits B unter QoS-Bedingungen von 5% maximaler Ausfallrate formuliert. Numerische Simulationen zeigen, dass es eine optimale Anzahl von Rückmeldungsbits B gibt, die die Energieeffizienz maximieren. Schließlich wird der Einfluss der Wahl kooperierender Sender auf die Energieeffizienz studiert, wobei gezeigt wird, dass eine optimale Gruppe kooperierender Sendeknoten, auch bekannt als Sendekoalition, gebildet werden kann, um die Energieeffizienz zu maximieren. Die untersuchten Techniken, einschließlich optimaler Rückmeldungsbits und Sendekoalitionsbildung, können eine 100-prozentige Steigerung der Energieeffizienz im Vergleich zum Stand der Technik Glossy bei gleichen Betriebsanforderungen in sehr dichten Netzwerken erreichen.

Zusammenfassend bieten die beiden Hauptthemen dieser Dissertation Einblicke in die möglichen Performancesteigerungen, die erzielt werden können, wenn kooperative Technologien in niederenergetischen Drahtlosnetzwerken eingesetzt werden.

Contents

List of Figures

Abbreviations

ACK	acknowledgment
AF	amplify-and-forward
ARQ	automatic repeat request
AWGN	additive white Gaussian noise
CDMA	code-division multiple-access
CF	compute-and-forward
CI	constructive interference
CPS	cyber-physical systems
CQI	channel quality information
CSI	channel state information
CVP	closest vector problem
D2D	device to device
DCBF	distributed collaborative beamforming
DDSS	distributed data storage systems
DF	decode-and-forward
DSSS	direct sequence spread spectrum
FCC	federal communications commission
FDMA	frequency-division multiple-access
FEC	forward error correction
FM	frequency modulation
FOS	flooding overlay structure
FPGA	field-programmable gate array
i.i.d.	independent and identically distributed

IEEE	institute of electrical and electronics engineers
IoT	internet of things
ISM	industrial, scientific and medical
LR-WPAN	low rate wireless personal access network
LWB	low-power wireless bus
MA	multiple access
MAC	media access control
MF-Glossy	multi-flow Glossy
MIMO	multiple-input multiple-output
MISO	multiple-input single-output
ML	maximum likelihood
MMSE	minimum mean square error
MTC	machine type communication
NC	network coding
OFDM	orthogonal frequency division multiplexing
O-QPSK	offset quadrature phase-shift keying
P2P	point-to-point
PLNC	physical layer network coding
QAM	quadrature amplitude modulation
QoS	quality of service
RVQ	random vector quantization
SDR	software defined radio
SIC	successive interference cancellation
SIMO	single-input multiple-output
SISO	single-input single-output

SNR	signal-to-noise ratio
USRP	universal software radio peripheral
WSN	wireless sensor network

Notation and Symbols

N	number of re-transmissions during a Glossy flood
c	Glossy packet relay counter
T_{slot}	time slot duration during a Glossy flood
$\boldsymbol{x}$	vector x
$\boldsymbol{X}$	matrix X
$\boldsymbol{I}_n$	identity matrix of size $n \times n$
$\mathrm{diag}(\dots)$	function that generates a matrix with the respective elements on the diagonal, zeros elsewhere
x^T	transpose operation
x^{H}	conjugate transpose operation
$\|\boldsymbol{x}\|$	ℓ_2-norm operation of a vector x
$\|x\|$	absolute value of a complex number x
$\log_2^+(x)$	$\max\{\log_2(x), 0\}$
$E[x]$	Expectation operation
$\oplus$	addition over the finite field
$\sum$	summation over the reals
$\mathcal{R}(x)$	real part of a complex number x
$\mathcal{I}(x)$	imaginary part of a complex number x
$\mathcal{CB}$	codebook, set of code words $\boldsymbol{c}$
B	number of feedback bits
$\mathbb{R}$	set of real numbers
$\mathbb{Z}$	set of integers
$\mathbb{C}$	set of complex numbers
$\mathbb{F}_q$	finite field of size q, where q is prime
Q	nearest neighbor quantizer
$\mathcal{V}$	voronoi region of a lattice
$\mathcal{NL}$	nested lattice code

$\mathcal{E}$	nested lattice code encoder
$\boldsymbol{v}_m$	lattice equation at receiver m
$\boldsymbol{a}_m$	lattice coefficient vector at receiver m
$\mathcal{CN}(0, \sigma^2)$	complex normal distribution with 0 mean and var $\frac{\sigma}{2}$

Chapter

1

Introduction

The use of vastly distributed wireless sensors has become very important in many fields of everyday life thanks to their small size, minimal energy consumption, low cost and ability to operate autonomously with limited maintenance effort. Some of those fields are commercial applications, such as smart homes, where sensors monitor home appliances and minimize energy consumption by controlling unnecessary energy demands [1]. Other fields are scientific applications, such as environmental monitoring, where these sensors have to operate independently and sometimes under extreme conditions (i.e. space exploration [2]). In emergency and health applications, sensor networks are utilized to make life easier and safer by monitoring personal health and activity data in order to perform accurate situation assessment [3]. While in industrial applications, sensor networks are used to monitor operation conditions and maintain quality of production [4].

As a result of their importance, wireless sensor networks (WSN) have been heavily investigated for the past decade in both physical and network layers. WSNs usually operate using low power communications following the IEEE 802.15.4 standards [5] where any transmission from a single node is not only heard by the intended receiver but also by nearby nodes. Moreover, when operating in the 2.4 GHz industrial scientific and medical (ISM) band, sensor devices have to share the available frequencies with other more powerful technologies such as WiFi. This is usually viewed as undesirable interference where receivers are instructed to avoid it and transmission protocols are optimized to limit it. However, in applications such as environmental monitoring and self-organizing networks, where knowledge about the network topology is limited or non-existent, routing information from a source node to a destination node and through a network of sensor nodes with limited capabilities, is very challenging and resource consuming. At the same time, these applications require high rate data collection systems for full functionality. These systems rely on time synchronization in order to calibrate measurements and network flooding to

send control signals such as adjusting sampling rates and initiating data transfers. This should be done as fast as possible to avoid clock synchronization errors. To satisfy these requirements, a new flooding mechanism for WSNs Glossy is introduced in [6] where time synchronization between nodes is implicitly achieved as the information packets travel through the network. Unlike most WSNs communication protocols, Glossy exploits interference instead of treating it as a problem like previously mentioned. In fact, it enforces simultaneous transmissions of the same information resulting in constructive interference at receiver nodes. It achieves 99% flooding reliability and micro second time synchronization. Low-Power Wireless Bus (LWB) is introduced in [7] based on Glossy, where it uses fast floods to transfer all data in the network. First, each transmission has to be scheduled by a central node where each sensor node has to request transmission slots in accordance with its operational demand. Then, communication is performed in a round based manner with a maximum round time of up to 30 seconds.

High performance, simplicity and low operational cost make Glossy seem perfect, but there are some challenges when using Glossy as a base for communication in a dense sensor network. In order for Glossy to achieve high performance results, it employs concurrent transmissions to enforce constructive interference at the receiver. Benefits of concurrent transmissions have been theoretically investigated [8] and experimentally demonstrated [9]. Moreover, the success of concurrent transmissions is proven to depend on simultaneously transmitting identical signals with a maximum synchronization error of 0.5 μsec. To this end, Glossy limits the number of concurrent information flows in the network to a single flow, by forcing nodes to wait and only transmit new information in assigned time slots. This hinders Glossy unsuitable for real time or delay sensitive applications without upgrades. Moreover, in order to achieve extreme simplicity and avoid software delays accompanying preliminary signal processing, sensor nodes using Glossy always use maximum power while transmitting. This increases energy consumption resulting in degraded energy efficiency and much lower battery life time. That being said, there are opportunities to further develop this technology. In the conclusion section of [10], it is noted that techniques such as distributed beamforming and lattice codes can promise significant improvements to the performance of concurrent transmission dependent flooding protocols such as Glossy. To address the previous issues, this dissertation poses several research questions and answers them by using transmission technologies to design novel communication protocols for WSNs, where the high reliability of Glossy is achieved while improving both latency and energy efficiency.

1.1 Challenges in Network Flooding using Glossy

Using Glossy as a network flooding protocol in WSNs has many advantages such as high reliability, simple transceiver design and embedded network wide clock synchronization. It can even achieve low latency in up to 8-hop size networks. However, there exists some obstacles in order to use it in highly dense networks or in scenarios with high network traffic. Figure 1.1 shows a simple illustration of a 2-hop WSN where nodes N_1 and N_2 want to transmit data packets A and B, respectively, using LWB. Nodes in green and blue are in transmit and receive mode, respectively.

Latency

Before the start of communication using LWB as shown in Figure 1.1a, each node looking to transmit new information must submit a transmission request to a central arbitrator (not depicted in the figure). Then, a transmission slot is assigned to each node following a first come, first served basis. Finally, transmission is carried out in a round basis and in the form of individual Glossy floods as shown in Figure 1.1b to Figure 1.1e. First, N_1 transmits A at maximum power. Nodes N_3 and N_4 receive A and re-transmit it simultanously in the following time slot as shown in Figure 1.1c. After node 2 receives A and the first Glossy flood is over, it proceeds to transmit B at maximum power as in Figure 1.1d. Then, similar to Figure 1.1c, nodes N_3 and N_4 re-transmit B in Figure 1.1e. Finally, node N_1 receives B and the second Glossy flood terminates. This results in node N_2 having double the latency of node N_1, because it had to wait until the first flood was over before initiating the second flood and transmitting B. This is fine for small networks like the one depicted in this example. However, in dense networks where large number of nodes require transmission slots regularly, it can lead to long delays for those scheduled to the last transmission slot. This issue calls for a communication protocol that reduces average latency in dense networks while preserving reliability of communication.

Energy Efficiency

A wireless sensor is typically a battery operated device with limited energy capacity, equipped with a low-power and low-rate radio transceiver. For example, one of the most popular commercial off-the shelf sensor nodes in WSNs and a typical device using Glossy is the Tmote Sky [11]. This device is equipped with a ChipCon CC2420 transceiver that operates in the 2.4GHz ISM band with compliance with the IEEE 802.15.4 standard,

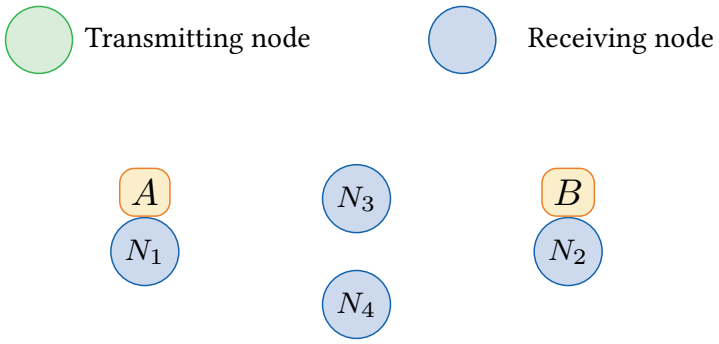

(a) Time slot 0: Before the protocol starts, each node with information to send has to request a transmission slot from a central arbitrator not depicted in this illustration. Nodes N_1 and N_2 would like to send data packets A and B, respectively. The central arbitrator replies with a time schedule where N_1 can transmit first, then N_2.

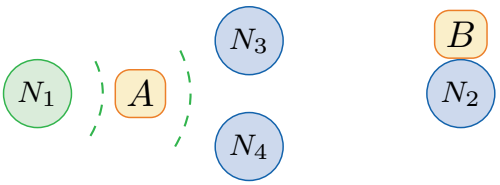

(b) Time slot 1: Node N_1 transmits A at maximum power. Nodes N_3 and N_4 receive A correctly. Node N_2 is out of reception range.

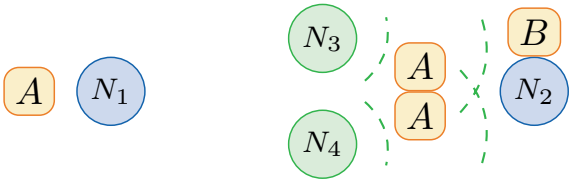

(c) Time slot 2: Thanks to the embedded synchronization of Glossy, nodes N_3 and N_4 can simultaneously transmit A at maximum power. Node N_2 receive A correctly.

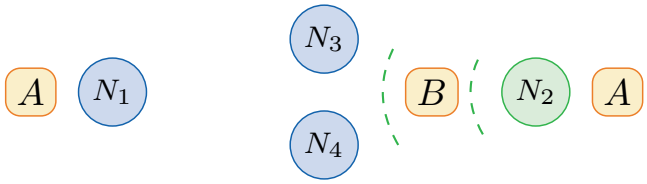

(d) Time slot 3: Node N_2 transmits B at maximum power. Nodes N_3 and N_4 receive B correctly. Node N_1 is out of reception range.

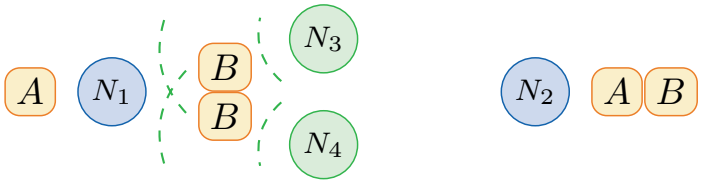

(e) Time slot 4: Nodes N_3 and N_4 can simultaneously transmit B at maximum power. Node N_1 receive B correctly. All nodes have A and B.

Figure 1.1: Transmission steps of LWB in a simple 2-hop network consisting of 4 identical nodes. Nodes N_1 and N_2 must transmit data packets A and B, respectively. Best case transmission scenario takes a minimum of 4 time slots for all nodes to receive both A and B.

while having a maximum transmit power and data rate of 0dBm and 250Kbps, respectively. The entire device is powered by only two AA batteries, which constitutes a limit on available energy and therefore, operating life time before batteries have to be replaced. This can prove challenging in applications like upper atmosphere monitoring, under water and space exploration; if not impossible. This makes energy efficiency the most important aspect when designing a WSN. The energy consumption of Tmote Sky is strongly affected by the radio transceiver, which is in idle (sleep) mode most of the time in order to save energy. Glossy takes advantage of the included micro second synchronization in order to have very small active times. Hence, reducing the energy consumed by the transceiver. However, it always uses the maximum transmit power regardless of the situation. For example, in the scenario depicted in Figure 1.1, each transmitting node uses the maximum available transmit power of 0dBm, while total energy consumption in the network will increase as the number of nodes in the network increases. Further, as the number of nodes in the network increases, the time spent in receiving mode, as well as the numbers of re-transmissions, increases. This results in an increased per-node energy consumption that can drastically reduce the battery life-time of the device. Changing that requires optimizing the energy consumption of the transceiver without affecting the current performance.

Tackling the previous challenges in a resource limited scenario such as WSNs requires us to use innovative transmission technologies, which presents another challenge.

Channel Information

In order to optimize transmit energy consumption, channel state information (CSI) must be available at the transmitter. However, in real network deployments, transmitters do not usually have CSI. Hence, known pilot signals may be sent from receivers to transmitters in order to estimate CSI, while relying on channel reciprocity. However, this constitutes an overhead in terms of energy consumption, as well as latency. This is a challenge in scenarios where sensor nodes are not aware of the network topology and requires innovative, energy efficient ways to exchange or make available the channel information for transmitting nodes in order to make calculated decisions that improves energy efficiency.

1.2 Scope and Objectives of the Dissertation

With the growing interest in massive deployment of wireless sensors and network densification, it is of paramount importance to investigate possible technologies that would aid in improving energy efficiency and decreasing latency in WSNs while focusing on the aforementioned challenges. To this end and based on state of the art Glossy, this dissertation investigates several approaches in order to achieve performance gains in energy efficiency, latency and energy consumption. This is done while using different combinations of transmission technologies such as network coding and transmission beamforming as well as mathematical tools such as convex optimization and game theory. First, investigated approaches are analytically constructed using mathematical means. Then, they are evaluated thoroughly using software simulations and judged based on different criteria depending on the used approach. Hardware implementation of the proposed approaches is discussed from a feasibility point of view. However, it is important to note that actual implementation lays outside the scope and time frame of this dissertation and is left for possible extensions and future work. Instead, we only focus on the theoretical formulation of protocol operations and software validation.

For a simple 2-hop network consisting of 4 nodes, LWB can be used to transmit 2 different data packets. In a best case scenario where no re-transmissions are required, a total of 4 time slots are needed to complete the operation. In this dissertation the following research questions are addressed and answered:

1. How can multiple nodes be enabled to flood the network with different data packets simultaneously and how does this affect performance including energy efficiency and latency?
2. How can transmission power be optimized and how does this affect performance including energy efficiency and latency?
3. How can channel information be made available without excessive transceiver complexity and communication overhead?
4. How does partial channel information affect performance compared to the optimal case of perfect channel information?
5. How can wireless sensor nodes dynamically self-organize into cooperative groups in order to improve energy efficiency?

1.3 Contributions and Outline of the Dissertation

In this dissertation we concentrate on answering the previous research questions. We start by proposing a novel WSN flooding communication protocol that allows multiple flows of different packets. Then, we propose an approach using optimization techniques and transmit beamforming in order to optimize transmit power and improve energy efficiency under perfect channel information. After that, we suggest a robust beamforming method using quantized feedback for more realistic scenarios where channel information is not available. Finally, we investigate the optimal number of cooperative transmitters that maximizes energy efficiency. The main contributions are detailed as follows:

Multi-flow Glossy - Chapter 3

Emerging applications like wireless control or drone swarms require low-latency communication across multiple hops among a large number of both static and mobile devices. Recent protocols based on concurrent transmissions can meet most of these requirements. In particular, Glossy comes extremely close to the minimum lower latency bound for flooding a *single* packet. However, when *multiple* packets need to be exchanged, the overall latency increases linearly since each packet must be mapped onto a distinct Glossy flood. This chapter explores the opportunities and challenges of physical-layer network coding to exchange more packets per unit of time. To this end, we present *Multi-flow Glossy (MF-Glossy)*, a communication scheme that simultaneously floods different packets from multiple sources to all nodes in the network. We determine upper bounds on the performance of Glossy and MF-Glossy using a communication-theoretic analysis. Further, we show by simulation that MF-Glossy has the potential to achieve several-fold improvements in goodput and latency across a wide spectrum of network configurations at lower energy costs and comparable packet reception rates. On the road to harnessing this potential in real low-power networks, we discuss the hardware implementation challenges and focus on the key research challenges and possible solutions lying ahead in order to harness the full power of MF-Glossy in embedded systems. The contributions in this chapter are partially published in the following publication:

A. Abdelkader, J. Richter, E. A. Jorswieck, and M. Zimmerling. “Multi-flow Glossy: Physical-layer Network Coding Meets Embedded Wireless Systems”. In: *Proceedings of the International Conference on Computer Communications and Networks*. Vancouver, Canada, July 2017 .

Beamforming with Perfect CSI - Chapter 4

We consider a device-to-device wireless multi-hop communication scenario with resource-constrained devices that require energy-efficient connectivity. Based on the recently proposed Glossy network flooding protocol and under the assumption of available channel information at all nodes, we develop both centralized and distributed beamforming and power control algorithms, and analyze their performance. The proposed schemes are compared in terms of their energy efficiency to the standard Glossy. Numerical simulations demonstrate that a centralized power control scheme can achieve several-fold improvements in energy efficiency over Glossy across a wide spectrum of network configurations at comparable packet reception rates. We also show how power control and beamforming can be applied in a distributed manner and demonstrate achievable gains compared to standard Glossy. The results indicate that adaptive power control and distributed beamforming strategies improve energy efficiency, which is one important performance indicator in 5G Internet-of-Things applications. The contributions in this chapter are partially published in the following publication:

A. Abdelkader, E. Jorswieck, and M. Zimmerling. "Centralized and Distributed Optimum Power Control and Beam-forming in Network Flooding". In: *European Wireless 2017; 23th European Wireless Conference*. May 2017, pp. 1–6 .

Robust Beamforming with Limited Feedback - Chapter 5

The energy efficiency of communication plays a significant role in network design and operation, when having power-limited devices in a multi-hop communication scenario. Based on the recently proposed Glossy network flooding approach, we introduce cooperation on 2 stages. First, between receiving and transmitting nodes for the process of channel estimation. Then, within transmitting nodes and formulate a robust multi-cast beamforming problem with imperfect channel state information, and analyze its performance. The level of cooperation is dependent on the number of limited feedback bits from receivers to transmitters. First, the impact of number of limited feedback bits B on energy efficiency is studied, and the programming problem for finding the optimal B is formulated subject to a maximum outage constraint of 5%. Numerical simulations show that there exists an optimal number of feedback bits that maximizes energy efficiency. Second, the effect of the number of cooperating transmitters on energy efficiency is investigated. Results show that an optimum group of cooperating transmit nodes, also known as a transmit coalition,

can be formed in order to maximize energy efficiency. Results show that the investigated techniques including optimum feedback bits and transmit coalition formation can achieve a 100% increase in energy efficiency when compared to state of the art Glossy under same operation requirements in very dense networks. The contributions in this chapter are partially published in the following publications:

A. Abdelkader and E. A. Jorswieck. "Robust Energy-Efficient Power Control and Beam-forming in Network Flooding". In: *WSA 2018; 22nd International ITG Workshop on Smart Antennas*. Mar. 2018, pp. 1–7.
A. Abdelkader and E. Jorswieck. "Robust adaptive distributed beamforming for energy-efficient network flooding". In: *EURASIP Journal on Wireless Communications and Networking* 2019.1 (June 2019), p. 154.

According to Figure 1.2, this dissertation is organized as follows: In Chapter 2, we present related work on low power WSNs, network flooding and concurrent transmissions leading to our choice of state-of-the-art Glossy, then we explain the operation of Glossy and LWB. In Chapter 3, we propose MF-Glossy, a novel WSN flooding protocol that enables multiple simultaneous data flows in the network using physical layer network coding. In Chapter 4, we discuss an approach using transmit beamforming to improve energy efficiency in network flooding. The discussed approach is analyzed under assumptions of perfect channel information. Then, we consider the more realistic scenario of no channel information in Chapter 5, where we propose an approach using robust beamforming and quantized feedback in order to optimize energy efficiency. Moreover, we explore the forming of cooperative coalitions and whether there exists an optimum size that maximizes energy efficiency. Finally, we conclude this dissertation and suggest future work in Chapter 6.

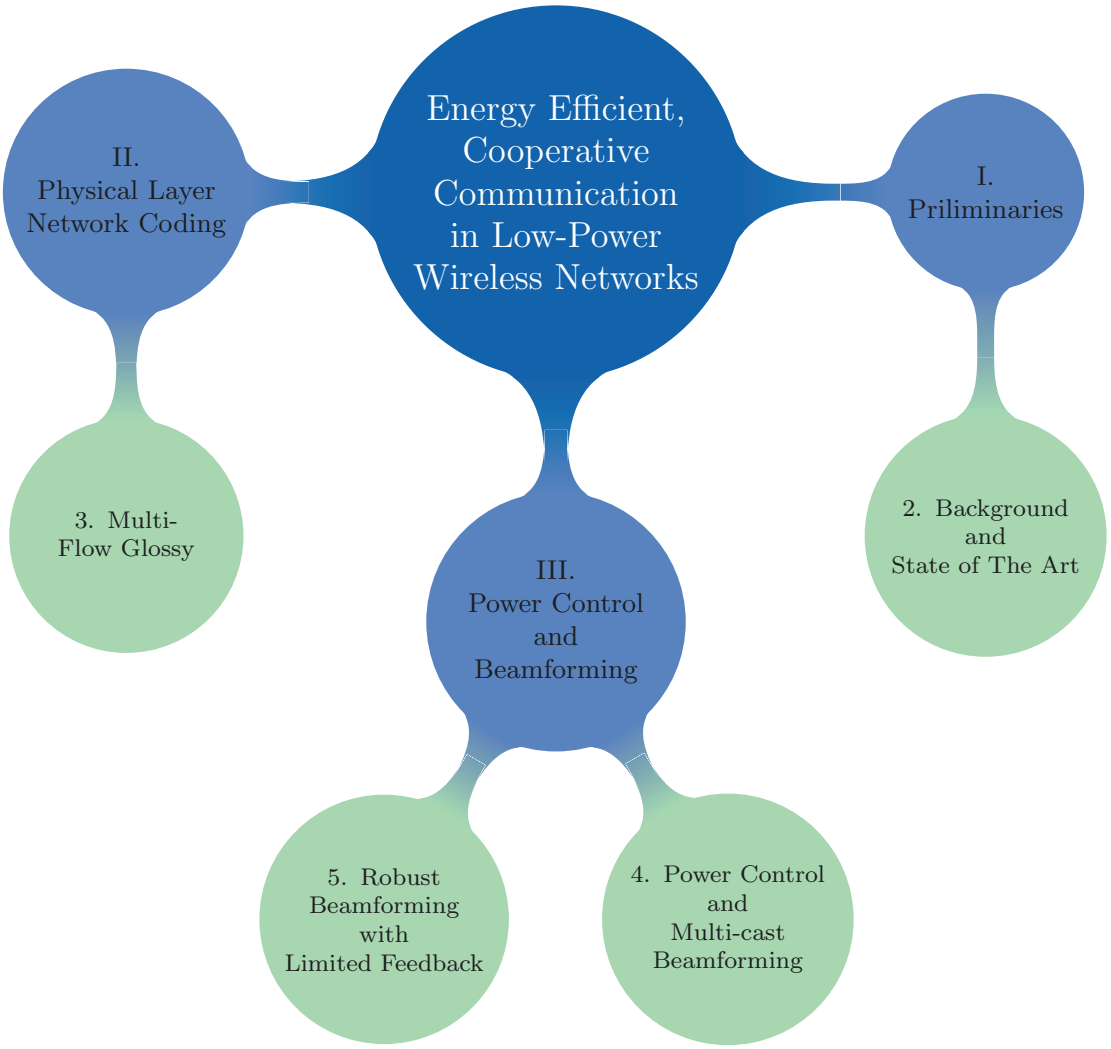

Figure 1.2: Graphical illustration of the contents of this dissertation.

Part I

Preliminaries

Chapter 2

Background and State of the Art

In this chapter we present a summary of related works on WSNs to this dissertation as well as important background information on state-of-the-art Glossy. First, we introduce the basics of low-power wireless networks leading to the choice of working on network flooding applications. Then, we review network flooding as a communication technology and present relevant works while motivating our focus on Glossy. After that, we discuss concurrent transmissions and its importance in order to classify previously discussed works in the literature. Finally, we explain the operation of state-of-the-art Glossy and introduce the advantages of building on it.

2.1 Low-power wireless Networks

Low-power wireless networking based on the IEEE 802.15.4 standard [5] has received a lot of attention over the last decade, especially in the sensor network community. Works in this area investigate the theoretical aspects [8, 9], as well as propose communication protocols for applications ranging from industrial automation [4, 12] to information dissemination or network flooding [6, 7, 13]. The 802.15.4 is developed as the communication standard for low-rate wireless personal area networks (LR-WPANs). It clearly specifies possible settings for both the physical and the MAC layers for LR-WAPNs. With lower data rate, simple connectivity and extended battery life time in mind, it serves as the foundation of upper layer communication protocols such as ZigBee [14] and WirelessHart [15]. It dictates that communication can occur in the 800 MHz, 900 MHz or 2.4 GHz ISM bands. While any of these bands can be used by 802.15.4 supported devices, the 2.4 GHz band is more popular due to its worldwide availability, where the 800 MHz band is specified primarily for European use and the 900 MHz band can only be used in FCC regulated territories. When operating in the 2.4 GHz ISM band, devices have to share the available fre-

quencies with other more powerful technologies such as WiFi which operates according to the IEEE 802.11 standard. Moreover, at 2.4 GHz the IEEE 802.15.4 standard stipulates a maximum data rate of 250 kbps using offset quadrature phase-shift keying (O-QPSK) with half-sine pulse shaping and direct-sequence spread spectrum (DSSS) in order to match the limited resources available on sensor nodes. However, due to communication overhead, only half the data rate is actually achievable. Due to the small communication range of only a few tens of meters, the devices collaborate via multi-hop communication.

Real deployments of low-power wireless networks range in application from permafrost monitoring in high alpine regions [16] to closed-loop lighting control in road tunnels [17]. However, many of these applications rely on a common notion of time across nodes (*e.g.*, to correlate sensor readings) and network flooding (*e.g.*, to send a command to all nodes). This demonstrates the importance of network flooding in low-power wireless networks as further explained in Section 2.2.

2.2 Network Flooding

Network flooding (also commonly known as data dissemination) is a communication protocol that delivers a message from one node to all other nodes in the network. Flooding is used in many applications ranging from environmental monitoring to industrial automation, in order to perform clock synchronization [18, 19], code distribution [20], or one-to-one routing [21]. For many of these applications, the main research focus is reliability and energy efficiency because of the limited battery lifetime of the sensor nodes. Many network flooding approaches are presented in literature over the years, where the simplest form is Simple Flooding, where each node that receives a new message forwards it to a neighboring node. However, this results in excessive redundancy and network congestion [22]. A method to treat this problem is presented in [23], where a flooding overlay structure (FOS) is proposed to increase network lifetime and reduce the overhead of flooding in a sensor network. Another example is Trickle, a network flooding algorithm for code propagation in WSNs [24]. Trickle uses an individual timer at each node to periodically send out a summary to neighboring nodes but obligates the node to stay silent in case of receiving information similar to its own. Unfortunately, Trickle is not suitable for real-time applications due to the long time until stable operation, which can go up to a few minutes. Recently, a significant contribution is made by proposing the Glossy flooding protocol [6]. As described in Section 2.4, the Glossy protocol provides both fast, reliable one-to-all communication and accurate network-wide time synchronization in multi-hop

wireless networks. In real IEEE 802.15.4 network deployments, consisting of more than 100 nodes, Glossy achieves unparalleled packet failure rates below 10^{-4} and latency of a few milliseconds, while synchronizing nodes to within sub-microsecond accuracy. The simple, yet disruptive approach of Glossy and the availability of an open-source implementation has arguably created a movement in the low-power wireless networking community, as visible, for example, from the many works building on the basic flooding primitive to improve the performance of stable network functionality, such as in-network processing [25] and data dissemination [26], or to enable entirely new networking abstractions suitable for mission-critical CPS applications [7, 27]. Thus, any innovation at the level of the communication primitive would immediately benefit the many works using it. Most of the works building on the Glossy primitive make use of concurrent transmissions in order to achieve high performance gains. Glossy achieves this by using concurrent transmissions of identical packets from multiple senders resulting in constructive interference and capture effects at receivers. Both phenomena are explained in Section 2.3.

2.3 Concurrent Transmissions

Concurrent transmission occurs when two or more nodes transmit signals simultaneously to a shared receiver node within the 1-hop range. At the receiver, the sum of both signals is received. In [28] theoretical gains are demonstrated when spatially diverse wireless transmitters cooperate to relay information. Later on, a series of experiments are presented in [29, 30] to further investigate the gains of concurrently sent information from multiple transmitters. In SourceSync [10] concurrent transmission gains are demonstrated in practice using an FPGA-based 802.11-like radio platform. Reduced bit error rates and higher throughput are demonstrated when multiple nodes transmit the same packet at the same time on the same OFDM subcarrier. In 2008, Backcast [31] utilizes automatically generated ACK reply signals in order to let transmitters know that at least one node successfully received the transmitted signal. It is also demonstrated for the first time that identical hardware-generated ACK signals in receiving nodes constructively interfere at the transmitter. Although Backcast does not depend on CI, it directly proves that collisions are not necessarily bad for reception. Therefore, A-MAC [32] and Flip-MAC [33] build upon Backcast and propose receiver-initiated protocols. Receivers periodically send out ACK request frames according to the IEEE 802.15.4 standard. Nodes that need to transmit will send an automatically generated ACK. Then, receiver nodes let their radio on while waiting for transmission. Until this point, only hardware generated ACK signals were concurrently

transmitted. Flash [13] transmits data packets from multiple nodes simultaneously ensuring that receivers receive the data from, at least, one sender. While previous works utilize concurrent transmission, they achieve gains in performance due to the capture effect [34].

Capture Effect

The capture effect in frequency modulation (FM) receivers was first introduced in [34] as a phenomena that occurs when a FM receiver has two different FM signals with unequal amplitudes at the same time. According to [25], the capture effect is defined such that; a receiver has a higher probability of successfully decoding a signal if the received signal is 3 dBm higher than the sum of interfering signals. However, the stronger signal must also arrive within 160 ms of the interfering signals. This is also applicable when two or more nodes transmit different signals. The previous requirements are confirmed experimentally in [35], where it is shown that the capture effect happens at the receiver when a stronger signal arrives no later than $96\mu\ s$ later than the preamble duration of the weaker signal. In few cases, signals might interfere destructively resulting in a partial or a complete reception error at the receiver. However, full destructive interference rarely happens which results in a high probability of successfully receiving packets due to CI and/or capture effect.

Constructive Interference

CI occurs as a possible side effect of concurrent transmissions, when multiple nodes transmit *the same data packet simultaneously*, which results in signal superposition at receiving nodes. Hence, data packets can be decoded successfully with high probability due to higher signal strength at receiving nodes. Non-destructive interference effects are reported in [31] when multiple sensor nodes simultaneously transmit identical, short acknowledgment frames generated in hardware. This observation also applies to variable-size packets generated in software as proven in [6], where Glossy is introduced. A statistical model for the one hop delay is derived in [35], where it is demonstrated that with a large frequency drift at the oscillators and long packet lengths, it is hard to obtain CI. Moreover, an experimentally validated model for the prediction of successful packet reception is proposed, where both capture effect and CI are considered. CI from the receiver perspective is studied in [36], where multiple factors affecting CI performance are inferred both theoretically and experimentally. The most important factor in deciding if CI occurs or not is that the time offset between concurrent transmissions must be below 500 ns. Therefore, a high level of synchronization is needed, which is provided by Glossy down to 0.5 μs for an

8-hop network. As described in Section 2.4, the Glossy protocol provides both one-to-all communication and time synchronization in multi-hop networks. The term CI-Flooding is used in [37], where a mathematical model of a CI based WSN is presented in order to study the overall network performance including throughput and life time. A comprehensive performance analysis of receiving concurrent transmissions from the physical layer perspective is presented in [38], where it is shown that the IEEE 802.15.4 DSSS plays a vital role in the successful reception of concurrent transmissions.

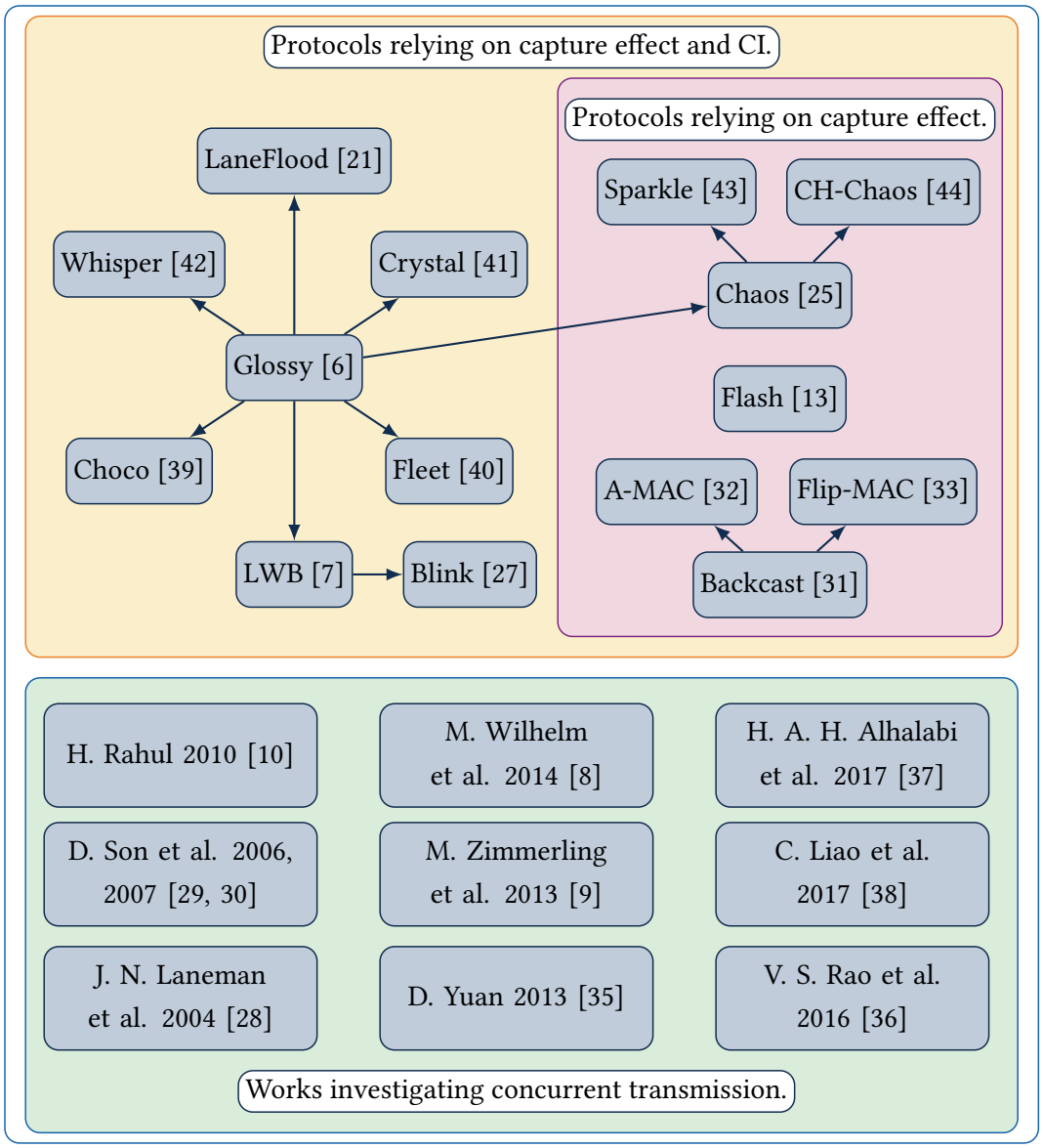

Figure 2.1: Classification of related works on concurrent transmissions. In the bottom works that studied concurrent transmissions either analytically or experimentally. On the right are proposed protocols relying mainly on the capture effect. On the left are proposed protocols relying on both the capture effect and CI. Arrows connect protocols to others that build upon them.

Related Works on Concurrent Transmissions

Several protocols have used concurrent transmissions to build communication primitives based on Glossy. A comprehensive overview of the works discussed here is shown in Figure 2.1. Works are classified according to the proposed approach and analysis provided. Classification is divided into (1) Works investigating concurrent transmissions, (2) Proposed protocols relying on the capture effect and (3) Proposed protocols relying on both the capture effect and CI.

To facilitate data exchange among multiple nodes, LWB [7] allocates non-overlapping time slots to individual nodes for flooding single packets via Glossy. Similarly, Blink [27] builds on LWB while following an earliest deadline first policy in order to achieve real time latency constraints. Choco [39] builds on Glossy to construct a low-power, low-delay and end-to-end reliable communication protocol. Whisper is presented in [42] to reduce the radio-on time of nodes in multi-hop networks while reliably flooding small amounts of data. It relies on concurrent transmissions to flood signaling packets through the network. Similarly, LaneFlood [21] also relies on concurrent transmissions in order to establish a route between any source and destination node in a multi-hop network in an effort to empower one-to-one IoT communication protocols. Crystal [41] proposes the concurrent transmission of multiple packets through simultaneous Glossy flows while performing data prediction in order to minimize the number of re-transmissions within each glossy flow. Senders compete while repeating transmission until they receive an ACK signal informing them that receivers have received the sent data correctly. Finally, Fleet [40] capitalizes on Glossy while performing node clustering in order to limit the radio-on time of sensor nodes. Hence, reducing energy consumption and latency. Chaos is proposed in [25], an all-to-all data sharing and in-network processing primitive for low-power wireless networks. During transmission, Chaos exploits Glossy through the concurrently transmitting packets with different payloads, where receiving nodes rely on the capture effect to receive one of them. CH-Chaos [44] improves Chaos by implementing channel hopping in order to add more robustness and resilience to interference at the receiver. For network control operations, Sparkle is proposed in [43]. Sparkle builds on Chaos where it relies on concurrent transmissions in order to control and optimize end-to-end communication flow. In summary, concurrent transmission dependent network flooding is an attractive approach well deserving of large interest in recent years. However, there is still a huge room for improvements in regards to energy efficiency and latency on the protocol operation level.

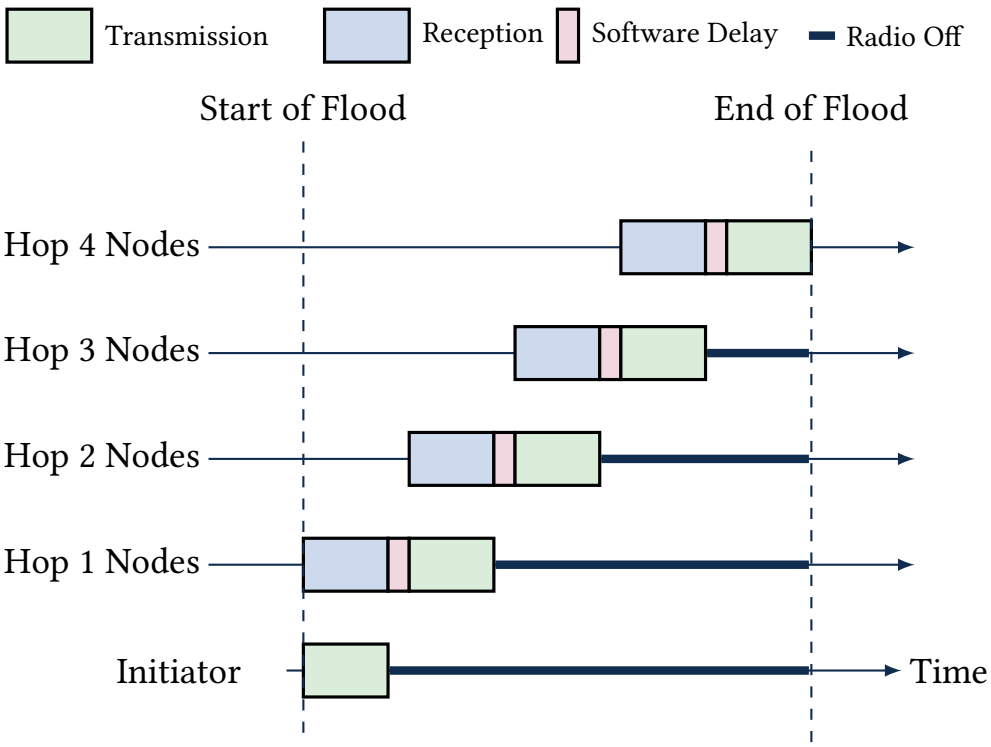

Figure 2.2: Series of concurrent transmissions and receptions as a Glossy flood propagates in a 4-hop network with re-transmission limit $N = 1$. Figure is adapted from [6], where network flooding using Glossy is first introduced.

2.4 Operation of State-of-the-art Glossy

This section briefly reviews the operation of state-of-the-art Glossy. A Glossy flood typically starts with one node transmitting certain information at maximum transmit power (0 dBm). Then, all nodes, which receive successfully and have not reached the limit on number of re-transmissions (N), transmit concurrently the received information with maximum transmit power. This continues until no more nodes are able to transmit due to the re-transmission limit N. The result of this procedure are waves of the same information propagating back and forth through the network until the Glossy flood is terminated. This simple yet effective operation primitive is the reason why we try to further improve the performance of state-of-the-art Glossy.

Figure 2.2 shows the actions during a Glossy flood in a multi-hop network. An *initiator* starts the flood by transmitting the packet; all other nodes have their radio on. Since wireless is a broadcast medium, all nodes within transmission range of the initiator, the

1-hop receiver nodes, receive the packet at about the same time. After a minimal processing delay, the 1-hop receivers relay the *same* packet at about the same time. Even though these *concurrent transmissions* collide at the *2-hop receivers*, these nodes can successfully receive and decode the packet with high probability. Then, the 2-hop receivers again re-transmit the same packet simultaneously, thereby propagating the flood deeper into the network. As a result, the flood spreads like a wave and reaches out to all nodes. Since each node transmits multiple times during the same flood up to a certain *re-transmission limit* N, there are multiple waves, boosting Glossy's reliability above 99.9 % [6]. Unlike prior practical low-power wireless communication schemes, Glossy purposely *forces packet collisions* rather than trying to avoid them (*e.g.*, using carrier sensing or scheduling non-interfering transmissions across individual links). To enable successful packet reception, Glossy aligns *identical* wireless signals from multiple concurrent senders within the 0.5 μs bound that allows them to interfere non-destructively using the IEEE 802.15.4 physical layer [6]. The synchronization of the concurrent senders is established on the fly and in a distributed fashion by using packet receptions during a flood as a reference point. For example, in Figure 2.2, the simultaneous reception of the packet from the 1-hop receivers serves to align the transmissions of the 2-hop receivers. Glossy achieves this through a careful software design that makes the processing time between reception and transmission as short and deterministic as possible. Glossy also capitalizes on the *capture effect* that lets a receiver demodulate only the strongest of multiple overlapping signals [34].

As a sort of by-product, Glossy can also time-synchronize all nodes in the network. To this end, packets carry an extra field, the *relay counter* c. The initiator sets $c = 0$ before starting the flood, and receivers increment c before relaying. Notably, the duration of a single *slot* T_{slot} during a Glossy flood, that is, the time from the start of a transmission with relay counter c to the start of the next transmission with $c + 1$, is a network-wide constant that can be locally measured by every node. By multiplying the received c by the measured T_{slot}, nodes obtain the elapsed time since the initiator started the flood. In this way, nodes synchronize to the initiator with sub-microsecond accuracy [6]. We build on Glossy because it approaches the lower latency bound for flooding single packets, achieves unparalleled packet delivery ratios above 99.99 % in diverse real-world networks, and seamlessly adapts to changes in the network (*e.g.*, due to mobile or failing devices) [6, 7].

Part II

Physical Layer Network Coding in Low-Power Wireless Networks

Chapter 3

Multi-Flow Glossy

In this chapter, we ask the question whether it is possible to overcome some limitations of Glossy while retaining its merits, including its seamless support for communication to all nodes in the presence of mobile devices. In particular, we explore the use of physical-layer network coding (PLNC) to enable *multiple sources to simultaneously flood different packets to all nodes*. This way, we aim at significantly increasing the goodput (*i.e.*, the amount of successfully exchanged data in the network per unit of time) over the state of the art for the same transmit bit rate (*e.g.*, 250 kbps for IEEE 802.15.4 radios).

3.1 Motivation and Contribution

Embedded wireless networks are a key factor to innovation in cyber-physical systems (CPS). Using wireless radios instead of wires cuts costs and clears physical barriers, allowing to tap into previously inaccessible information and to create applications with unprecedented opportunities, from industrial wireless control [45] to emergency response via aerial drones [46]. These emerging applications often rely on multi-hop communication with stringent requirements on latency and reliability [45, 46]. For instance, coordination and control tasks require short end-to-end latency of 10–250 ms [12] and tolerate only small packet loss rates [47]. Further, industrial applications and drone swarms typically need to exchange messages among a large number of static and/or mobile devices [45, 48], which are often also subject to energy constraints [49].

Given the state of the art in low-power wireless networking presented in Section 2.1, one possible solution to meet these requirements is to map the communication demands onto a sequence of Glossy floods [6]. Similar to LWB [7], each node that wishes to transmit is allocated a time slot in which it can flood one packet to all other nodes in the network as demonstrated in Section 2.4. For flooding an *individual packet* using half-duplex radios,

Glossy achieves almost the theoretical minimum communication latency, while providing a reliability higher than 99.9 % in diverse scenarios regardless of whether the devices are static or mobile[6, 7]. However, Glossy supports only one source node (or *flow*) per flood. Therefore, the overall latency increases linearly with the number of packets if *multiple packets from different source nodes* are exchanged using Glossy, as well as the network size. In order to avoid interference between consecutive Glossy floods with different packets, the next flood can only start after the previous one is over [7]. This operation bounds the number of packets that can be exchanged within, for example, the cycle time of a control or coordination task, which may limit the applicability of low-power wireless technology to control systems with slow-changing dynamics and to swarms with not many more than a handful of drones. Moreover, it performs sub-optimally from an energy point of view and may not be suitable for monitoring applications, where multiple sensors need to transmit their readings regularly while having as long battery life time as possible [12]. Hence, it would be highly desirable to support not just one but multiple flows from different initiators during a flood.

3.1.1 Contributions and structure

To the best of our knowledge, we are the first to consider PLNC in a low-power wireless setting. We realize that a lot of research needs to be done before MF-Glossy runs on off-the-shelf devices just like Glossy. As such, our goal in this chapter is two-fold: We intend to (*i*) shed light on the performance gains we can hope to achieve over Glossy by using the compute-and-forward approach, which has thus far never been implemented on IEEE 802.15.4 compliant hardware, and (*ii*) identify the key challenges that must by solved to harness these performance gains in a MF-Glossy implementation on wireless devices.

To this end, this chapter contributes the following:

- We introduce MF-Glossy, a many-to-all communication scheme that builds upon state-of-the-art Glossy and exploits PLNC based on the compute-and-forward approach [50] to simultaneously flood multiple packets in a multi-hop low-power wireless network.
- By conducting a communication-theoretic analysis, we provide thus far unknown upper bounds on the performance of the widely used state-of-the-art Glossy and our proposed MF-Glossy scheme.

- We show in simulation that MF-Glossy has the potential to outperform Glossy across a wide spectrum of network configurations. Relative to Glossy, MF-Glossy can reduce latency by 9× and boost goodput by 3×, while consuming less energy and providing the same high reliability.
- Based on the first implementation of the compute-and-forward approach on a small testbed of SDRs presented in [51], we study the hardware implementation challenges facing MF-Glossy. Using the findings in [51], we measure 2.4 ms and 5.3 ms for encoding and decoding one byte, respectively, on an Intel i5 processor. We discuss several directions to significantly improve on these figures.

Overall, we show that MF-Glossy promises significant performance gains and is indeed implementable. Our analytical performance upper bounds, while interesting in their own right, determine the processing overhead an implementation of MF-Glossy can afford to not outweigh the gains. Not withstanding its limitations, the proof-of-concept implementation shown in this chapter serves as a stepping stone to making MF-Glossy viable for state-of-the-art wireless embedded platforms (*e.g.*, leveraging 32-bit ARM Cortex-M microcontrollers).

After presenting the state of the art and explaining basic operation of PLNC in Section 3.2, we propose in Section 3.3 a novel scheme, called Multi-flow Glossy (MF-Glossy), that exploits PLNC to enable the simultaneous flooding of multiple different packets in multi-hop low-power wireless networks. Then, we conduct in Section 3.4 a communication-theoretic analysis, at the most fundamental level, of the state-of-the-art Glossy and the proposed scheme MF-Glossy. Our analysis provides thus far unknown upper bounds on the performance of this widely-used, practical protocol. Then, results from numerical simulations in Section 3.6 demonstrate that MF-Glossy greatly outperforms Glossy across a wide spectrum of network configurations. For instance, compared to Glossy, MF-Glossy reduces latency by 9× and increases goodput by 3× while consuming less energy and providing similar reliability. After that, we discuss hardware implementation challenges and suggest possible solutions in Section 3.7 while demonstrating a proof-of-concept implementation of PLNC based on the compute-and-forward approach. We end the chapter in Section 3.8 with brief concluding remarks.

3.2 Physical-layer Network Coding (PLNC)

The concept of linear network coding (NC) is first proposed by Ahlswede et al. in [52] for wired networks. In their seminal paper, they refer to NC as coding at a node in a network, where, by coding, they mean an arbitrary, causal mapping from inputs to outputs. The model used in NC is, however, assuming point-to-point error-free links. NC can also be described as defined in [53]: "... if any receiver of a multi-cast session could, in the absence of other receivers of the same session, receive at a certain rate, then it can do it in the presence of any other number of receivers. NC removes the competition among users for finite resources." The basic idea is to allow intermediate nodes in a network to combine the received data packets and forward a superposition. The intended receivers will be able to decode the original data packets if they receive enough linearly independent combinations of the original data packets. For wired networks, we can see a paradigm shift from packet-switched networks, where each data packet is routed individually through the network, to code-centric networks, where data packets are combined on their way through the network. This helps resolve bottlenecks on frequently used routes. But network coding is not limited to wired networks. The concept is also applicable in wireless networks, where interference is no longer considered a disadvantage but instead exploited.

3.2.1 State of the art

In 2006, physical-layer network coding (PLNC) is first introduced in [54] as a way to take advantage of the natural coding that occurs when electromagnetic waves come together within the same physical space. After that, the first PLNC implementation on software-defined radios (SDRs) is demonstrated by Katti et al. [55] in 2007, where they adopt an *amplify-and-forward* approach, such that a relay does not decode the received superposition but simply amplifies and forwards the signal. This approach is often referred to as analog network coding. Amplify-and-forward does not decode the signals, but forwards an amplified version of the received signal. The downside is the noise amplification, which accumulates as the signal is forwarded through the network, making it effective only in high signal to noise ratio channels [56]. Moreover, time synchronization poses a practical problem that many try to battle [57]. A first design and implementation of a PLNC protocol is proposed in [58] using Viterbi decoder to treat timing and sampling offsets between interfering signals. For the two-way relay channel, [59] conducts an analysis of the performance of practical PLNC. The authors of [60, 61] go even further and show a real-time implementation of PLNC.

A peak for PLNC research is in 2011, when Nazer and Gastpar show that a *compute-and-forward* approach, where relays de- and encode linear combinations of packets, can achieve higher goodput than amplify-and-foward [50]. Using nested lattice codes, it can achieve the additive white Gaussian noise (AWGN) channel capacity with lattice decoding instead of maximum-likelihood decoding [62]. There have been a few efforts to use compute-and-forward applicable in practical systems [63]. In [64, 65] the performance of the compute-and-forward approach is analyzed using low density lattice codes [66]. However, the analysis is limited to scenarios with perfect channel alignment. To make compute-and-forward practical, an efficient implementation of the corresponding coding schemes is essential. Although in a different context, Sheppard et al. [67] designed and implemented lattice coding schemes using digital signal processing techniques, and Wang et al. [68] integrate the leech lattice into IEEE 802.11a. Recent studies explore lattice codes for future 5G networks [69]. So, thus far, compute-and-forward based on lattice codes has been a theoretical topic that lacked a practical implementation, whereas we demonstrate the first hardware setup on a small SDR testbed.

We investigate the use of the compute-and-forward approach by Nazer and Gastpar [50] to enable the simultaneous flooding of multiple packets in a multi-hop embedded wireless network. We refer to this many-to-all communication scheme as *Multi-flow Glossy (MF-Glossy)*. Using MF-Glossy, a given number of sources K initiate the flood by simultaneously transmitting K different source packets. At the end of a MF-Glossy flood, every node in the network is aware of all K source packets.

Like Glossy, PLNC is based on concurrent transmissions. Unlike Glossy, however, the transmitted packets have *different* payloads. As an example, consider the classical two-hop relay network in Figure 3.1, where nodes N_1 and N_2 want to exchange a message with one another through relay N_3. Using Glossy, node N_1 "floods" its packet via N_3 to N_2, and then node N_2 "floods" its packet via N_3 to N_1. So exchanging two packets takes 4 time slots. PLNC achieves the same in 2 time slots. In particular, nodes N_1 and N_2 transmit their packets simultaneously in the first time slot. Due to the coding that naturally occurs when electromagnetic waves come together within the same physical space, relay N_3 receives and decodes the sum (*i.e.*, a linear combination) of both packets, which it then encodes and transmits in the second time slot. Because N_1 and N_2 know the packets they transmitted, they can subtract them from the received sum to get the other packet. Thus, using PLNC, we double the goodput in this example compared with Glossy. In order to further explain the proposed MF-Glossy in Section 3.3, we present some background definitions for PLNC in Section 3.2.2.

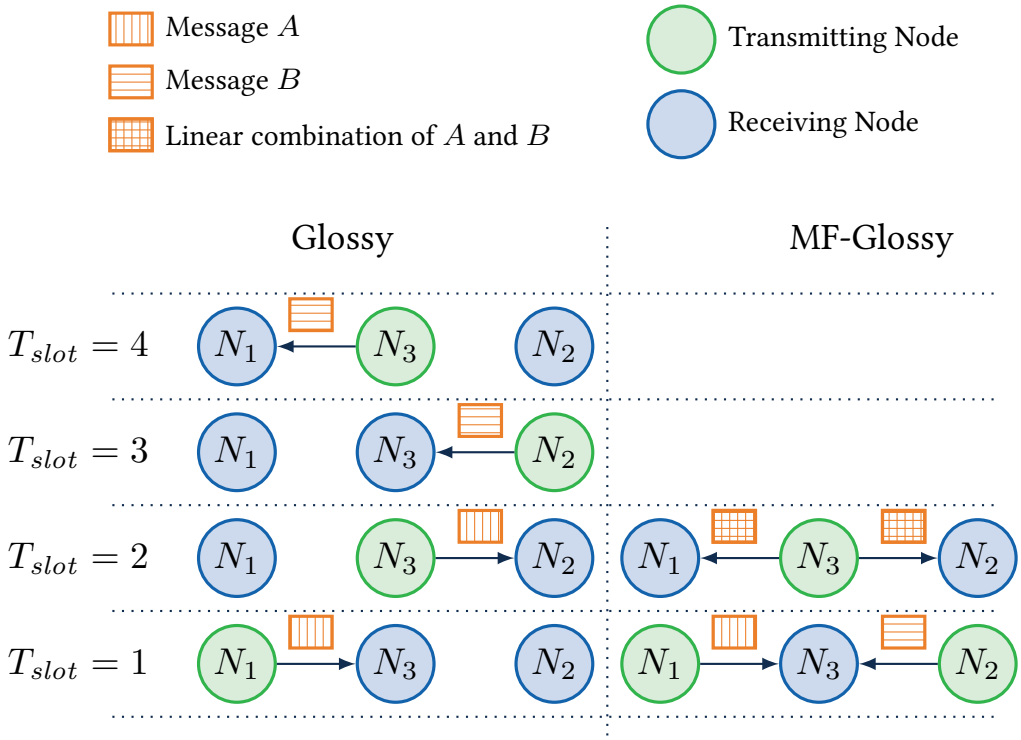

Figure 3.1: Comparison between Glossy and MF-Glossy in two-hop relay WSN, where nodes N_1 and N_2 intend to exchange messages with each other via relay N_3. Using physical-layer network coding, N_1 and N_2 send simultaneously. N_3 receives and decodes the sum of both packets, which it encodes and transmits. N_1 and N_2 substract their own packet to get the other packet. This doubles the goodput compared with the current approach used by Glossy.

3.2.2 Introduction to PLNC

In a wireless setup, it is possible to exploit the superposition property of the wireless channel. The transmitted signals are combined in the air and the receiver gets a superposition plus noise. Since the network coding occurs on the physical layer, we call this kind of network coding PLNC. If the receiver is an intermediate node that will relay a linear combination of the received signals, we call this node a *relay*. A relay can choose among different relaying strategies, including

- *decode-and-forward*, where the relay decodes the individual data and forwards a new linear combination;

- *amplify-and-forward*, where the relay amplifies the received superposition and forwards the signal;
- *compute-and-forward*, where the relay directly decodes a linear combination of the original data.

Using decode-and-forward strategy, a relay decodes just one signal and treats all others as noise. Treating interference as noise reduces the achievable rate.

Compute-and-forward combines the advantages of both: The relay decodes a linear combination of the signal (interference is exploited and not treated as noise) and the noise is removed from the signal (no noise amplification and accumulation). This strategy was first introduced by Nazer et al. in [50].

Channel codes such as Reed-Solomon provide forward error correction (FEC) for communication over noisy channels. A code is a finite set of codewords of length n. The data to be sent is divided into messages from an index set $\{1, \ldots, 2^{nR}\}$, where $R = \frac{q}{n}$ is the code rate, and q is the code dimension (*i.e.*, the message length). After encoding, the codewords get mapped to complex-valued samples using a modulation scheme. However, conventional modulation schemes, such as quadrature amplitude modulation (QAM), are not suitable for compute-and-forward, because the superposition of two modulation points is not necessarily a valid modulation point. For this reason, compute-and-forward uses *nested lattice codes*, which offer the required properties.

In the following, we define a few necessary terms related to nested lattice codes and the compute-and-forward framework. For a more detailed introduction, we refer the reader to [70]. Afterwards, we use an example to illustrate the communication using compute-and-forward based on lattice codes. Lets assume there are K source nodes and M relay nodes.

3.1 Definition (Lattice). A lattice Λ is a subgroup of $\mathbb{C}^n$ which is isomorphic to $\mathbb{Z}^n + j\,\mathbb{Z}^n$. If $\boldsymbol{s}, \boldsymbol{t} \in \Lambda$, then $\boldsymbol{s} + \boldsymbol{t} \in \Lambda$. ◁

3.2 Definition (Nearest Neighbor Quantizer). The nearest neighbor quantizer Q is defined as

$$Q(\boldsymbol{x}) \triangleq \arg\min_{\boldsymbol{\lambda} \in \Lambda} \|\boldsymbol{x} - \boldsymbol{\lambda}\| \ . \tag{3.1}$$

◁

3.3 Definition (Voronoi Region). The fundamental Voronoi region $\mathcal{V}$ of a lattice Λ is the set of all points in $\mathbb{C}^n$ closest to the zero point, that is, $\mathcal{V} = \{\boldsymbol{x} : Q(\boldsymbol{x}) = 0\}$. ◁

3.4 Definition (Quantization Error). The quantization error can be expressed by the modulo-Λ operation with respect to the lattice, which is defined as $\boldsymbol{x} \bmod \Lambda = \boldsymbol{x} - Q(\boldsymbol{x})$.◁

3.5 Definition (Nested Lattice Code). A nested lattice code $\mathcal{NL}$ is the set of all points of a fine lattice Λ_F that are within the fundamental Voronoi region $\mathcal{V}_C$ of a coarse lattice $\Lambda_C \subset \Lambda_F$,

$$\mathcal{NL} = \Lambda_F \cap \mathcal{V}_C = \{\boldsymbol{\lambda} \bmod \Lambda_C,\, \boldsymbol{\lambda} \in \Lambda_F\}\,. \tag{3.2}$$

◁

3.6 Definition (Lattice Encoder). The encoder $\mathcal{E}$ used at source node k maps data messages $d_k \in \mathbb{F}_q$ to lattice codewords $\boldsymbol{x}_k \in \mathcal{NL} \subset \mathbb{C}^n$ such that,

$$\mathcal{E} : \mathbb{F}_q \mapsto \Lambda_F \cap \mathcal{V}_C\,. \tag{3.3}$$

◁

3.7 Definition (Lattice Equation). A lattice equation $\boldsymbol{v}_m$ at relay m is an integral combination of lattice codewords $\boldsymbol{x}_k$ modulo the coarse lattice

$$\boldsymbol{v}_m = \left[\sum_{k=1}^{K} a_{mk}\boldsymbol{x}_k\right] \bmod \Lambda_C \tag{3.4}$$

with $a_{mk} \in \mathbb{Z} + j\,\mathbb{Z}$. We call $\boldsymbol{a}_m = (a_{m1}, \ldots, a_{mK})^T$ the lattice coefficient vector. ◁

Figure 3.2 illustrates encoding, transmission, and decoding of two messages over an AWGN channel using the compute-and-forward approach. Each transmitter encodes its messages by a nested lattice code encoder $\mathcal{E}$; that is, it maps a message $d_k \in \mathbb{F}_q$ to a lattice codeword $\boldsymbol{x}_k \in \mathcal{NL} \subset \mathbb{C}^n$ such that $\mathcal{E}(d_k) = \boldsymbol{x}_k$. This encoding process is equivalent to modulation schemes in classical communication systems. Whereas a classical modulation scheme maps messages to one-dimensional complex-valued samples, a lattice encoder maps messages to n-dimensional complex-valued samples, which are transmitted sequentially.

Receiver m in Figure 3.2 now aims to decode a lattice equation specified by the lattice coefficient vector $\boldsymbol{a}_m$ as in (3.4). Unfortunately, it receives a noisy superposition of the transmitted codewords

$$\boldsymbol{y}_m = \sum_{k=1}^{K} h_{mk}\boldsymbol{x}_k + \boldsymbol{z}_m, \tag{3.5}$$

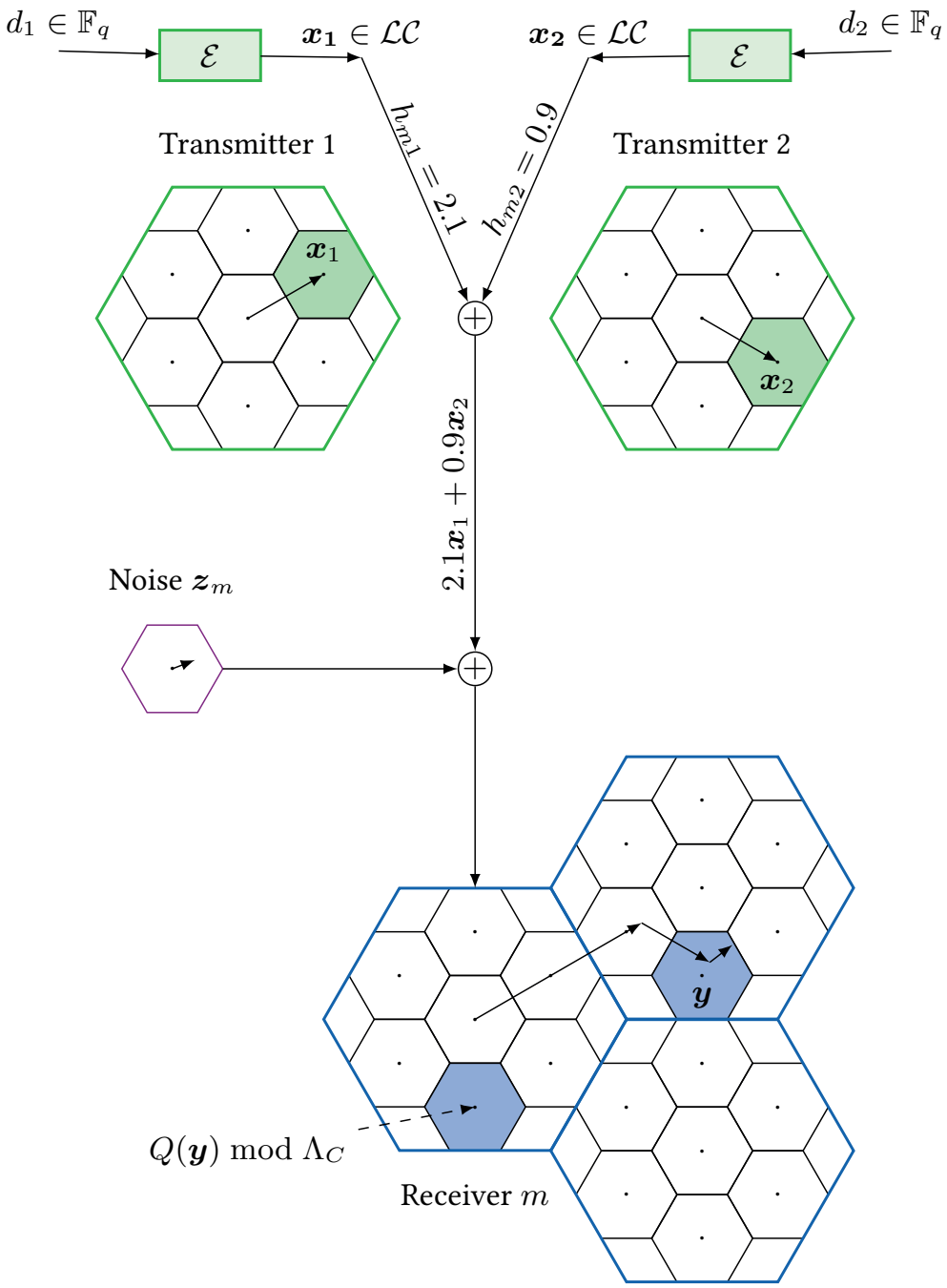

Figure 3.2: Illustration of a compute-and-forward transmission over an additive white Gaussian noise (AWGN) channel using nested lattice codes. Figure is adapted from [71] and [51].

where each transmitted codeword $\boldsymbol{x}_k$ is multiplied by a channel coefficient h_{mk} and summed up. Additionally, a noise vector $\boldsymbol{z}_m$ with $\boldsymbol{z}_m \sim \mathcal{CN}(0, \sigma^2 \boldsymbol{I}_n)$ gets added to the received signal. The channel coefficients are complex values that do not necessarily belong to the set of Gaussian integers, whereas each relay wants to decode a linear combination with coefficients from the set of Gaussian integers. Thus, a receiver must scale the channel output with a factor α_m, such that $\boldsymbol{s}_m = \alpha_m \boldsymbol{y}_m$. The goal of this operation is to scale the received signal such that the channel values become Gaussian integer values. However, there is a trade-off because scaling the received signal also scales the noise. The optimal scaling factor for a desired lattice equation with coefficients $\boldsymbol{a}_m$ is the minimum mean square error (MMSE) coefficient

$$\alpha_m^{MMSE} = \frac{P \boldsymbol{h}_m^H \boldsymbol{a}_m}{\sigma^2 + P \left\| \boldsymbol{h}_m \right\|^2}, \tag{3.6}$$

where $\boldsymbol{h}_m$ is the channel coefficient vector from all sources to relay m. After the scaling operation, the receiver is able to detect a linear combination of the transmitted codewords plus some noise. To get an estimate of the lattice equation $\boldsymbol{v}_m$, vector $\boldsymbol{s}_m$ is quantized onto the fine lattice Λ_F modulo the coarse lattice Λ_C

$$\hat{\boldsymbol{v}}_m = [Q(\boldsymbol{s}_m)] \bmod \Lambda_C. \tag{3.7}$$

If the noise $\boldsymbol{z}_m$ is small enough such that $\boldsymbol{z}_m \in \mathcal{V}_F$, the quantization step removes the noise and the linear combination can be reliably decoded. Since each decoder tries to decode a superposition of codewords, we call the rate at which decoding is done reliably *computation rate*. The achievable computation rate of the compute-and-forward framework is given by

$$\mathcal{R}(\boldsymbol{h}_m, \boldsymbol{a}_m) = \log_2^+ \left(\left(\left\| \boldsymbol{a}_m \right\|^2 - \frac{P |\boldsymbol{h}_m^H \boldsymbol{a}_m|^2}{\sigma^2 + P ||\boldsymbol{h}_m||^2} \right)^{-1} \right) \tag{3.8}$$

with $\log_2^+(x) \triangleq \max\{0, \log_2(x)\}$. This means all relays can simultaneously decode equations with coefficients $\boldsymbol{a}_m$ as long as the message rates are within the computation rate region

$$R_k < \min_{a_{mk}} \mathcal{R}(\boldsymbol{h}_m, \boldsymbol{a}_m). \tag{3.9}$$

3.3 Multi-flow Glossy (MF-Glossy)

We now present MF-Glossy, a many-to-all communication scheme that exploits PLNC based on compute-and-forward to simultaneously flood $2 \leq K \leq V - 1$ different packets (or *flows*) from K different sources to all V nodes in a multi-hop wireless network. The source nodes initiate the flood by concurrently transmitting their packets at the same source rate R. Afterward, each node follows the operating steps shown in Algorithm 1 until it reaches the re-transmission limit N. In essence, MF-Glossy inserts steps 2–6 of Algorithm 1 between the Rx and Tx phases of state-of-the-art Glossy as shown in Figure 2.2.

Figure 3.3 shows an example with $K = 2$ packets injected by source nodes N_1 and N_2; the re-transmission limit is $N = 2$. For simplicity, we focus on nodes N_1–N_4, which may in fact be part of a larger wireless multi-hop network.

In the first time slot (see Figure 3.3a), nodes N_1 and N_2 simultaneously transmit two different packets A and B, which are encoded using lattice codes. Due to the broadcast nature of the wireless channel, nodes N_3 and N_4 receive a superposition of the transmitted signals and each decode a linear combination of the source packets ($a_1A + a_2B$ and $a_3A + a_4B$, respectively) as explained in steps 3 and 4 of Algorithm 1.

In the second time slot (see Figure 3.3b), N_3 and N_4 transmit an encoded linear combination as explained in steps 6 and 7 of Algorithm 1, which are received and decoded by nodes N_1 and N_2. According to step 5 in Algorithm 1, because nodes N_1 and N_2 have acquired $K = 2$ independent linear combinations, they can already retrieve the two source packets A and B.

In the third time slot (see Figure 3.3c), N_1 and N_2 transmit again linear combinations $a_5A + a_6B$ and $a_7A + a_8B$ of packets A and B, since they have not yet reached the re-transmission limit $N = 2$. Nodes N_3 and N_4 receive and decode linear combinations of the transmitted linear combinations. Assuming that the newly received linear combinations are independent of the previously received linear combinations, they can now retrieve packets A and B.

Algorithm 1 Key operating steps of a node in MF-Glossy

1: **while** re-transmission counter $\leq$ re-transmission limit N **do**

2: **Wait for incoming signal.** Listen to the channel waiting for a transmitted signal to be detected.

3: **Receive signal.** When a signal is detected, receive it and verify successful reception by checking that there exists a coefficient vector $\boldsymbol{a}$ for which the achievable rate $\mathcal{R}(\tilde{\boldsymbol{h}}, \boldsymbol{a})$ is greater than or equal to the source rate R, $\mathcal{R}(\tilde{\boldsymbol{h}}, \boldsymbol{a}) \geq R$, where $\mathcal{R}(\tilde{\boldsymbol{h}}, \boldsymbol{a})$ is given by (3.8). If the rate condition is not satisfied, reception is unsuccessful and the node goes back to 2.

4: **Decode signal.** After successful signal reception, decode and store any linear combination of source packets with associated coefficient vector $\boldsymbol{a}$ for which $\mathcal{R}^*(\tilde{\boldsymbol{h}}, \boldsymbol{a}) \geq R$. The decoding maps each coefficient vector to the corresponding lattice point.

5: **Rank check.** Check if the rank of the coding coefficient matrix is at least K. If so, retrieve the K source packets.

6: **Encode signal.** Choose and encode one linear combination to be transmitted provided it is linearly independent on previously transmitted linear combinations. The encoding process maps each linear combination to the closest lattice point.

7: **Transmit signal.** Transmit the corresponding signal and increment the re-transmission counter.

8: **end while**

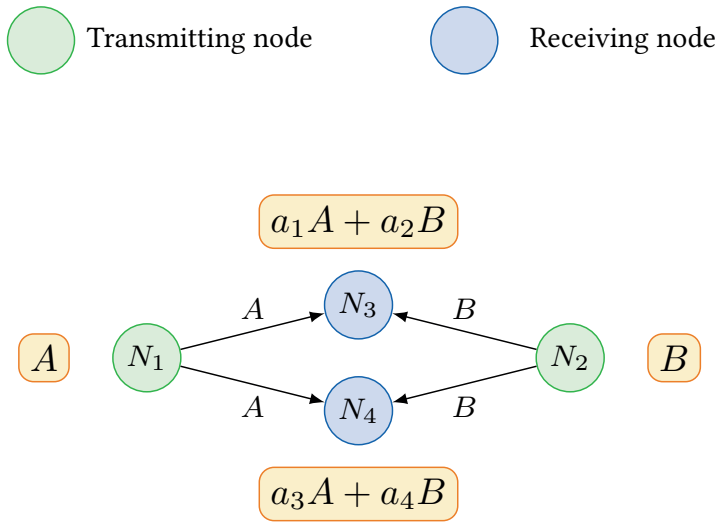

(a) Time slot 1: Nodes N_1 and N_2 initiate the flood by simultaneously transmitting different source packets A and B. N_3 and N_4 receive and decode linear combinations a_1A+a_2B and a_3A+a_4B, respectively.

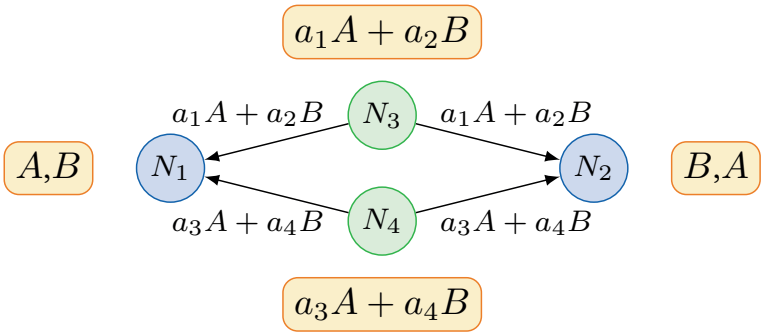

(b) Time slot 2: Nodes N_3 and N_4 encode and transmit their respective linear combinations. N_1 and N_2 receive and decode linear combinations, allowing them to retrieve the source packets A and B.

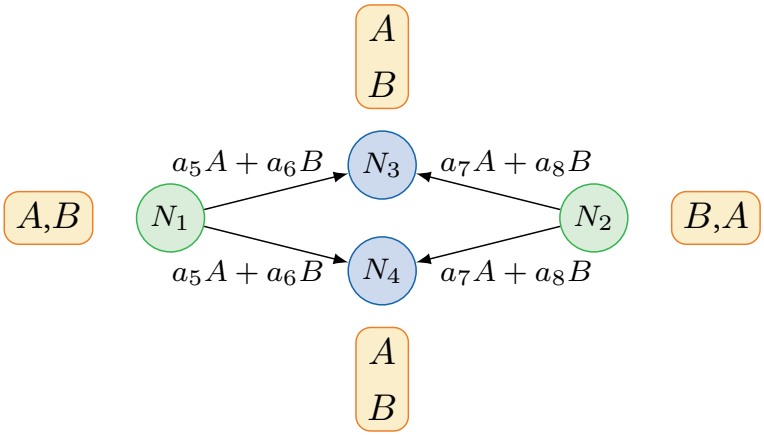

(c) Time slot 3: Nodes N_1 and N_2 transmit again a linear combination of packets A and B, *i.e.*, a_5A+a_6B and a_7A+a_8B, respectively. N_3 and N_4 receive and decode new linear combinations. Assuming these are linearly independent on their previously received linear combinations, they can now also retrieve the source packets A and B.

Figure 3.3: Example illustrating the operation of MF-Glossy with $K = 2$ source packets injected by nodes N_1 and N_2; the re-transmission limit is $N = 2$. This illustration shows only the communication among nodes N_1–N_4 in a 2-hop network, which may in fact be part of a much larger multi-hop wireless network.

(a) Point-to-point channel.

(b) Multiple-access channel.

Figure 3.4: The two basic cases in our communication-theoretic analysis.

3.4 Communication-theoretic Analysis

In this section, we derive bounds on the outage probability (*i.e.*, packet loss rate) of Glossy and MF-Glossy These bounds provide valuable insights on the theoretically possible goodput of Glossy and MF-Glossy, and thus allow us to quantitatively compare both schemes independent of the implementation.

3.4.1 Glossy

To derive the outage probability of Glossy, we decompose a full flood. At the start of a flood, there is one node sending to one or several nodes (see Figure 2.2), which can be modeled as point-to-point channels as depicted in Figure 3.4a. During the flood, instead, multiple nodes broadcast their data to their neighbors: one node receives from several transmitting nodes (see Figure 2.2). This can be modeled as multiple-access channels as depicted in Figure 3.4b.

Point-to-point channel (P2P)

We start with the point-to-point channel shown in Figure 3.4a. Node S transmits a signal $\boldsymbol{x}$ at rate R and node D receives the signal $\boldsymbol{y} = \boldsymbol{x}h + \boldsymbol{z}$, where $\boldsymbol{z}$ is AWGN with $\boldsymbol{z} \sim \mathcal{CN}(0, \sigma^2\mathcal{I}^n)$ and $h \in \mathbb{C}$ is the channel gain. The channels for low-power wireless devices are typically slow-fading channels (*i.e.*, they can be considered constant over the block length). The maximum achievable rate over this channel is upper bounded by its capacity, which is given by [72, Chapter 2]

$$C_{\text{P2P}} = \log_2\left(1 + \frac{|h|^2 P}{\sigma^2}\right), \tag{3.10}$$

where $P = \mathrm{E}[\boldsymbol{x}^2]$ is the average transmit power of node S. If S sends at a rate higher than the channel capacity, the reception is not error-free and outage occurs. Hence, the outage

probability (*i.e.*, packet loss rate) is given by $\Pr(C_{\text{P2P}} < R)$ [73].

Multiple-access channel (MA)

We turn to the multiple-access case shown in Figure 3.4b. Each node S_k with $k \in \{1, 2, \ldots, K\}$ simultaneously transmits a signal $\boldsymbol{x}_k$ at rate R to node D.

$$\boldsymbol{y} = \sum_{k=1}^{K} \boldsymbol{x}_k h_k + \boldsymbol{z}\,, \tag{3.11}$$

where $h_m \in \mathbb{C}$ is the channel gain between S_k and D. In Glossy, all nodes send the same signal, so $\boldsymbol{x}_1 = \cdots = \boldsymbol{x}_K$.

If the transmitters have no channel state information, the maximum achievable rate R_{MA} is the maximum rate at which node D can successfully receive all data transmitted by nodes $S_1, S_2, \ldots, S_K$. This rate is given by [74]

$$R_{\text{MA}} = \log\left(1 + \frac{|\sum_{k=1}^{M} h_k \sqrt{P_k}|^2}{\sigma^2}\right)\,, \tag{3.12}$$

where $P_k = \mathrm{E}[|\boldsymbol{x}_k|^2]$ is the average transmit power of node S_k. The corresponding outage probability is $\Pr(R_{\text{MA}} < R)$.

3.4.2 MF-Glossy

In MF-Glossy, the point-to-point channel model is valid as derived above. However, the multiple-access channel model changes, because node D decodes a superposition of the signals instead of the individual signals. We assume that there are K flows during a flood, that is, K nodes initiated a flood, whereas each node k with $k \in \{1, 2, \ldots, K\}$ sent a data packet $\boldsymbol{d}_k$. Using the notation in Figure 3.5, we assume that each relay node RL_m transmits a linear combination $\boldsymbol{x}_m = \sum_{k=1}^{K} a_{mk}\boldsymbol{d}_k$ of the data packets $\boldsymbol{d}_k$. Receiver node D receives the signal

$$\boldsymbol{y} = \sum_{m=1}^{M} h_m \boldsymbol{x}_m + \boldsymbol{z} = \sum_{m=1}^{M} h_m \left(\sum_{k=1}^{K} a_{mk}\boldsymbol{d}_k\right) + \boldsymbol{z} \tag{3.13a}$$

$$= \sum_{m=1}^{M}\sum_{k=1}^{K} h_m a_{mk}\boldsymbol{d}_k + \boldsymbol{z} = \sum_{k=1}^{K} \boldsymbol{d}_k \sum_{m=1}^{M} h_m a_{mk} + \boldsymbol{z} \tag{3.13b}$$

$$= \sum_{k=1}^{K} \tilde{h}_k \boldsymbol{d}_k + \boldsymbol{z}\,, \tag{3.13c}$$

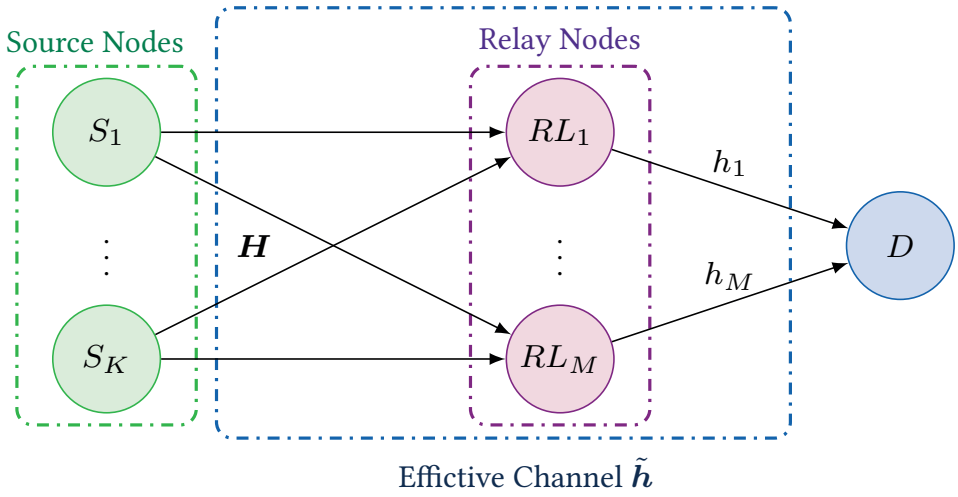

Figure 3.5: System model of general relay networks with K source nodes, M relay nodes and 1 destination node. Matrix $\boldsymbol{H}$ represents the channel gains from the source nodes to the relay nodes and has the size $K \times M$. Vector $\tilde{\boldsymbol{h}} = [\tilde{h}_1, \ldots, \tilde{h}_K]$ represent the effective channel gain from the source nodes to the destination node passing through the relay nodes.

where $\tilde{h}_k = \sum_{m=1}^{M} h_m a_{mk}$ is the effective channel from source node k to destination node D passing through all M relay nodes. The maximum achievable rate for decoding a linear combination $\boldsymbol{a}_D$ (compute-and-forward coefficient vector at node D) of the data packets $\boldsymbol{d}_k$ follows from (3.8) and is given by $\mathcal{R}(\tilde{\boldsymbol{h}}, \boldsymbol{a}_D)$. The outage probability (*i.e.*, packet loss rate) is $\Pr(\mathcal{R}(\tilde{\boldsymbol{h}}, \boldsymbol{a}_D) < R)$.

All coefficient vectors $\boldsymbol{a}_D$ for which $\mathcal{R}(\tilde{\boldsymbol{h}}, \boldsymbol{a}_D)$ is greater than or equal to the transmit rate R are used for decoding and stored. If a node cannot find a coefficient vector that satisfies the rate condition, the reception is considered unsuccessful and the node goes back to the listening state. In order to maximize the benefits of each transmission, each node only transmits a linear combination with a coefficient vector if this vector is linearly independent of previously transmitted vectors. As soon as K linearly independent coefficient vectors are acquired by a node, the source packets are decoded at this specific node. The resulting outage probability at node D for the entire flood is the probability that node D acquires less than K linearly independent combinations of the original data packets $\boldsymbol{d}_k$, which is unlikely to happen due to the random nature of Gaussian channels.

3.5 Evaluation Settings and Metrics

We present in this section the settings used in the system level simulations including network topology, transmission parameters, channel model and compared simulation scenarios. Moreover, we define performance metrics that we use later in comparing Glossy and MF-Glossy in Section 3.6.

Network topology

We generate network topologies using a binomial point process with λ nodes randomly and independently placed in a square of side length L. We vary λ and L to study their impact on performance; our results are averaged over 10,000 independent realizations for the same λ and L.

Transmission parameters

Irrespective of the network topology, all nodes transmit with rate $R = 250\,\text{kbps}$ and a power of 0 dBm, which correspond to the maximum settings as prescribed by the IEEE 802.15.4 standard.

Channel model

We model the channel gains h_i as stationary independent according to $h_i = w_i\, g_i$, such that small-scale fading w_i follows a complex normal distribution $\mathcal{CN}(0,1)$, and large-scale fading g_i depends on the distance d between transmitter and receiver [5, E 5.3] as follows:

$$g_i = \begin{cases} 40.2 + 20\log(d)\,, & d \leq 8\,\text{m}\,, \\ 58.5 + 33\log(d/8)\,, & d > 8\,\text{m}\,. \end{cases} \tag{3.14}$$

This corresponds to a path loss exponent of 2 for the first 8 m and a path loss exponent of 3.3 for distances larger than 8 m. To ensure $g_i > 0$ according to (3.14), we consider only topologies where the distance between any pair of nodes exceeds 0.1 m, which is reasonable in real deployments [75].

Compared schemes

We compare our proposed MF-Glossy against state-of-the-art Glossy. To do so in a fair manner for $K \geq 2$ flows, using Glossy, we consider K successive floods initiated by K different randomly selected nodes; our results for Glossy refer to these K successive floods as a whole. We set the re-transmission limit of Glossy to $N = 3$ based on experience from extensive real-world experiments [6, 7], and use $N = 6$ for MF-Glossy. We study the impact of N on the performance of both schemes in dedicated simulation runs.

Performance metrics

We consider the following performance metrics of real-world applications[17]:

- *Packet reception ratio (PRR)*: The number of nodes that correctly receive (or decode, in case of MF-Glossy) all packets divided by the total number of nodes in the network λ.
- *Latency*: The time from the start of the flood until a node correctly receives (decodes) all packets, averaged over all nodes in the network. Given a certain packet size, the duration of a single slot during a Glossy flood is a network-wide constant [6]. We compute latency of Glossy and MF-Glossy for 8-byte packets, purposely ignoring the overhead of the de- and encoding in MF-Glossy to get an upper bound on the theoretically possible performance gains. As result, varying the packet size has no impact on the relative performance between MF-Glossy and Glossy in our simulations. We evaluate and discuss MF-Glossy's overhead in Section 3.7 using dedicated experiments.
- *Global energy consumption*: The total energy consumed by all λ nodes for communication between the start and the end of a MF-Glossy flood or K consecutive Glossy floods. To compute energy consumption, we take the current draws from the data sheet of the widely used CC2420 radio chip in states transmit, receive, listening, and idle, assuming batteries constantly supply 2000 mAh at 3 V. We consider a node to be idle only when its radio is turned off after reaching its re-transmission limit N.
- *Goodput*: The average amount of data a node receives (or decodes) successfully per time unit. Formally, we calculate goodput as follows:

$$\text{Goodput} = \frac{PRR \times 64 \times K}{Latency}, \tag{3.15}$$

where 64 is the number of bits in a single packet. In other words, goodput is a measure of the level of "service" provided, while energy measures the associated "cost."

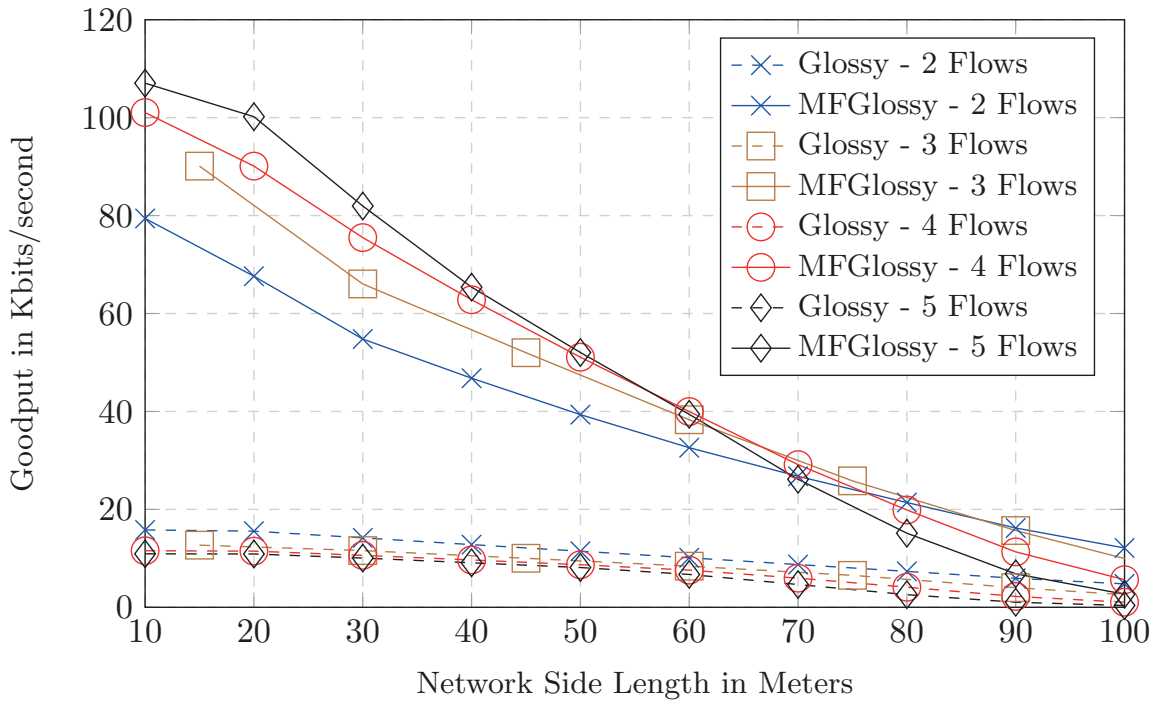

Figure 3.6: Impact of the number of flows and network side length in a 50-node network on the goodput of MF-Glossy and Glossy.

3.6 Results and Discussion

We use the models from Section 3.4 to evaluate and compare the performance of MF-Glossy and Glossy in simplified system level simulations according to the settings and metrics defined in Section 3.5.

3.6.1 Goodput

Figure 3.6 shows goodput of MF-Glossy and Glossy against network side length for 50 nodes and different number of flows. We see that by serving multiple flows within the same flood MF-Glossy achieves several-fold improvements over Glossy across a wide range of network side lengths (*i.e.*, node densities). Using more flows K benefits MF-Glossy up to a network wide length of about 60 m, while Glossy generally suffers as K increases. We also see that the decrease in goodput for MF-Glossy becomes steeper for larger K till we reach crossing points that tell us exactly which value of K to use for a given network size. Figure 3.7 shows goodput against network side length for $K = 3$ flows and different number of nodes. Again, we see that MF-Glossy is particularly good at leveraging a higher

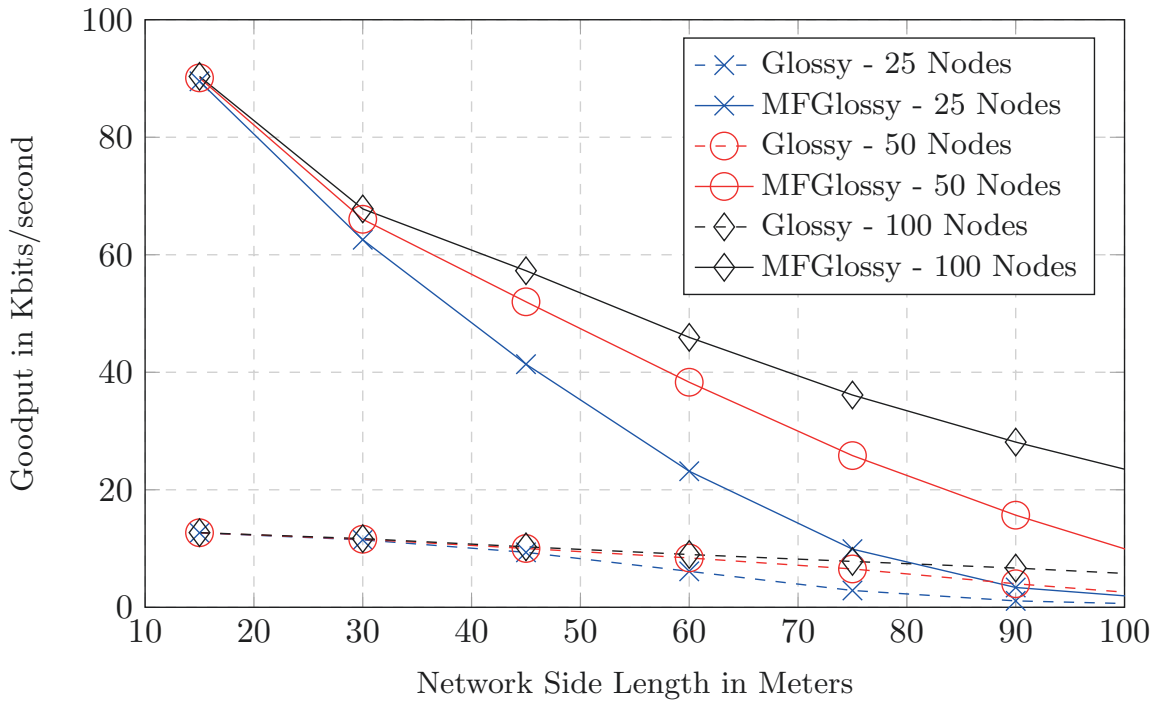

Figure 3.7: Impact of the number of nodes and network side length for 3 flows on the goodput of MF-Glossy and Glossy.

node density to boost goodput, which confirms the trend we observed before in Figure 3.6.

3.6.2 Latency and PRR

To understand the goodput results, we look at latency and PRR as a function of network side length for 50 nodes and different number of flows. Looking at Figure 3.8, we see that the latency of Glossy increases linearly and significantly with the number of flows, because each flow is mapped onto a single independent flood. MF-Glossy, instead, accommodates multiple flows in the same flood, which comes only at a slight increase in latency per flow. As a result, for 5 flows, MF-Glossy reduces latency by about $9\times$ compared with Glossy. Note that the comparison in Figure 3.8 is fair only when considering the same number of flows K.

Looking at Figure 3.9, we observe a faster decay in PRR as the number of flows increases. This is expected because, intuitively, delivering, say, 5 packets successfully is more difficult than delivering only 4 packets successfully. Nevertheless, by increasing the re-transmission limit N, it is possible to boost the PRR of MF-Glossy at the expense of a higher latency.

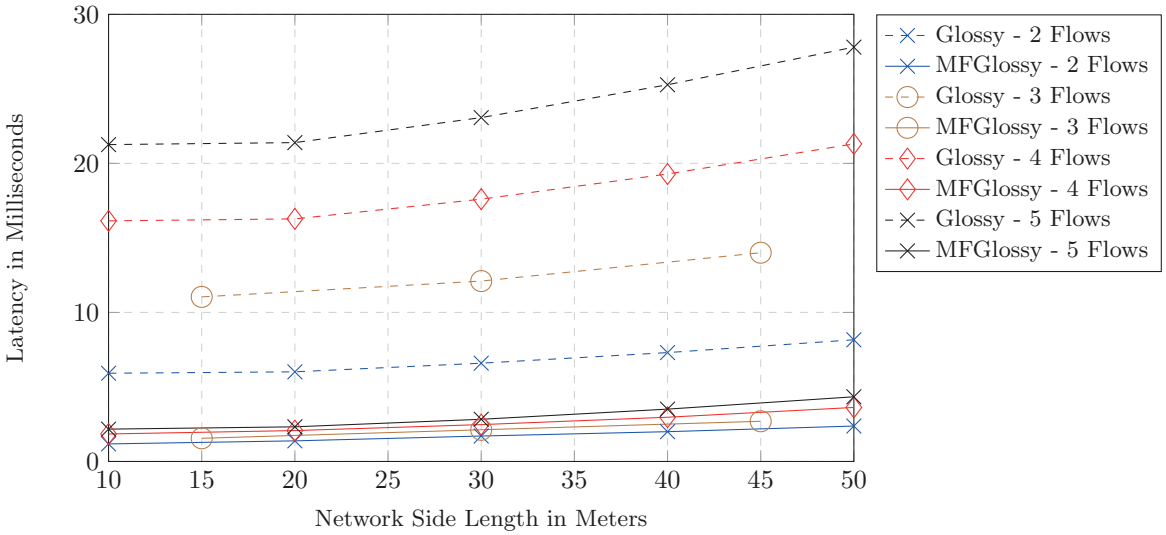

Figure 3.8: Latency of MF-Glossy and Glossy against network side length for 50 nodes and different number of flows.

3.6.3 Goodput vs. energy

Having examined the factors impacting the level of "service" provided by MF-Glossy and Glossy, we now relate this to the associated "costs." To this end, we plot in Figure 3.10 goodput against global energy consumption for different number of flows K and re-transmission limits N, considering a 50-node network that is 60 m $\times$ 60 m in size.

We see that MF-Glossy provides a significantly better trade-off than Glossy: MF-Glossy always provides higher goodput or reduced energy consumption without impairing the other metric in comparison to Glossy. Moreover, we find that for a given number of flows K there exists a distinct setting for the re-transmission limit N that maximizes goodput. Increasing N beyond this point helps PRR, yet this improvement cannot counter the effect of increased latency, thus ultimately resulting in lower goodput and higher energy consumption.

We also see that using more flows K increases the goodput of MF-Glossy, but the relative improvements become smaller and smaller for higher K. Based on the network characteristics and application requirements at hand, users can decide on the best parameter setting (*e.g.*, N and K), thereby trading higher (lower) goodput for higher (lower) energy consumption.

We see that there exists an optimum setting for N that maximizes goodput while minimizing energy consumption, which we call *Pareto-optimal*. This Pareto-optimal point dif-

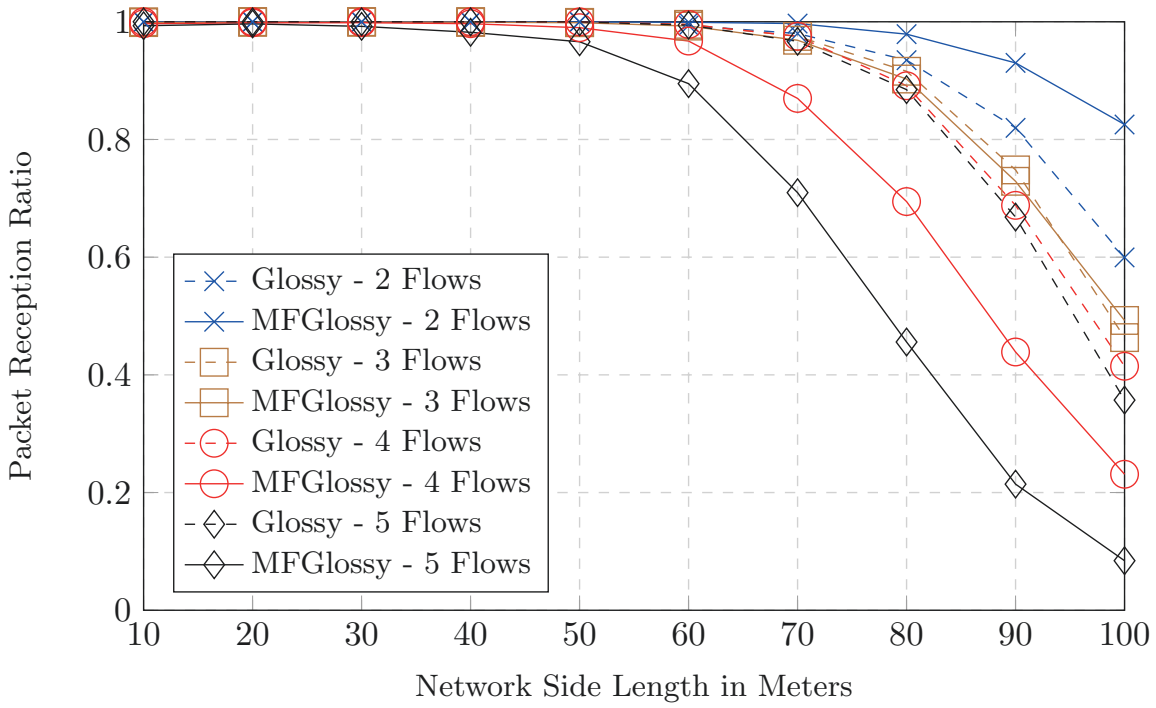

Figure 3.9: PRR of MF-Glossy and Glossy against network side length for 50 nodes and different number of flows.

fers between different values of K as well as network scenarios. For the scenario considered in our discussion in Figure 3.10 we can calculate that for $K = 2, 3$ and 4, the Pareto-optimum values for N are $3, 4$ and 5 respectively. Increasing N beyond the Pareto-optimal point will result in higher PRR but not high enough to counter the effect of increased latency, therefor resulting in a slight degrade of performance while consuming even more energy. By using the same approach, we are able to optimize settings for MF-Glossy in any network scenario to maximize goodput and minimize energy consumption. We also note that by using MF-Glossy we are not only achieving higher goodput than Glossy, but we are doing it with lower energy consumption.

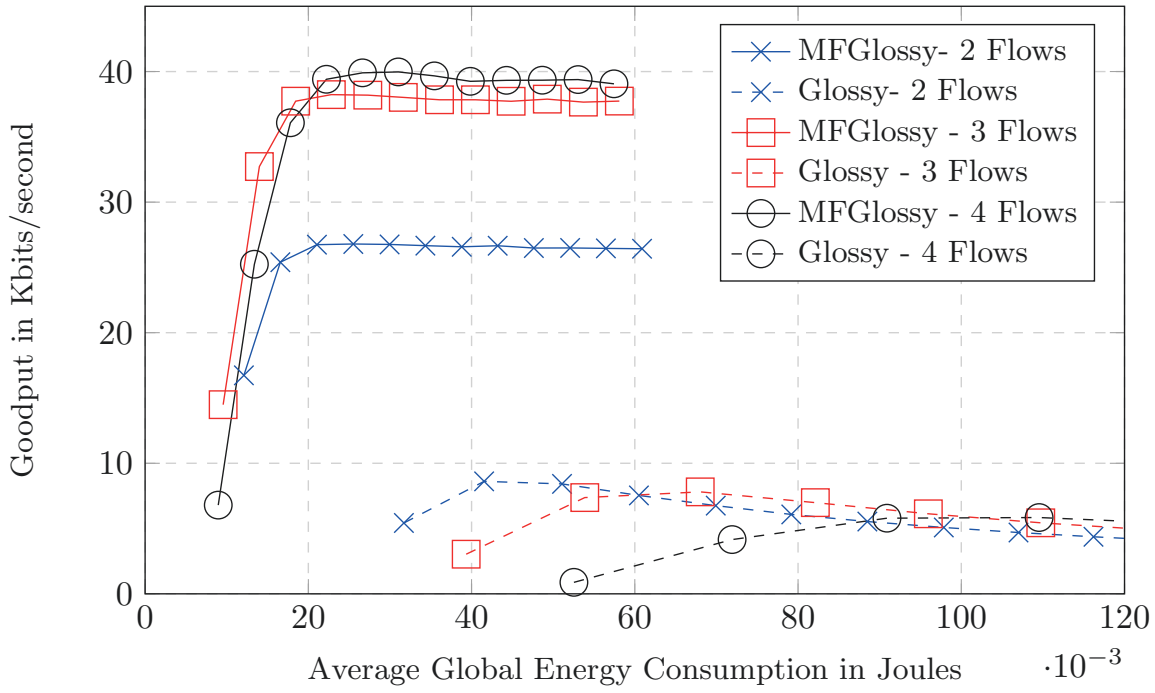

Figure 3.10: Trade-off between goodput and global energy consumption in MF-Glossy and Glossy for different number of flows and re-transmission limits, in a network that consists of 50 nodes and is 60 m $\times$ 60 m in size.

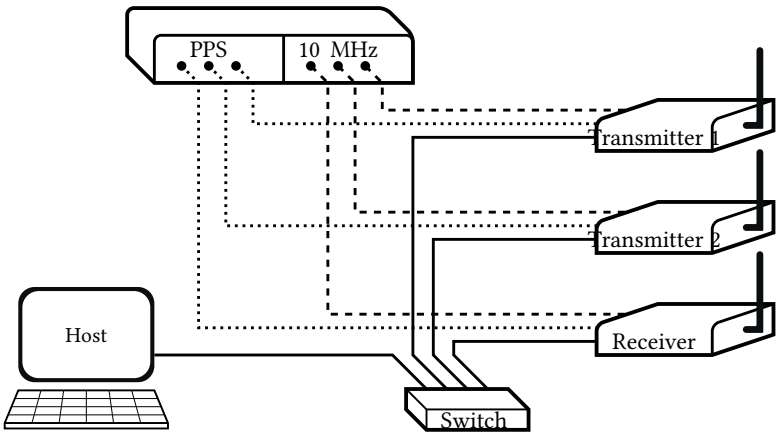

Figure 3.11: Hardware setup used in the first implementation of compute-and-forward using nested lattice codes as presented in [51].

3.7 Challenges of Hardware Implementation

MF-Glossy uses the compute-and-forward framework based on nested lattice codes. We report here on the first implementations of this framework on real hardware, thus demonstrating that the key concept underlying MF-Glossy is indeed implementable. We also highlight the main challenges in the way of using MF-Glossy on embedded, resource-constrained devices and suggest possible solutions.

PLNC Implementation based on [51]

Three USRP N210 SDRs are used in [51], such that two act as transmitters and one act as a receiver, as shown in Figure 3.11. This setup corresponds to what happens during the first time slot of a MF-Glossy flood with $K = 2$ sources. The SDRs are time-synchronized by a 10 MHz signal as well as a pulse per second (PPS) signal. A host PC, which features an Intel i5 processor, interacts with the three SDRs via a switch over Ethernet and manages all computations.

GNU radio [76] is used to implement the interaction between the host PC and the three SDRs, and SageMath [77] to implement the encoding and decoding on the host. In addition to the lattice code, Reed-Solomon code is used for forward error correction. GNU radio as well as SageMath are general open-source frameworks, and hence do not provide optimized algorithms for our peculiar lattice encoding and decoding operations. Nevertheless, this implementation provides a benchmark that allows the evaluation of the compute-and-forward framework performance in a practical setting.

To this end, the two transmitters are allowed to simultaneously send two different 19 kB files. After encoding both files on the host, this triggers 80 simultaneous transmissions of 235-byte data frames by the two transmitters. The receiver forwards received signals to the host, that performs the decoding.

Results of the expirments performed in [51] reported the following results:

- All data frames were correctly decoded.
- 2.4 ms and 5.3 ms were measured for encoding and decoding one byte, respectively.

Challenges and solutions

After including the processing overheads presented in the aforementioned implementation in our simulations, we get, for example, a latency of 241 ms for 5 flows with MF-Glossy in a 50-node network with a side length of 45 m (see Figure 3.8). Therefore, about 10× faster encoding and decoding are required for MF-Glossy to be faster than Glossy, which has a latency of 28 ms for this network configuration. Therefore, it is clear that the biggest obstacle in the way of an efficient implementation of MF-Glossy is that encoding and decoding take a significant amount of time. Nevertheless, a very large part is spent in methods that just provide data models for finite fields, vector and matrix arithmetic, etc. Significant speedups are possible by using optimized libraries for these operations (*e.g.*, [78]). Further, it is possible to optimize the algorithms for the modulo operation of a certain lattice. Since the modulo operation is costly and frequently used, optimizing it will bring a significant performance boost. In standardized protocols, there is typically a finite set of modulation and coding schemes from which the nodes choose depending on certain system parameters. The same holds for lattice codes. One can design a set of good lattices with optimized algorithms from which the nodes choose one. A practical implementation of a lattice encoder and decoder is presented in [79] on SDR hardware, where the implementation takes into account the channel misalignment between distributed nodes resulting from hardware impairments. The algorithm requires very low-overhead feedback to align the channels of superposing signals. A lattice shaping method is also proposed in order to reduce computations in decoding operations based on low-density lattice codes (LDLC)[66] and lattice code word power control. Moreover, efficient algorithms exist to compute the coding coefficients [80] and to map the receive vector to a valid lattice point [81], which we exploited only partially. Thus, we believe an implementation on embedded devices is indeed possible, especially in light of the trend towards more powerful, yet highly energy-efficient 32-bit micro-controllers with rich instructions sets (*e.g.*, ARM Cortex-M series).

A second challenge is time and frequency synchronization of the distributed nodes. The compute-and-forward framework requires and assumes perfect synchronization, yet we only discuss its feasibility in practice based on SDR implementations. Therefore, an important question must be answered; How large can the delays and offsets among nodes (without dedicated synchronization hardware) can be without greatly affecting performance? On the other hand, Glossy is able to provide sub-micro second time synchronization between nodes. However, this is a result of the deterministic and identical processing delay at all nodes, which will change when lattice encoding and decoding operations are introduced at the nodes. Therefore, the processing delay must be kept deterministic and constant across all nodes to keep the inherit time synchronization of original Glossy.

3.8 Conclusions

In this chapter, we have explored the opportunities and challenges of using PLNC to enable the simultaneous flooding of different packets from different sources to all nodes in the network. We thus introduced MF-Glossy and performed a communication-theoretic analysis of Glossy and MF-Glossy to determine upper bounds on their performance. Simulation results showed that MF-Glossy has the potential to achieve several-fold improvements in goodput and latency at lower energy costs and comparable packet reception rates. Based on several actual implementations of PLNC using lattice codes on SDRs, we demonstrated that our protocol design is indeed implementable. Our work thus represents the first step towards utilizing PLNC in embedded wireless networks, and shows its potential—a potential that, if harvested efficiently, can result in huge performance gains and resource savings.

Part III

Power Control and Transmit Beamforming

Chapter 4

Beamforming with Perfect CSI

In this chapter, we consider a device-to-device wireless multi-hop communication scenario with resource-constrained devices that require energy-efficient connectivity. Based on the recently proposed Glossy network flooding protocol presented in Section 2.4, we develop power control algorithms that utilize multi-cast beamforming in order to cooperatively flood the same information to all nodes in the network. Hence, improving energy efficiency while conserving the many other merits of Glossy.

4.1 Motivation and Contribution

The energy efficiency of a sensor node is strongly affected by the energy consumption in the radio transceiver. Glossy takes advantage of the embedded sub-micro-second time synchronization between nodes in order to achieve very small radio active times (Radio On time) and save energy. However, it employs no power control, no cooperation and more importantly, no spatial processing schemes such as distributed beamforming. Therefore, the total energy consumption of the network increases linearly with increasing number of nodes in a network and results in excess energy consumption and degraded energy efficiency. This is sub-optimal for the long-term operation of sensor networks (*e.g.*, in monitoring applications [16]) that need energy conservation to assist in elongating their battery life. To this end, we explore possible advantages of using power control schemes to more efficiently manage network resources and achieve higher energy efficiency in state-of-the-art Glossy.

4.1.1 Contributions and structure

In [43], *Sparkle* is proposed, a novel WSN protocol for control operations. In *Sparkle*, transmission power control is applied to Glossy to optimize end-to-end flows by performing

control on the flow. It uses topology control methods to map the best route from the source to the destination node. Then, it chooses transmission powers empirically at each intermediate node in order to save energy and satisfy application specific reliability and latency constraints. Experiments performed on two different test-beds show the following results:

- On one hand, using a single path from the source node to the destination node severely damages reliability, which shows the advantage of using concurrent transmissions in improving reliability of communication.
- On the other hand, having all nodes participate with maximum transmit power in the flood may also decrease reliability.
- Latency decreases when the number of participating nodes in the flood is moderately limited compared to all nodes transmitting at maximum or minimum power.
- Energy consumption is decreased significantly when the number of participating nodes in the flood is moderately limited compared to all nodes transmitting at maximum or minimum power.

All in all, *Sparkle* presents the first effort to use power control with Glossy in order to achieve better energy efficiency. However, the results presented are purely empirical and solely based on experimental trials. Values for transmission powers used are set arbitrary in different modes and iterated until a proper mode is found. This calls for a more theoretically formulated approach to the use of power control with state-of-the-art Glossy. To this end, this chapter contributes the following:

- We introduce an elaborate theoretic system model formalizing the communication phases in Glossy including the multi-cast and general multi-cast channels.
- Assuming a centralized decision approach and availability of perfect CSI, we formulate the problem of centralized power control and beamforming in Glossy as a convex optimization problem and provide a solution to the relaxed approximation of the problem.
- Assuming a distributed decision approach and availability of perfect local CSI, we formulate the problem of distributed power control and beamforming in Glossy as a list of independent individual problems and provide a solution to each one of them.

- We compare the proposed approaches in terms of their energy efficiency to the standard Glossy through numerical simulations across a wide spectrum of network configurations at comparable packet reception rates.

Our numerical simulations show that a centralized power control scheme can achieve several-fold improvements in energy efficiency over Glossy. They also demonstrate that distributed power control promises significant gain in energy efficiency compared to standard Glossy in specific operation scenarios. Results tell us that careful network planning is required when choosing between no power control (as in Glossy) and distributed power control, which agrees with the findings presented in [43].

After presenting related works on power control and transmit beamforming methods in Section 4.2, we present in Section 4.3 a communication-theoretic system model, of the communication phases of state-of-the-art Glossy. Then, in Section 4.4, we explore and compare different power control and beamforming schemes with respect to their energy efficiency. First, we consider a centralized approach in Section 4.4.1, where a single arbitrator has full network topology and network-wide channel state information, and is thus able to make global resource allocating decisions, which we consider to be the upper bound on the achievable performance. Then, we propose a distributed power control and beamforming scheme in Section 4.4.2, comparing it against both the centralized approach and standard Glossy in Section 4.6. Finally, we present some concluding remarks in Section 4.7.

4.2 Power Control and Beamforming

The problem of optimizing transmission power in wireless communications has received a lot of attention due to its potential in allocating resources more efficiently [82]. A set of nodes that simultaneously transmit the same information can be regarded as a virtual antenna array [83]. Hence, accurately choosing the transmit power of each node can be seen as focusing available transmit energy in specific directions or a form of beamforming. Moreover, this introduces spatial diversity, which can improve performance and increase received signal strength at receiving nodes [28]. The performance of different power control algorithms is studied in [84], where bounds and stability conditions for the studied algorithms are presented. Transmit power optimization for the MISO multi-cast channel is studied in [85], and the joint transmit beamforming for the dissemination of common information is studied in [86], where a problem formulation is proposed to minimize transmit power under multiple-rate constraints. This problem is shown to be *NP*-hard. However, an approximate solution can be devised using relaxation methods [87]. An overview of

convex optimization techniques applied to beamforming is presented in [88], where it is made clear that convex optimization allows the formulation of complex beamforming design problems. In [89] the challenges of distributed transmit beamforming are investigated, where two or more transmitters simultaneously send a common message while controlling their power and phase such that the message is successfully received and decoded at a certain receiving node. Several proof-of-concept prototypes are discussed, and their results are summarized. Significant gains in energy efficiency achieved by using distributed transmit beamforming are accompanied by a trade-off against implementation complexity and overhead [90].

4.3 System Model

In order to formulate our power control and beamforming problem, we introduce our communication-theoretic system model and derive expressions for the outage probability of different transmission cases in Glossy. Then, we present the quality of service (QoS) constraints on the achievable rate, which we then use as constraints in our optimization problems.

4.3.1 Outage Probability

To derive the outage probability, we must separate the different fundamental transmission cases happening within one flood. At the start of a flood, there is one node sending to one or several other nodes. This communication can be modeled as a multi-cast channel consisting of L point-to-point links as depicted in Figure 4.1a. During the flood, instead, multiple nodes simultaneously transmit the same data to their neighbors and each node in receiving mode receives from several transmitting nodes. This communication can be modeled as a general multi-cast channel with M transmitters as demonstrated in Figure 4.1b, which can be further broken down into L multiple-input-single-output (MISO) channels.

Multi-cast channel

We start with the multi-cast channel shown in Figure 4.1a. Node S transmits a signal $\boldsymbol{x}$ at rate R and nodes $D_1, ..D_l, ..D_L$ receive the signal $\boldsymbol{y}_l = \boldsymbol{x}h_l + \boldsymbol{z}_l$, where $\boldsymbol{z}_l$ is AWGN with $\boldsymbol{z} \sim \mathcal{CN}(0, \sigma^2\mathcal{I}^n)$, and $h_l \in \mathbb{C}$ is the complex channel gain from transmitter S to receiver D_l. The channels for low-power wireless devices can be assumed quasi-static, independent, and experience flat-fading on the block length, which is a valid assumption

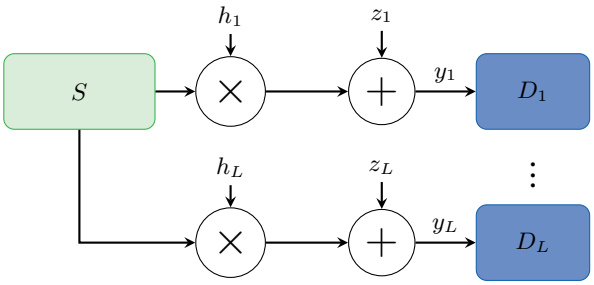

(a) Multi-cast channel consisting of L point-to-point links. Such is the case at the start of any Glossy flood.

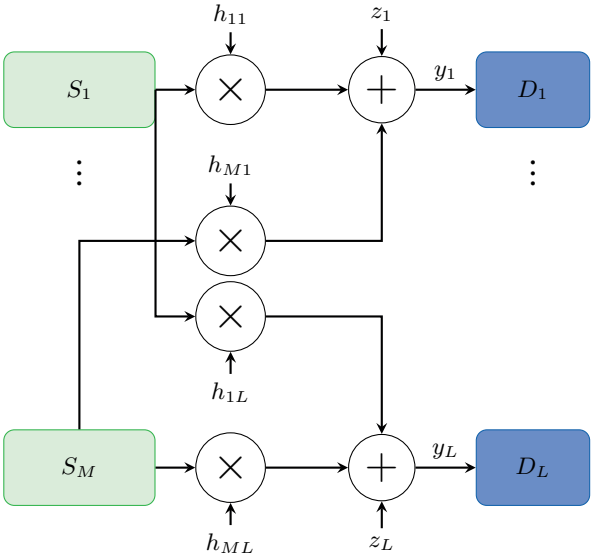

(b) General multi-cast channel (M transmitters sending the same data) consisting of L multiple input single output (MISO) channels. Such is the case at any intermediate time slot within a Glossy flood.

Figure 4.1: The basic cases of our communication-theoretic system model.

for low-power wireless devices such as Zigbee [5, E 5.3]. The maximum achievable rate R_l^* over these L point-to-point channels is upper bounded by their capacity, which is given by [72, Chapter 2]

$$R_l^* = \log_2\left(1 + \frac{|h_l|^2 P}{\sigma_l^2}\right), \tag{4.1}$$

where $P = \mathrm{E}[\boldsymbol{x}^2]$ is the average transmit power of node S. If S sends information at a rate R higher than the channel capacity, the reception will be erroneous and outage will occur. The outage probability is given by $\Pr(R_l^* < R)$, which is also a lower bound on the packet error probability [73].

General multi-cast channel

We move to the general multi-cast case shown in Figure 4.1b, which represents any intermediate time slot T_{slot} within a Glossy flood where M nodes have just received the same data in the previous time slot $T_{slot}-1$ and retransmit it simultaneously. Each node S_m with $m \in \{1, 2, \ldots, M\}$ concurrently transmits a signal $\boldsymbol{x}_m$ at rate R, while node D_l receives the signal

$$\boldsymbol{y}_l = \sum_{m=1}^{M} \boldsymbol{x}_m h_{ml} + \boldsymbol{z}_l;\ \forall l \in \{1, 2, \ldots, L\}, \tag{4.2}$$

where $\boldsymbol{z}_l$ is additive white Gaussian noise with $\boldsymbol{z} \sim \mathcal{CN}(0, \sigma^2 \mathcal{I}^n)$ and $h_{ml} \in \mathbb{C}$ is the complex channel gain between source node S_m and destination node D_l. In Glossy, all nodes send the same signal. Hence, $\boldsymbol{x}_1 = \boldsymbol{x}_2 = \cdots = \boldsymbol{x}_m$. If the transmitters have no channel state information, the maximum rate at which node D_l can successfully receive all data transmitted by nodes $S_1, S_2, \ldots, S_M$ is the achievable rate R_l^*. This rate is given by [74]

$$R_l^* = \log\left(1 + \frac{|\sum_{m=1}^{M} h_{ml}\sqrt{P_m}|^2}{\sigma_l^2}\right), \tag{4.3}$$

where $P_m = \mathrm{E}[\boldsymbol{x}\boldsymbol{x}^H]$ is average transmit power of node S_m, and $[\,]^H$ is the conjugate transpose operation.

4.4 Glossy Meets Power Control

There is no doubt that Glossy excels at providing ultra-fast and highly reliable network flooding along with accurate time synchronization [6]. However, in standard Glossy, all nodes transmit with rate $R = 250\,\text{kbps}$ and typically with a power of 0 dBm [7]; these values correspond to the default and maximum settings as prescribed by the IEEE 802.15.4 standard, respectively. Hence, P_m is a constant value for all $m \in M$ the transmitting set. The corresponding outage probability in this case is $\Pr(R_l^*(h_m) < R)$, which is independent of the transmit power P_m. As we will show, this approach performs sub-optimally from an energy point of view and can be further improved by using power control and beamforming to efficiently allocate power resources which leads to a decrease in energy consumption of the entire network, hence, improved energy efficiency.

To do so, a receiving set of nodes $\mathcal{L}_m$ has to be established for each transmit node m. The communication range threshold θ is defined such that any node within a distance θ of a transmitting node m is added to the receiving set $\mathcal{L}_m$ of this transmitter. Choosing the value of θ and its effect on the energy efficiency is distinct for each of the following approaches and will be analyzed and discussed thoroughly.

4.4.1 Centralized Power Control and Beamforming

In order to examine the effect of introducing power control and beamforming on the energy efficiency of Glossy, we begin with the centralized scheme, which produces global optimum power control and beamforming decisions. This scheme utilizes the assumption of having a central arbitrator with complete channel state information knowledge of the entire network. Thus, it is able to determine the global optimum strategy for power assignment and beamforming.

Operation

As illustrated in Figure 4.2 each transmitting node m has a specific transmission range θ in which all non-transmitting nodes $l \notin M$ are considered possible receivers. This transmission range is identical and fixed for all nodes in the network. In case of more than one transmitter $M \geq 2$, the global receiving set $\mathcal{L} = \bigcup_{i=1}^{M} \mathcal{L}_m$ includes all nodes within the transmitting range of any transmitter m, as can be seen in Figure 4.3 where both nodes N_1 and N_2 are transmitting.

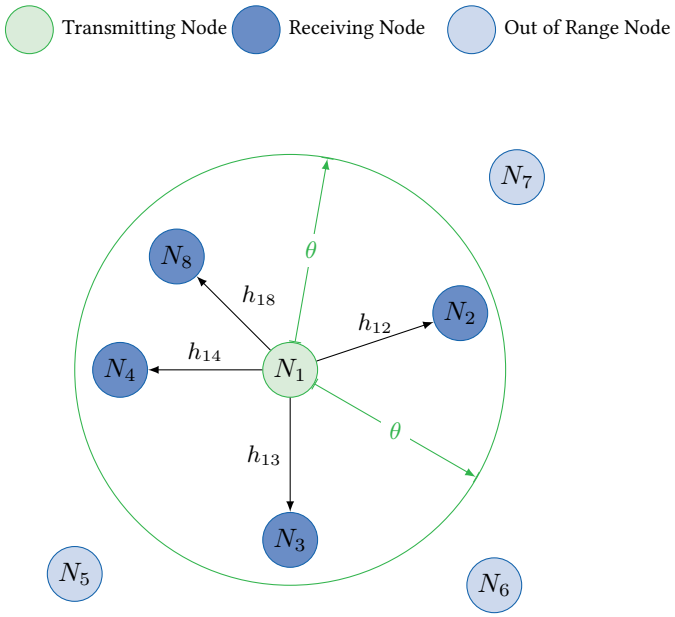

Figure 4.2: Global receiving set of nodes $\mathcal{L}$ in the centralized power control and beamforming scheme for the case of one transmitter N_1. The receiving set is $\mathcal{L} = \mathcal{L}_1 = \{N_2, N_3, N_4, N_8\}$.

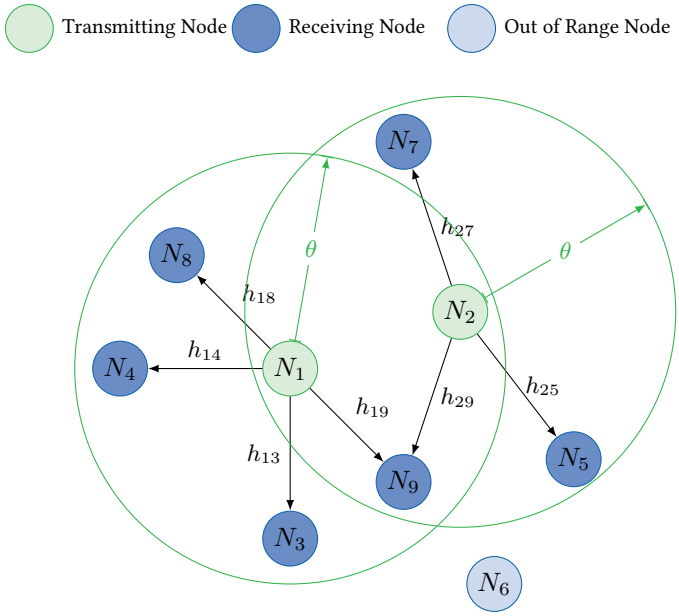

Figure 4.3: Global receiving set of nodes $\mathcal{L}$ in the centralized power control and beamforming scheme for the case of $M = 2$ transmitters N_1, N_2. The receiving set is $\mathcal{L} = \mathcal{L}_1 \bigcup \mathcal{L}_2$.

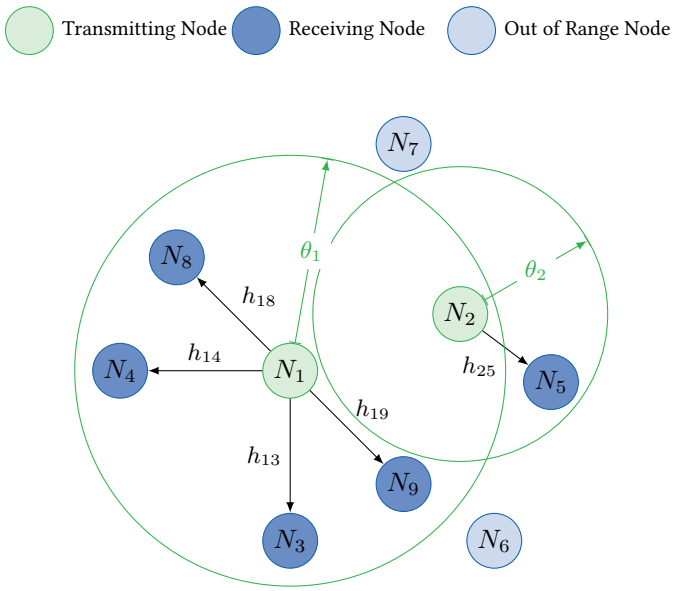

Figure 4.4: Local receiving sets of nodes $\mathcal{L}_1, \mathcal{L}_2$ in the distributed power control scheme for the case of $M = 2$ transmitters N_1, N_2. The receiving sets are $\mathcal{L}_1 = \{N_3, N_4, N_8, N_9\}, \mathcal{L}_2 = \{N_5\}$.

Analysis

Let $\boldsymbol{w}$ denote the beamforming weight vector (i.e. transmit power weights) applied to the M transmitters, and let $\boldsymbol{h_l}$ denote the $M \times 1$ complex vector representing the channel gains from each transmitter m to the receiver $l \in \mathcal{L}$. Under the assumption of zero-mean transmit signals with unit variance, the received *SNR* for receiver l is

$$SNR_l = |\boldsymbol{w}^{\boldsymbol{H}} \boldsymbol{h_l}|^2 / \sigma_l^2 \,, \tag{4.4}$$

Therefore, the outage probability expression becomes

$$\Pr\left(|\boldsymbol{w}^{\boldsymbol{H}} \boldsymbol{h_l}|^2 < (2^R - 1)\sigma_l^2\right) \,. \tag{4.5}$$

In order to get the constraint for successful reception, *i.e.*, quality of service (QoS) constraint, the *normalized channel vector* is defined as

$$\tilde{\boldsymbol{h_l}} := \boldsymbol{h_l} / \sqrt{(2^R - 1)\sigma_l^2} \,, \tag{4.6}$$

such that

$$\left(|\boldsymbol{w}^{\boldsymbol{H}} \tilde{\boldsymbol{h}}_{\boldsymbol{l}}|^2 \geq 1\right) \,. \tag{4.7}$$

Hence, the power allocation and beamforming problem that minimizes transmit power, subject to QoS constraints in (4.7) on all receiving nodes $l \in \mathcal{L}$, can be formulated as

$$\begin{aligned} \min_{\boldsymbol{w}} \quad & ||\boldsymbol{w}||^2 \,, \\ \text{subject to} \quad & |\boldsymbol{w}^{\boldsymbol{H}} \tilde{\boldsymbol{h}}_{\boldsymbol{l}}|^2 \geq 1; \quad \forall l \in \mathcal{L} \,. \end{aligned} \tag{4.8}$$

Unfortunately, the optimization problem in (4.8) is a well known NP-hard problem [86]. Therefore, we use the same approach presented in [91] to recast the problem as follows:

$$\begin{aligned} \min_{\boldsymbol{w}} \quad & \mathrm{tr}\left(\boldsymbol{w}\boldsymbol{w}^{\boldsymbol{H}}\right) \,, \\ \text{subject to} \quad & \mathrm{tr}\left(\tilde{\boldsymbol{h}}_{\boldsymbol{l}}{}^{H} \boldsymbol{w}\boldsymbol{w}^{H} \tilde{\boldsymbol{h}}_{\boldsymbol{l}}\right) \geq 1 \,; \quad \forall l \in \mathcal{L} \,. \end{aligned} \tag{4.9}$$

Using the definition of Gram matrix [92, p. 55], we can rewrite (4.9) as follows:

$$\begin{aligned} \min_{\boldsymbol{G}} \quad & \mathrm{tr}(\boldsymbol{G}) \,, \\ \text{subject to} \quad & \tilde{\boldsymbol{h}}_{\boldsymbol{l}} \boldsymbol{G} \tilde{\boldsymbol{h}}_{\boldsymbol{l}}{}^{H} \geq 1; \; \forall l \in \mathcal{L} \,, \\ & \boldsymbol{G} \succeq 0 \,, \end{aligned} \tag{4.10}$$

where inequality $\boldsymbol{G} \succeq 0$ means that $\boldsymbol{G}$ is a symmetric positive semi-definite matrix such that

$$\boldsymbol{G} = \boldsymbol{w}^{H} \boldsymbol{w} \,, \tag{4.11}$$

$\tilde{\boldsymbol{h}}_{\boldsymbol{l}}$ is the normalized channel gain vector from all M transmitters to receiver $l \in \mathcal{L}$ the receiving set and $\tilde{\boldsymbol{h}}_{\boldsymbol{l}}{}^{H} \boldsymbol{G} \tilde{\boldsymbol{h}}_{\boldsymbol{l}} = \mathrm{tr}\left(\tilde{\boldsymbol{h}}_{\boldsymbol{l}}{}^{H} \boldsymbol{G} \tilde{\boldsymbol{h}}_{\boldsymbol{l}}\right)$ [87]. The $M \times M$ matrix $\boldsymbol{G}$ contains the transmit power of each node m on the diagonal and the cross-correlation of transmit signals on the non-diagonal. In this way, we reach our goal. This technique is called a Lagrangian relaxation [93] and, in the general case of single stream transmission, requires that $\mathrm{rank}[\boldsymbol{G}] = 1$. However, our problem can be viewed as a multi-stream transmission as presented in [94] and explained in Section 5.3. Hence, the rank constraint can be dropped.

The programming problem in (4.10) is a convex problem with a linear objective function, convex constraint set and is formulated as explained in [86]. To solve this problem, we use CVX, a Matlab package for solving convex programs [95, 96].

The centralized approach is considered our upper bound on performance and energy efficiency, since a global optimum power allocation decision is made at a central node which possesses network wide CSI. This is a theoretical approach and serves as a benchmark of comparison to other approaches. For a more realistic approach we introduce in 4.4.2 a distributed power allocation scheme that requires only local CSI, a valid assumption in many networks.

4.4.2 Distributed Power Control

We introduce a distributed approach to transmit power allocation in Glossy assuming available local CSI at transmitting nodes .

Operation

We assume that each node in the network has only local CSI and topography information. This allows each transmitting node m to make independent transmit power decisions, based on the available information. A minimum communication range θ_{min} is specified, but each transmitting node m is allowed to increase the value of θ_m dynamically in order to include at least one receiving node in its own local receiving set $\mathcal{L}_m$ as seen in Figure 4.4 where $\theta_1 \neq \theta_2$.

Analysis

In order to minimize the transmit power consumption of all transmitters while still satisfying the rate constraints in (4.5), we must solve (4.9). However, each transmitter m must adapt its own transmit power to accommodate the receiver l with the worst channel h_{ml}. Therefore, we arrive at the following problem

$$\begin{aligned} \min_{P_m} \quad & P_m \,, \\ \text{subject to} \quad & h_{ml}^* P_m h_{ml} \geq (2^R - 1)\sigma_l^2; \forall l \in \mathcal{L} \,, \\ & P_m \geq 0 \,, \end{aligned} \tag{4.12}$$

where P_m is the non-negative transmit power of transmitter node m. This can be solved independently for each transmitter m using the closed form solution

$$P_m = \frac{(2^R - 1)\sigma_l^2}{\min\limits_{l \in \mathcal{L}} |h_{ml}|^2} \,. \tag{4.13}$$

Therefore, satisfying the rate constraint in (4.5) for all receivers in its own local receiver set $\mathcal{L}_m$.

4.5 Evaluation Settings and Metrics

This section uses simplified system level simulations to evaluate and compare the performance of different power control and beamforming schemes when applied to state-of-the-art Glossy. We follow the same simulation settings presented in Section 3.5. However, we define new compared schemes and performance metrics to better evaluate our proposed approaches.

Compared schemes

We compare standard Glossy to both a centralized and distributed power control schemes. We set the re-transmission limit of Glossy to $N = 3$ based on experience from extensive real-world experiments [6, 7]. For the proposed approaches, we set $N = 1$ since the reception of data is insured by the constraints of our power optimization problem. We study the impact of θ on the performance of both schemes.

Performance metrics

We compare the previously mentioned schemes in terms of *energy efficiency*, which is defined as the average amount of data successfully disseminated through the network during one Glossy flood, divided by the energy consumed by the entire network in the process. We compute energy efficiency in Kbit/Joule of the network for packets that carry an 8-byte payload. It is important to note that although the power optimization is done under QoS constraints, this guarantees QoS of individual stages within one flood but not the QoS of an entire flood. Therefore, some nodes may not be able to receive the data due to topography limitations, for example.

4.6 Results and Discussion

To assess the gains of introducing power control and beamforming in terms of energy efficiency, we plot in Figure 4.5 the energy efficiency of Glossy without power control, Glossy with centralized power control and beamforming, and Glossy with distributed power control and beamforming. We consider a network of 50 nodes placed in a 50 m $\times$ 50 m area for different values of the communication range threshold θ.

Looking at the centralized scheme, we see that the optimum value for θ is around 20 meters achieving almost 10 Kbit/Joule, which corresponds to a three-fold increase in energy

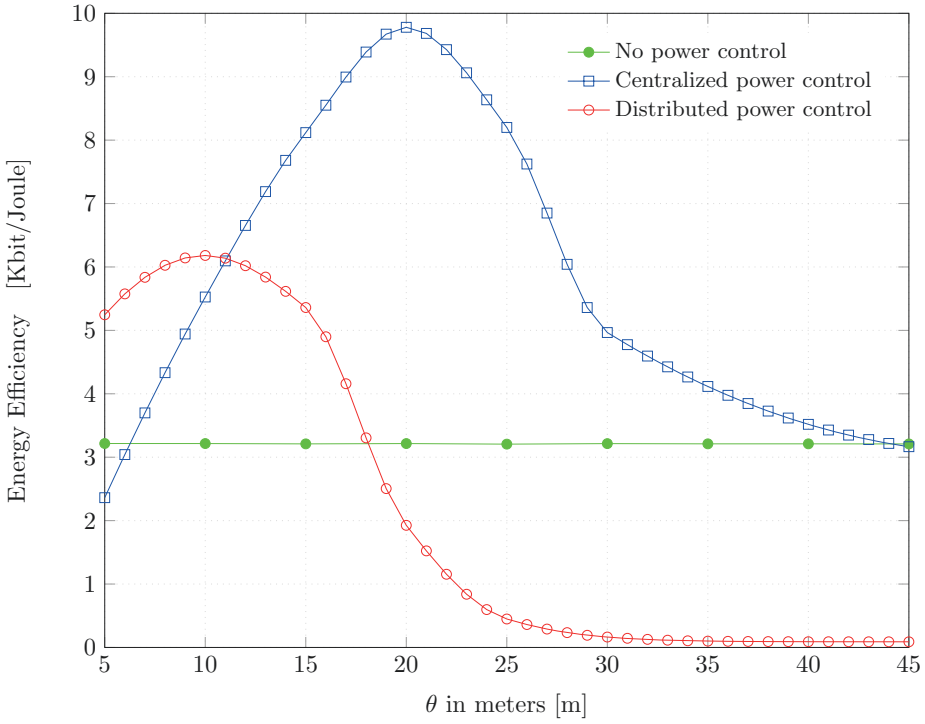

Figure 4.5: Energy efficiency of standard glossy, centralized and distributed power control and beamforming schemes for different θ values, in a network that consists of 50 nodes and is 50 m $\times$ 50 m in size.

efficiency over state-of-the-art Glossy. This, in a sense, serves as an upper bound on the energy efficiency of Glossy when using power control and beamforming. It can also be seen that the centralized approach performs worst for small values of θ. This is a consequence of having an unconnected graph due to the small range of receiving sets θ, resulting in very low packet reception ratios (defined as the number of nodes that correctly receive all packets divided by the total number of nodes in the network), hence low energy efficiency.

For the distributed scheme, we observe a gains in energy efficiency over state-of-the-art Glossy up to $\theta = 15$ m. Since each node chooses its own θ dynamically depending on the network topology information, the distributed scheme does not experience graph non-connectivity. Therefore, it outperforms all other schemes for lower values of θ. However, for higher values of θ, each node has a large receiving set $\mathcal{L}_m$ and must satisfy the rate conditions for all $l \in \mathcal{L}_m$ together with stronger overlap between receiving sets $\mathcal{L}_m$. This results in excess transmit power usage, which in turn lowers the energy efficiency significantly.

We now examine a sparser network in Figure 4.6 where we consider only 25 nodes placed

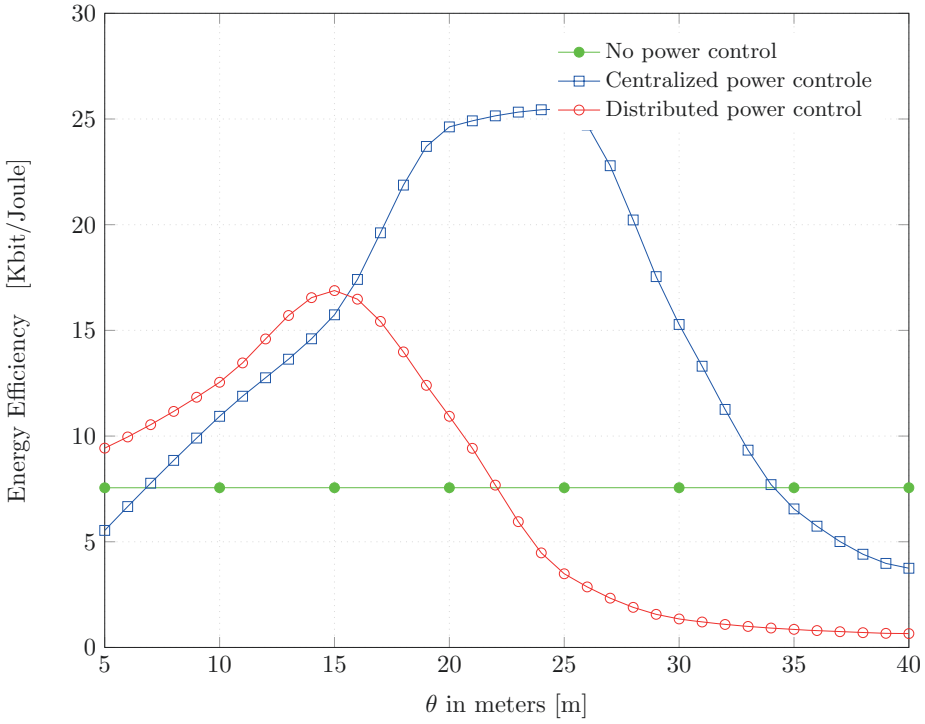

Figure 4.6: Energy efficiency of standard glossy, centralized and distributed power control and beamforming schemes for different θ values, in a network that consists of 25 nodes and is 50 m $\times$ 50 m in size.

in the same 50×50 meter square area. We notice that the optimum values of θ for the centralized and distributed power control schemes have increased. This is intuitive; due to the sparsity of the network, transmission ranges need to be expanded in order to achieve network graph connectivity. The total amount of energy consumed in disseminating the packet in a 25 node network is significantly less than that consumed in a 50 node network, resulting in increased maximum energy efficiency of all schemes. This means that nodes must use more transmit energy to reach further away (i.e. larger θ). However, this is compensated by the lower number of transmitters. This is valid until θ becomes too large and, in turn,the transmit power becomes too large without achieving higher packet reception ratios, which results in a degradation of energy efficiency. Therefore, a fine tuning of θ is crucial to an energy efficient operation.

Challenges and solutions

There are many ways to formulate a distributed power control and beamforming strategy. By exploring different approaches to applying power control and beamforming in Glossy

in a distributed, or *semi-distributed* fashion, we can achieve eventually higher energy efficiency gains while approaching the upper bound. In [97] the best response team power control problem for interference channel with local CSI is studied. An algorithm converging to a best response power control policy is introduced and optimum power control policies can be computed. Applying team decision strategies to our power control and beamforming problem in network flooding is an interesting direction and represents the logical next step following this work. However, there is one more challenge. The availability of CSI at the transmitter is crucial to successfully solving the presented beamforming problem. In the next chapter, we further investigate this challenge and present a robust beamforming approach that relies on limited feedback in order to acquire imperfect quantized CSI.

4.7 Conclusions

In this chapter, we studied the Glossy protocol with clean-slate physical and medium access control layer that use power control and transmit beamforming methods under the assumption of perfect CSI availability. It was shown that flexible power control and distributed multi-cast beamforming approaches, well known from coordinated multi-point transmission and reception in cellular communications and standardized in LTE/A, can lead to significant gains in terms of energy efficiency. By studying centralized power assignment, an upper bound on the energy efficiency was acquired which exceeds the energy efficiency of standard Glossy by several folds. We proved that optimal operating setting is dependent on the radius of the receiving set θ; and that for small values of θ, energy efficiency is degraded. Distributed power control and beamforming was shown to be most advantageous for smaller values of θ, due to the dynamically chosen values of θ independently by each transmitter based on topography information. This suggests to take another look at the corresponding PHY and MAC standards in order to make the system ready to address the scalability and efficiency challenges facing the massive deployment of low-power sensor networks.

Chapter 5

Robust Beamforming with Limited feedback

In this chapter we move towards a more realistic scenario where CSI is not available at the sensor nodes, as is the case for most WSNs. Therefore, a two-stage cooperative scheme is required. First, receiving nodes must cooperate with transmitting nodes in order to perform channel estimation. Then, transmitting nodes *collaborate* with each other in order to successfully perform distributed transmit beamforming without a central controller. The cost of cooperation in terms of energy consumption is taken into account and is represented by the energy consumed in the process of channel state information feedback from receiving to transmitting nodes. We note that there are several other factors that contribute to the processing overhead of collaborative distributed multi-cast beamforming [98] in actual hardware implementations, but for the scope of this dissertation we focus on the theoretical analysis of the proposed approach. We leave the physical implementation and accompanying impairments for future research. The result of this analysis is a clear trade-off between implementation complexity and energy efficiency [90] as will be shown in Section 5.5. Moreover, we analyze the consequences of increasing the number of collaborating nodes on energy efficiency. We use the term coalition to denote a number of transmitters that collaborate in order to perform multi-cast beamforming during any intermediate stage of a Glossy flood. We describe and analyze the performance of an algorithm that maximizes energy efficiency in cooperative network flooding by forming coalitions of transmit nodes.

5.1 Motivation and Contribution

Vastly distributed sensors are becoming an important part of our daily lives where they are utilized in many applications and diverse fields such as smart homes, environmental monitoring, emergency and health [99, 100]. Furthermore, recent 5G initiatives show a

clear focus on energy efficient smart cooperative transmission protocols [101]. These initiatives are partially motivated by the importance of energy efficiency in large-scale wireless networks for internet of things (IoT) and cyber-physical systems applications [102]. The devices used in these applications are usually heavily distributed, which makes it very challenging to replace or recharge them in a frequent manner. Therefore, extending their battery life becomes crucial. Optimizing energy will help extend the expected lifetime of these small battery operated devices, and facilitate their large scale deployment. To this end, we have proposed in Chapter 4 a power control and beamforming approach in order to improve energy efficiency and extend sensor nodes' battery life. However, this approach is based on the assumption of CSI availability at all nodes. In real WSN deployments, individual sensor nodes do not have CSI knowledge. However, in some cases network topography information might be available. This calls for a scheme where sensor nodes are able to acquire CSI in an energy efficient manner, in order to successfully perform multi-cast beamforming.

5.1.1 Contribution and Structure

In order to tackle the problem of CSI unavailability in sensor nodes, we extend the development presented in Chapter 4 where a device-to-device wireless multi-hop communication scenario with resource-constrained devices that require energy-efficient connectivity is considered. Based on the recently proposed Glossy network flooding protocol [6], that follows the IEEE 802.15.4 low-rate wireless personal area networks (LR-WPANs) standard, the beamforming and power control problem is formulated, analyzed and assessed in network scenarios where the same information needs to be shared with all nodes. Performance measures are compared, where the use of beamforming has proven to improve energy efficiency significantly. Moreover, this chapter contributes the following:

- We introduce a new system model for the general multi-cast channel that takes into consideration the feedback process needed for channel estimation.
- We formulate the problem of robust multi-cast beamforming under the assumption of imperfect CSI as a convex optimization problem and provide a solution to the relaxed approximation of the problem.
- We propose and describe a scheme where the beamforming problem can be solved independently at each node in an energy efficient manner.

- We discuss the effect of feedback quantization on energy efficiency and show there exists an optimum number of quantization bits that maximizes energy efficiency.
- We propose a greedy algorithm that allows nodes to form *coalitions* where the participating nodes are chosen in a way that maximizes energy efficiency.
- We compare the proposed approaches in terms of their energy efficiency to the standard Glossy through numerical simulations.

First, we begin with presenting a brief overview of distributed and collaborative beamforming (DCBF) in Section 5.2. Then, we describe the system model in Section 5.3, where we also explain the proposed CSI feedback approach and introduce our problem statement. In Section 5.4, we formulate our general robust multi-cast beamforming problem under limited feedback, building therefore upon the analysis and results presented in Chapter 4. Then, we analyze the effect of feedback bits B and coalition size on energy efficiency in Section 5.4.1 and Section 5.4.2, respectively. Next, we support this analysis with simulation results presented and discussed in Section 5.5, where we illustrate how the robust beamforming problem can be solved for application specific requirements. Finally, we present some concluding remarks in Section 5.6.

5.2 Distributed and Collaborative Beamforming (DCBF)

Cooperation in wireless networks is a topic that has attracted the attention of researchers for many years [103]. One form of cooperation is distributed and collaborative beamforming, which is defined as a technique where independent and randomly located source nodes cooperate to transmit a common radio frequency signal, hence forming a virtual antenna array [83]. This cooperation improves the life time of the sensor nodes [104], proving to be valuable for systems with limited battery life. It also shines as a promising technique to empower many 5G technologies such as machine type communication (MTC), device to device communication (D2D), and internet of things (IoT).

Initially, research on collaborative distributed beamforming in sensor networks was divided into two directions [105]: Collaborative and Distributed. On one hand, collaborative beamforming focused on beam pattern analysis while assuming perfect phase and carrier synchronization between sensor nodes [106]. On the other hand, distributed beamforming focused on the feasibility of achieving synchronization between those nodes [107]. However, some work was done in order to explore the possibility of achieving cooperation without synchronization such as in [108]. Later on, both directions started merging

Figure 5.1: Research directions in DCBF in wireless networks. The purple colored node "Energy efficiency maximization" represents the direction to which our work belongs.

forming distributed collaborative beamforming. The recent survey [105] classifies research trends in this area very clearly, from which the mind map in Figure 5.1 is adapted. This classification indicates that our work, where we maximize energy efficiency in network flooding by applying distributed collaborative beamforming (DCBF), lies within the scope of power minimization and lifetime maximization, more precisely under energy efficiency maximization.

Previous research efforts in this direction has several performance metrics for the evaluation of DCBF. Network life time is usually defined as the time duration from the start of network operations till the first node runs out of battery [104]. In [109] a power allocation algorithm using convex optimization is used to maximize network lifetime. On the other hand, total energy consumption is defined as the sum of total consumed energy of each node in transmit, receive and idle phases of operation [6]. In some works *e.g.*, [104], only transmit power is considered in the total energy consumption. In [110] an algorithm using a convex optimization is proposed to minimize total energy consumption under individual power constraints in two-hop networks. Another approach by [104] using genetic algorithm is proposed to minimize transmit energy consumption and increase network lifetime. Moreover, maximizing energy efficieny is the goal of [111] where sequential quadratic programming is used to solve the problem of optimal node allocation, they also show the effects on spectral efficiency. Robust distributed beamforming is considered in [112], where beamforming is used to minimize total relay transmit power under signal-to-noise ratio constraints with the availability of perfect channel state information. Recently, more works have investigated the performance of beamforming with imperfect CSI in an effort to make it more robust. In [113], a robust adaptive beamforming approach is proposed to battle the effect of signal steering vector mismatches. The proposed approach is based on the optimization of worst case performance and shows significant performance gains over other adaptive beamforming methods. Another scenario where receivers have perfect CSI and can specify beamforming vectors to transmitters is investigated in [114], where random vector quantization is shown to be asymptotically optimal. Later in [115], robust beamforming is used to optimize worst case received power gains when transmitters have imperfect CSI. The worst case achievable rates are derived based on a deterministic uncertainty model for the channel estimation error. An effort to investigate distributed beamforming under limited feedback in cooperative networks is made in [116], where an optimal beamforming vector is proposed to maximize the received signal-to-noise ratio at the receiver. Although only a fixed number of feedback bits is considered, results prove that this scheme is indeed beneficial in terms of performance.

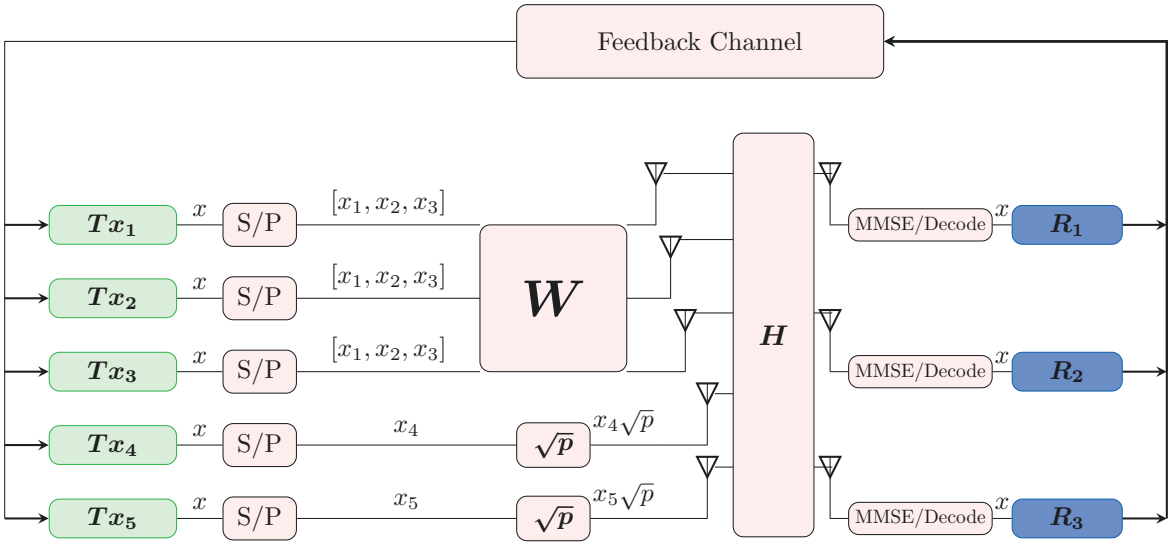

Figure 5.2: System model of a single-hop multi-cast beamforming channel, consisting of $K = 5$ transmitting nodes and $L = 3$ receiving nodes. $K_1 = 3$ nodes are cooperating and $K_2 = 2$ nodes are operating individually, where $K = K_1 + K_2$. Feedback channels are considered error-free.

5.3 System Model

Our approach can be viewed as an adaptive transmit diversity scheme. The transmission protocol starts, as in standard Glossy, with one node initiating the flood. This initial phase is a simple multi-cast transmission as explained in Section 4.3, where one node transmits a message, and nodes within reception range receive it. After successful reception of the message by, let us say, K nodes, these nodes become transmitters in the next time slot. In standard Glossy, all K nodes proceed to transmit the same information simultaneously in a non-cooperative way using the maximum transmit power setting. Here, we propose to define $K_1 \subseteq K$ of cooperating nodes which acquire CSI from the receiver through limited feedback, in order to perform multi-cast beamforming. The remaining $K_2 = K - K_1$ nodes do not cooperate and operate as in standard Glossy. Please note that the case of $K_1 = \emptyset$ is standard Glossy. An example of the system model is shown in Figure 5.2, where $K = 5$ nodes, which have successfully received and decoded the message from last transmission, send the same data $\boldsymbol{x}$ to $L = 3$ receiving nodes. First, CSI is sent back from the receivers to the transmitters through a limited-bandwidth error-free feedback channel as shown in Figure 5.2 using quantization as thoroughly explained in Section 5.3.1. Then, each transmitting node constructs an imperfect estimated channel matrix $\boldsymbol{H}$ using the acquired

feedback and proceeds to calculate an energy efficient coalition to which all or subset of the K nodes (K_1 nodes), can participate. The formation of this coalition is based on a greedy approach that can be executed at each transmitting node independently. This is explained in more details in Section 5.4.2. Afterwards, the information is divided into $K = 5$ symbols where the first 3 symbols $[x_1, x_2, x_3]$ are cooperatively transmitted by K_1 nodes one to three, while symbols x_4 and x_5 are transmitted by K_2 nodes four and five, respectively. The coalition of three nodes, solves an energy efficiency optimization problem that will be formulated and discussed in Section 5.4, and cooperatively transmits the information forming a virtual antenna array that uses energy efficient robust beamforming by applying the precoding matrix (beamforming matrix) $\boldsymbol{W}$, while the remaining two nodes operate in standard Glossy mode and transmit using maximum power p. The received signal at any receiver l can be characterized as follows

$$y_l = \boldsymbol{x}^T \boldsymbol{U} \boldsymbol{h}_l + z_l, \tag{5.1}$$

where cooperation is controlled by the KxK matrix

$$\boldsymbol{U} = \begin{bmatrix} & & & 0 & 0 \\ & \boldsymbol{W} & & 0 & 0 \\ & & & 0 & 0 \\ 0 & 0 & 0 & \sqrt{p} & 0 \\ 0 & 0 & 0 & 0 & \sqrt{p} \end{bmatrix}. \tag{5.2}$$

$\boldsymbol{x}^T = [x_1 ... x_5]$ are the data symbols, $\boldsymbol{W}$ is the K_1xK_1 beamforming matrix, $\boldsymbol{h}_l^T = [h_{1l}, ... h_{5l}]$ is the channel gain vector between receiver l and the transmitting nodes, and z_l is the receiver noise. The $[\,]^T$ describes the transpose operation. After the signal reception, interference cancellation methods (*i.e.*, minimum mean square error (MMSE) and successive interference cancellation (SIC)) are applied at each receiving node before the original message $\boldsymbol{x}$ can be retrieved. The maximum rate achieved by applying such processing at any receiver node l to the received signals can then be calculated as following

$$R_l^* = \max_{\boldsymbol{U}} \quad E\left[\log\left(1 + \frac{\boldsymbol{h}_l^H \boldsymbol{U}^H \boldsymbol{x}^* \boldsymbol{x}^T \boldsymbol{U} \boldsymbol{h}_l}{\sigma_l^2}\right)\right], \tag{5.3}$$

where the expectation operation $E[\,]$ is over channel state information $\boldsymbol{h_l}$. However, receivers provide CSI feedback to transmitting nodes. Therefore, choosing an optimal beamforming matrix for fed-back channel realizations can lead to a maximum achievable rate

of:

$$R_l^* = \log\left(1 + \frac{\boldsymbol{h}_l^H \boldsymbol{U}^H \boldsymbol{x}^* \boldsymbol{x}^T \boldsymbol{U} \boldsymbol{h}_l}{\sigma_l^2}\right). \tag{5.4}$$

By applying MMSE and SIC techniques as demonstrated in [117, ch. 10], it can be equivalently described as:

$$R_l^* = \log\left(1 + \frac{\begin{bmatrix} h_{1l} \\ h_{2l} \\ h_{3l} \end{bmatrix}^H \boldsymbol{W}^H \boldsymbol{D}_3 \boldsymbol{W} \begin{bmatrix} h_{1l} \\ h_{2l} \\ h_{3l} \end{bmatrix}}{\sigma_l^2} + \frac{|h_{l4}|^2 p}{\sigma_l^2} + \frac{|h_{l5}|^2 p}{\sigma_l^2}\right), \tag{5.5}$$

where h_{il} is the channel gain coefficient from transmitter i to receiver l, $\boldsymbol{D}_3$ is a diagonal matrix with the weights of data streams and is equal to the identity matrix $\boldsymbol{I}$, $[\boldsymbol{W}^H \boldsymbol{D}_3 \boldsymbol{W}]$ is the transmit covariance matrix as shown in [94], the $[\,]^*$ and $[\,]^H$ describe the conjugate and conjugate transpose operations, respectively. Using the definition of Gram matrix [92, p. 55], we can rewrite the achievable rate equation as follows:

$$R_l^* = \log\left(1 + \frac{\begin{bmatrix} h_{1l} \\ h_{2l} \\ h_{3l} \end{bmatrix}^H \boldsymbol{G} \begin{bmatrix} h_{1l} \\ h_{2l} \\ h_{3l} \end{bmatrix}}{\sigma_l^2} + \frac{|h_{l4}|^2 p}{\sigma_l^2} + \frac{|h_{l5}|^2 p}{\sigma_l^2}\right), \tag{5.6}$$

where

$$\boldsymbol{G} = \boldsymbol{W}^H \boldsymbol{W} \tag{5.7}$$

is a positive semi-definite matrix. This can be generalized to the case of $K = K_1 + K_2$ transmitters with K_1 cooperating nodes and K_2 non-cooperating nodes as follows

$$R_l^* = \log\left(1 + \frac{\boldsymbol{h}_l \boldsymbol{G} \boldsymbol{h}_l^H}{\sigma_l^2} + \sum_{i=K_1+1}^{K} \frac{|h_{il}|^2 p}{\sigma_l^2}\right) \tag{5.8}$$

where $\boldsymbol{h}_l^T = [h_1, h_2 ... h_{K_1}]$, $\boldsymbol{G}$ is a K_1xK_1 positive semi-definite matrix, and p is the maximum transmit power of the node. Moreover, for the case where all transmitting nodes are

cooperating, the maximum achievable rate can be described as

$$R_l^* = \log\left(1 + \frac{\boldsymbol{h}_l \boldsymbol{G} \boldsymbol{h}_l^H}{\sigma_l^2}\right) \tag{5.9}$$

with KxK positive semi-definite matrix $\boldsymbol{G}$.

Channel Model

In order to examine the effect of limited feedback on a complex communication scenario such as Glossy, we must specify our channel characteristics, similar to the channel model used in Chapter 4. We start with the signal received at receiver l, described in (5.1). Channel vectors of receivers 1 to L with $\boldsymbol{h}_l^T = [h_{1l}, h_{2l}, ...h_{Kl}]$ and $h_{kl} \in \mathbb{C}$ is the channel gain from transmitter k to receiver l modeled as quasi-static, independent, and experience flat-fading on the block length, which is a valid assumption for low-power wireless devices such as Zigbee [5, E 5.3]. These coefficients are calculated according to $h_{kl} = w_{kl} g_{kl}$, where small-scale fading w_{kl} follows a complex normal distribution $\mathcal{CN}(0, 1)$, and large-scale fading g_{kl} depends on the distance d_{kl} between transmitter k and receiver l [5, E 5.3] as follows

$$g_{kl} = \begin{cases} 40.2 + 20\log(d_{kl}), & d_{kl} \leq 8\,\text{m}, \\ 58.5 + 33\log(dkl/8), & d_{kl} > 8\,\text{m}. \end{cases} \tag{5.10}$$

which corresponds to a path loss exponent of 2 for the first 8 m and a path loss exponent of 3.3 for distances larger than 8 m. To ensure $g_{kl} > 0$ according to (3.14), we consider only topologies where the distance between any pair of nodes exceeds 0.1 m, which is reasonable in real deployments [75]. We denote the normalized channel vector $\tilde{\boldsymbol{h}}_l = \frac{\boldsymbol{h}_l}{||\boldsymbol{h}_l||}$, where $\tilde{\boldsymbol{h}}_l$ is a unit vector that describes only the channel direction. Moreover, in our model, transmitters are assumed to know the channel quality information (CQI), represented by $||\boldsymbol{h}_l||$, perfectly, while each receiver l is assumed to know local CSI $\boldsymbol{h}_l$ through pilot training [118, 119] at the beginning of transmission which is not the focus of this work. CSI is then quantized and shared with transmitting nodes through a limited feedback channel as described in Section 5.3.1. Finally, z_l is additive white Gaussian noise with a complex normal distribution $z_l \sim \mathcal{CN}(0, \sigma_l^2)$.

5.3.1 CSI Feedback

Quantization is done using randomly generated vector quantization codebooks independently at each receiver. A code book $\mathcal{CB}$ contains 2^B K-dimensional unit norm vectors randomly drawn from the isotropic distribution on the K-dimensional unit sphere where

$\mathcal{CB} \triangleq \{\boldsymbol{c}_1, \boldsymbol{c}_2, ...\boldsymbol{c}_{2^B}\}$. In addition to being mathematically tractable, RVQ performs close to optimal quantization as feedback bits $B \to \infty$ [114]. This can be independently applied at each receiver l where the closest vector $\boldsymbol{c}_i$ to the normalized real channel $\tilde{\boldsymbol{h}_l}$ is chosen. The index i is then transmitted to active transmitters using B feedback bits. The RVQ process is performed such that the closest vector $\boldsymbol{c}_i$ to the normalized real channel $\tilde{\boldsymbol{h}_l}$ has to be chosen. We consider the Euclidean distance, defined as the norm of the difference between $\boldsymbol{c}_i$ and $\tilde{\boldsymbol{h}_l}$, as a measure of closeness. Each receiver must choose the closest vector $\boldsymbol{c}_i$ to the normalized channel $\tilde{\boldsymbol{h}_l}$ independently. This is done by solving the following problem

$$i_l = \arg \quad \min_{1 \leq i \leq 2^B} ||\tilde{\boldsymbol{h}_l} - \boldsymbol{c}_i||^2. \tag{5.11}$$

Since the norm of the error vector is

$$||\delta_l||^2 \quad = ||\tilde{\boldsymbol{h}_l} - \hat{\boldsymbol{h}_l}||^2, \tag{5.12}$$

where the $\hat{\boldsymbol{h}_l}$ is the quantized channel vector based on the Euclidean distance, this manner of choosing the quantized channel vector results in the smallest error norm possible. Unfortunately, the statistical behavior of this error is not available in closed form. However, we assume that ϵ_l is an upper bound on the norm of quantization error such that $||\delta_l|| \leq \epsilon_l$.

Feedback Overhead

Feedback is the operation of sharing quantized CSI between receivers and transmitters. Each receiver node l must quantize and share its CSI using the feedback channel. Thanks to the broadcast nature of the wireless medium and assuming error free feedback channels, it is safe to assume that any wireless signal received successfully by the furthest node, can be received by all other nodes and the power needed for reliable transmission is at least

$$P_l = (2^B - 1) \max_{1 \leq j \leq K, j \neq l} |d_{lj}|^2, \tag{5.13}$$

where d_{lj} is the distance from receiver l to transmitter j, operator $|.|$ denotes the Euclidean norm and P_l is defined as the transmission power needed to distribute CSI from receiver l to all transmitters. The total feedback energy overhead is computed as follows

$$P_{coop} = (2^B - 1) \sum_{l=1}^{L} \max_{1 \leq j \leq K, j \neq l} |d_{lj}|^2, \tag{5.14}$$

where we can see the exponential dependency of P_{coop} on the number of feedback bits B and linear dependency on the distances between receivers and transmitters. This means

that increasing the number of feedback bits B will result in a higher cooperation over head in terms of P_{coop}, but will also result in a more accurate estimation of the channels, leading to less transmit power. Therefore, there must be an optimum number of feedback bits B that minimizes total energy consumption and maximizes energy efficiency. This brings us to our problem statement, which we present in Section 5.3.2.

5.3.2 Problem Statement

In order to efficiently manage network resources and achieve high energy efficiency in state-of-the-art Glossy [7, 27], we seek to analyze the feasibility of using power control and transmission cooperation schemes such as coherent multicast beamforming. To achieve our goal, we first look at the problem of limited feedback, where receiving nodes try to share their CSI with transmitting nodes using B feedback bits. Increasing the number of feedback bits B used in CSI sharing results in a better representation of the channels and lower quantization error. However, the consumed energy overhead by reliably transmitting these feedback bits increases as well. This results in a clear trade-off between the cooperation gain achieved by coherent multicast beamforming amongst the K transmitting nodes and the consumed energy overhead due to CSI feedback. Therefore, there must exist an optimal B, dependent on network parameters such as topology, number of transmitters K and density of the network, that maximizes energy efficiency. This allows us to solve a programming problem, that depends on the CSI uncertainty parameter ϵ_l and in turn optimal B, that maximizes energy efficiency under quality of service constraints (QoS) and guarantees successful reception as follows

$$\min_{\boldsymbol{G}} \quad \mathrm{tr}(\boldsymbol{G}) \ , \tag{5.15}$$

$$\text{subject to} \qquad \left(\hat{\boldsymbol{h}}_l + \boldsymbol{\delta}\right) \boldsymbol{G} \left(\hat{\boldsymbol{h}}_l + \boldsymbol{\delta}\right)^H \geq \frac{(2^R - 1)\sigma_l^2}{||\boldsymbol{h}_l||^2} \ ; \ \forall l \in \mathcal{L} \ , \tag{5.16}$$

$$\forall \boldsymbol{\delta} : ||\boldsymbol{\delta}|| \leq \epsilon \, , \tag{5.17}$$

$$\boldsymbol{G} \succeq 0 \, , \tag{5.18}$$

where all transmitters are assumed to be cooperating, and minimizing the beamforming transmit powers $\mathrm{tr}(\boldsymbol{G})$ and the feedback power under 3 inequality constraints. Inequality (5.16) ensures the achievable rate robustness against CSI uncertainty, inequality (5.17) limits the maximum CSI uncertainty error, and inequality (5.18) insures that cooperation multicast beamforming covariance matrix $\boldsymbol{G}$ is positive semi-definite. This programming

problem results in maximizing the energy efficiency and is solved and discussed in more details in Section 5.4 and Section 5.4.1. lastly, we look at the problem of choosing cooperating nodes. We investigate how the choice of cooperating transmitters K_1 affect energy efficiency, whether there exists an optimum coalition and how to form it.

5.4 Beamforming with Limited Feedback

In Chapter 4, we considered the case of multicast beamforming under the assumption of perfect CSI available at both transmitter and receiver. The following programming problem was solved in Section 4.4 for the optimal precoder $\boldsymbol{G}$

$$\begin{aligned} \min_{\boldsymbol{G}} \quad & \mathrm{tr}(\boldsymbol{G}) \,, \\ \text{subject to} \quad & \boldsymbol{h}_l \boldsymbol{G} \boldsymbol{h}_l^H \geq (2^R - 1)\sigma_l^2 \,;\, \forall l \in \mathcal{L} \,, \\ & \boldsymbol{G} \succeq 0 \,, \end{aligned} \tag{5.19}$$

where the inequality $\boldsymbol{G} \succeq 0$ means that $\boldsymbol{G}$ is a positive semi-definite matrix. The programming problem in (5.19) is a convex problem with a linear objective function, convex constraint set and is formulated as explained in [86]. To solve it, we use CVX, a Matlab package for solving convex programs [95, 96].

Unfortunately, perfect CSI knowledge at the transmitter side is not always possible, as in scenarios where limited feedback is considered. Therefore, based on the available CSI provided to the transmitters through limited feedback channels and using the uncertainty model explained in Section 5.3.1, the transmitter has to estimate the real channels in order to calculate the appropriate beamformer. First, in order to satisfy the QoS constraints at each receiver l the following must hold

$$\log\left(1 + \frac{\boldsymbol{h}_l \boldsymbol{G} \boldsymbol{h}_l^H}{\sigma_l^2}\right) \geq R \;;\, \forall l \in \mathcal{L} \,. \tag{5.20}$$

The real channel $\boldsymbol{h}_l$ can be written in terms of the quantized channel direction $\hat{\boldsymbol{h}}_l$ and the channel norm $||\boldsymbol{h}_l||$ as such

$$\boldsymbol{h}_l = ||\boldsymbol{h}_l|| \tilde{\boldsymbol{h}_l} = ||\boldsymbol{h}_l|| \left(\hat{\boldsymbol{h}}_l + \boldsymbol{\delta}_l\right) \,. \tag{5.21}$$

We assume that both $\hat{\boldsymbol{h}}_l$ and $||\boldsymbol{h}_l||$ are known by the transmitter. Therefore, after some algebraic manipulations, (5.20) can be written as

$$\begin{aligned} & \left(\hat{\boldsymbol{h}}_l + \boldsymbol{\delta}_l\right) \boldsymbol{G} \left(\hat{\boldsymbol{h}}_l + \boldsymbol{\delta}_l\right)^H \geq \frac{(2^R - 1)\sigma_l^2}{||\boldsymbol{h}_l||^2} \,; \\ & \forall l \in \mathcal{L} \;,\; \forall \boldsymbol{\delta}_l : ||\boldsymbol{\delta}_l|| \leq \epsilon_l \,, \end{aligned} \tag{5.22}$$

where ϵ_l is an upper bound on the norm of quantization error. In order to design a beamformer that is robust against quantization error, the transmitters must minimize the trans-

mit power while satisfying the rate constraints in (5.22). Using (5.22) and (5.19), the robust beam-forming optimization problem can be formulated as in (5.15)

Since the quantization error vector $\boldsymbol{\delta}_l$ is random and exact knowledge of its direction is not available at the transmitter, we modify the optimization problem mathematically so it can be solved numerically. To that purpose, we apply some simplification and algebraic modifications to the constraints in (5.22) similar to the analysis done in [120]. The robust beam-forming optimization problem in (5.15) becomes equivalent to the following semi definite programming problem which can be solved by a matlab tool for convex optimization known as CVX [95, 96]

$$\begin{aligned} \min_{\boldsymbol{GQ},\mu} \quad & \mathrm{tr}(\boldsymbol{G}) \ , \\ \text{subject to} \quad & \hat{\boldsymbol{h}}_l \left(\boldsymbol{G}-\boldsymbol{Q}\right) \hat{\boldsymbol{h}}_l^{\,H} - \epsilon_l^2 \mu \geq \frac{(2^R-1)\sigma_l^2}{||\boldsymbol{h}_l||^2} \ ; \\ & \forall l \in \mathcal{L} \ , \ \mu \geq 0 \ , \ \boldsymbol{G} \succeq 0 \, , \\ & \begin{bmatrix} \boldsymbol{Q} & \boldsymbol{G} \\ \boldsymbol{G} & \boldsymbol{G}+\mu \boldsymbol{I} \end{bmatrix} \succeq 0 \, . \end{aligned} \tag{5.23}$$

Based on S-procedure and Schur Complement as explained in Appendix A and B, respectively, we first transform the rate constraints in (5.22) as

$$\begin{aligned} & \boldsymbol{\delta_l} \boldsymbol{G} \boldsymbol{\delta}_l^H + 2\mathcal{R}\left\{\hat{\boldsymbol{h}}_l \boldsymbol{G} \boldsymbol{\delta}_l^H\right\} + \hat{\boldsymbol{h}}_l \boldsymbol{G} \hat{\boldsymbol{h}}_l^{\,H} - z \geq 0 \, ; \\ & \forall l \in \mathcal{L} \ , \ \forall \boldsymbol{\delta}_l : -||\boldsymbol{\delta}_l||^2 + \epsilon_l^2 \geq 0 \, , \end{aligned} \tag{5.24}$$

where $z = \frac{(2^R-1)\sigma_l^2}{||\boldsymbol{h}_l||^2}$, and $||\boldsymbol{\delta}||^2 = \boldsymbol{\delta}^H \boldsymbol{\delta}$. According to S-Procedure, this holds if and only if there exists $\mu \geq 0$ such that

$$\begin{bmatrix} \boldsymbol{G}+\mu \boldsymbol{I} & \boldsymbol{G} \tilde{\boldsymbol{h}}_l^{\,H} \\ \tilde{\boldsymbol{h}}_l \boldsymbol{G} & \tilde{\boldsymbol{h}}_l \boldsymbol{G} \tilde{\boldsymbol{h}}_l^{\,H} - \epsilon_l^2 \mu - z \end{bmatrix} \succeq 0 \, , \tag{5.25}$$

This provides us with 2 separate cases for μ. First, we examine the case where $\mu > 0$. Using Schur Complement, (5.25) can be written as

$$\begin{aligned} & \tilde{\boldsymbol{h}}_l \boldsymbol{G} \tilde{\boldsymbol{h}}_l^{\,H} - \epsilon_l^2 \mu - z - \tilde{\boldsymbol{h}}_l \boldsymbol{G} \left[\boldsymbol{G}+\mu \boldsymbol{I}\right]^{-1} \boldsymbol{G} \tilde{\boldsymbol{h}}_l^{\,H} \geq 0 \, , \\ & \tilde{\boldsymbol{h}}_l \boldsymbol{G} \tilde{\boldsymbol{h}}_l^{\,H} - \tilde{\boldsymbol{h}}_l \boldsymbol{G} \left[\boldsymbol{G}+\mu \boldsymbol{I}\right]^{-1} \boldsymbol{G} \tilde{\boldsymbol{h}}_l^{\,H} - \epsilon_l^2 \mu \geq z \, . \end{aligned} \tag{5.26}$$

We introduce $\boldsymbol{Q}$, where $\boldsymbol{Q} \succeq \boldsymbol{G}\left[\boldsymbol{G}+\mu \boldsymbol{I}\right]^{-1} \boldsymbol{G}$. The robust beam-forming optimization

problem in (5.15) can be rewritten as

$$\begin{aligned} \min_{\boldsymbol{GQ},\mu} \quad & \mathrm{tr}(\boldsymbol{G}) \ , \\ \text{subject to} \quad & \hat{\boldsymbol{h}}_l \boldsymbol{G} \hat{\boldsymbol{h}}_l^{\,H} - \hat{\boldsymbol{h}}_l \boldsymbol{Q} \hat{\boldsymbol{h}}_l^{\,H} - \epsilon_l^2 \mu \geq z \ , \\ & \forall l \in \mathcal{L} \ , \ \mu > 0 \ , \ \boldsymbol{G} \succeq 0 \, , \\ & \boldsymbol{Q} - [\boldsymbol{G} + \mu \boldsymbol{I}]^{-1} \boldsymbol{G} \succeq 0 \, . \end{aligned} \tag{5.27}$$

By applying Schur Complement to the constraint in (5.27), it can be transformed equivalently into

$$\begin{aligned} \min_{\boldsymbol{GQ},\mu} \quad & \mathrm{tr}(\boldsymbol{G}) \ , \\ \text{subject to} \quad & \hat{\boldsymbol{h}}_l \left(\boldsymbol{G} - \boldsymbol{Q}\right) \hat{\boldsymbol{h}}_l^{\,H} - \epsilon_l^2 \mu \geq z \, ; \\ & \forall l \in \mathcal{L} \ , \ \mu > 0 \, , \boldsymbol{G} \succeq 0 \, , \\ & \begin{bmatrix} \boldsymbol{Q} & \boldsymbol{G} \\ \boldsymbol{G} & \boldsymbol{G} + \mu \boldsymbol{I} \end{bmatrix} \succeq 0 \, . \end{aligned} \tag{5.28}$$

Second, for $\mu = 0$, (5.25) amounts to

$$\begin{bmatrix} \boldsymbol{G} & \boldsymbol{G} \tilde{\boldsymbol{h}}_l^{\,H} \\ \tilde{\boldsymbol{h}}_l \boldsymbol{G} & \tilde{\boldsymbol{h}}_l \boldsymbol{G} \tilde{\boldsymbol{h}}_l^{\,H} - z \end{bmatrix} \succeq 0 \, . \tag{5.29}$$

From the definition of a positive semi-definite matrix, it follows that

$$\begin{bmatrix} -\tilde{\boldsymbol{h}}_l^{\,H} & 1 \end{bmatrix} \begin{bmatrix} \boldsymbol{G} & \boldsymbol{G} \tilde{\boldsymbol{h}}_l^{\,H} \\ \tilde{\boldsymbol{h}}_l \boldsymbol{G} & \tilde{\boldsymbol{h}}_l \boldsymbol{G} \tilde{\boldsymbol{h}}_l^{\,H} - z \end{bmatrix} \begin{bmatrix} -\tilde{\boldsymbol{h}}_l \\ 1 \end{bmatrix} = -z \geq 0 \tag{5.30}$$

holds only for $z = 0$, which means that the constraints in (5.28) can be satisfied for the case of $\mu = 0$ by having $\boldsymbol{Q} = \boldsymbol{G}$ and can hereby be included into (5.28), arriving to the final result in (5.23). Algorithm 2 shows the operations done at each transmitting node after receiving the feedback signal.

Algorithm 2 Transmitter Operations

1: **Input:** Pr_o, K, ϵ_l.

2: **Output:** $\boldsymbol{G}$.

3: **Calculate:**

$$\boldsymbol{G} = \begin{cases} \arg \min\limits_{\boldsymbol{G},\boldsymbol{Q},\mu} & \mathrm{tr}(\boldsymbol{G})\,, \\ \text{subject to} & \hat{\boldsymbol{h}}_l \left(\boldsymbol{G} - \boldsymbol{Q}\right) \hat{\boldsymbol{h}}_l^{\,H} - \epsilon_l^2 \mu \geq \dfrac{(2^R - 1)\sigma_l^2}{||\boldsymbol{h}_l||^2}\,; \\ & \forall l \in \mathcal{L}\,,\ \mu \geq 0\,,\ \boldsymbol{G} \succeq 0, \\ & \begin{bmatrix} \boldsymbol{Q} & \boldsymbol{G} \\ \boldsymbol{G} & \boldsymbol{G} + \mu \boldsymbol{I} \end{bmatrix} \succeq 0. \end{cases}$$

4: **Multicast transmission**.

Algorithm 3 Feedback Generation

1: **Input:** Pr_o, K, R.

2: **Output:** B^*.

3: **Calculate:**

$$B^* = \begin{cases} \arg \min\limits_{B,\epsilon_l,\boldsymbol{G},\boldsymbol{Q},\mu} & \mathrm{tr}(\boldsymbol{G}) + (2^B - 1) \max\limits_{1 \leq j \leq K, j \neq l} |d_{lj}|^2, \\ \text{subject to} & \hat{\boldsymbol{h}}_l \left(\boldsymbol{G} - \boldsymbol{Q}\right) \hat{\boldsymbol{h}}_l^{\,H} - \epsilon_l^2 \mu \geq \dfrac{(2^R - 1)\sigma_l^2}{||\boldsymbol{h}_l||^2}\,; \\ & \mu \geq 0\,,\ \boldsymbol{G} \succeq 0, \\ & \begin{bmatrix} \boldsymbol{Q} & \boldsymbol{G} \\ \boldsymbol{G} & \boldsymbol{G} + \mu \boldsymbol{I} \end{bmatrix} \succeq 0. \end{cases}$$

4: **Transmit feedback with power** $P_l = (2^{B^*} - 1) \max\limits_{1 \leq j \leq K, j \neq l} |d_{lj}|^2$.

5.4.1 Feedback Optimization

First, we evaluate the effect that the number of feedback bits B has on energy efficiency of an arbitrary single hop within a Glossy flood. This is the first step towards optimizing the number of feedback bits B from an energy efficiency point of view. To do so, we must define our performance measures. So we begin by defining energy efficiency as introduced in [121] as follows

$$EE = \frac{\text{Goodput}}{\text{Total energy consumption}}, \tag{5.31}$$

where, in our scenario, the average Goodput is defined, similar to the formulation in [122], as the average successfully received rate at each receiver, and the total energy consumption is the sum of transmit energies for all K transmitters and the cooperation overhead P_{coop} as defined in (5.14). For more info about the definition of the metrics used we refer the reader to Section 3.5 where we introduce and define Goodput and energy efficiency. The energy efficiency can be rewritten as such

$$EE = \frac{(1 - \mathrm{Pr}_o)R}{\mathrm{tr}(\boldsymbol{G}) + P_{coop}}, \tag{5.32}$$

where Pr_o is the outage probability fixed to an application specific minimum acceptable value, and R is the source rate fixed at 250 kbps as in the IEEE 802.15.4 standard [5].

In order to maximize energy efficiency we need to consider the following optimization problem

$$\max_{B(\epsilon)} \quad EE = \frac{(1 - \mathrm{Pr}_o)R}{\mathrm{tr}(\boldsymbol{G}) + P_{coop}}. \tag{5.33}$$

Due to the fixed nominator, this problem is equivalent to

$$\min_{B(\epsilon)} \quad \mathrm{tr}(\boldsymbol{G}) + (2^{B(\epsilon)} - 1) \max_{1 \le j \le K, j \neq l} |d_{lj}|^2 . \tag{5.34}$$

Unfortunately, due to the lack of a closed form expression for B in terms of ϵ, this optimization problem can not be simultaneously solved for $\boldsymbol{G}$ and B. Therefore, an offline database created using network statistics is saved at each node, where ϵ can be chosen as a function of K, B, and Pr_o. An example of the offline database is shown in Figure 5.3 for $Pr_o = 5\%$. After that, the programming problem in (5.34) can be solved independently at each receiver node for each B in order to find B^* that achieves the minimum consumed

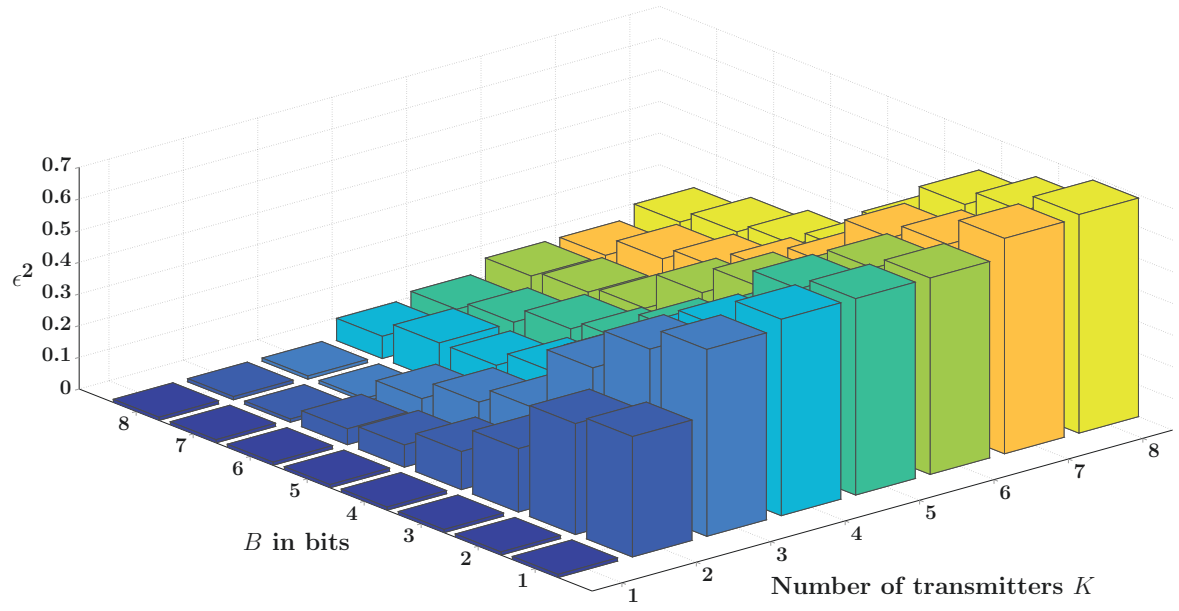

Figure 5.3: An example of the offline database saved at each node where ϵ can be chosen as a function of K, B, and Pr_o. In this example, Pr_o is set to 5%.

energy for the application specific Pr_o requirement. The feedback generation algorithm in Algorithm 3 shows the operational steps carried out at each receiver node, while the flow chart in Figure 5.4 shows the protocol operations flow at each node.

A simple example can be seen in Figure 5.5 with 4 transmitting nodes waiting for receiver feedback, and 3 receiving nodes executing Algorithm 3. Due to different positions, each receiver will have a relation between consumed energy and B. The dependency of consumed energy on the number of feedback bits B for each receiver is calculated and shown in Figure 5.6. We can see there that it is possible that B^* would be different for each receiver depending on its position in the network. In our example, receiver 1,2 and 3 will choose 2,3 and 5 bits, respectively for feedback transmission.

5.4.2 Coalition Formation

The proposed cooperation scheme for network flooding based on Glossy is divided into 2 parts. The first part is feedback generation at receiving nodes, followed by multicast beamforming at transmitting nodes as explained above. The second part is a coalition formation strategy that chooses cooperating transmitters in order to maximize energy efficiency. In this section, we analyze the effect of coalition size and participant transmitters on energy efficiency, and if there exists an optimal choice of cooperating nodes that maximizes energy

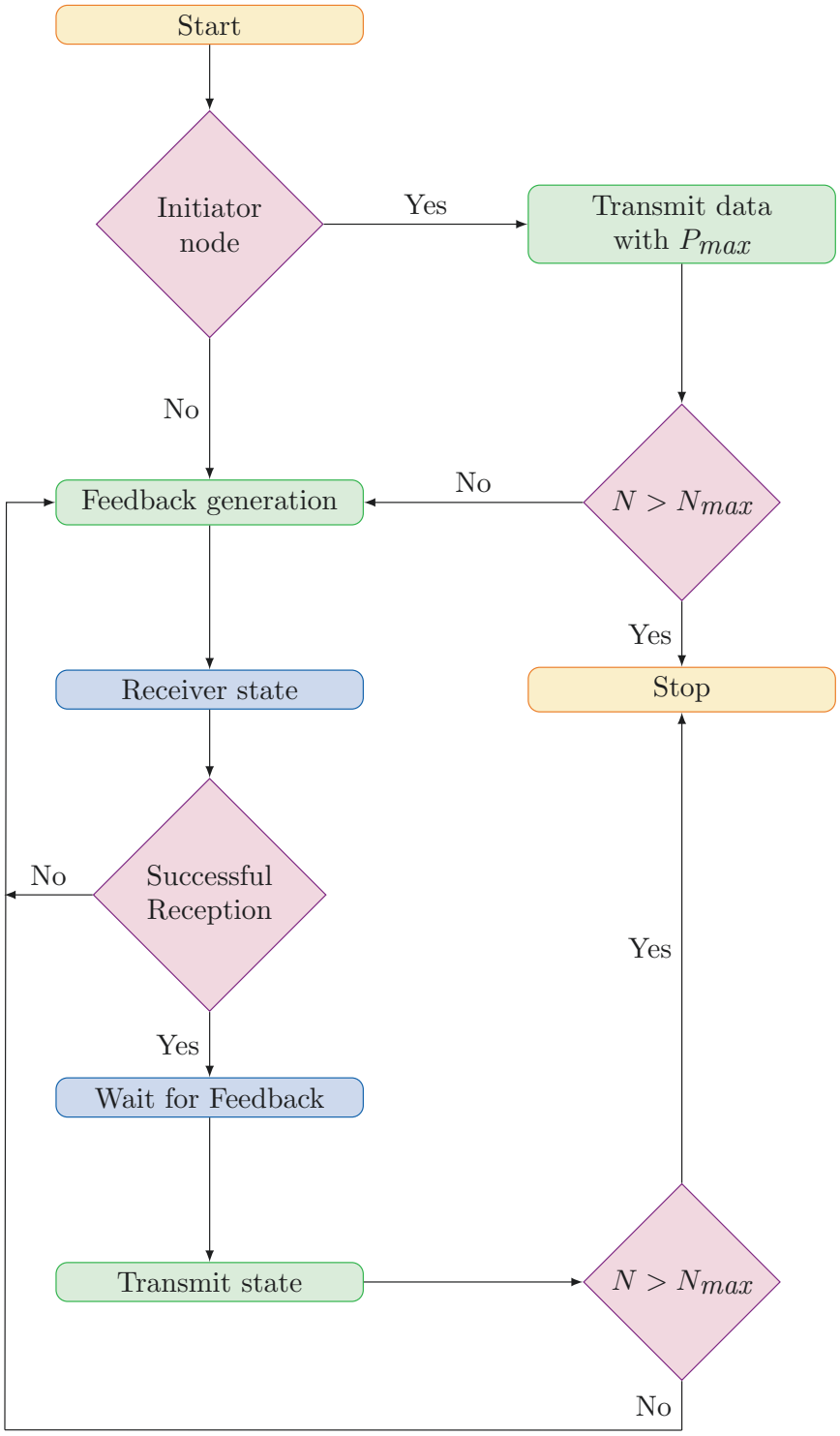

Figure 5.4: Commands executed at any node during the proposed protocol.

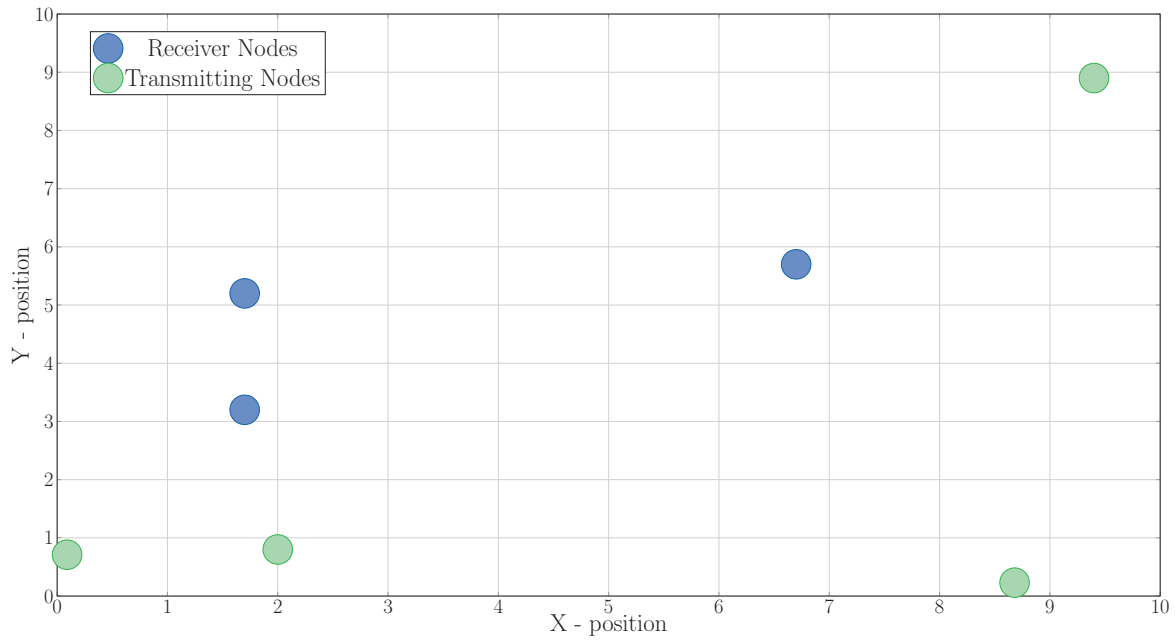

Figure 5.5: Sensor network example of an intermediate step during a flood with 4 transmitters in green and 3 receivers in blue. Receivers generate feedback to provide transmitters with imperfect quantized CSI.

efficiency.

For this part, we allow a subset of all transmitting nodes to cooperate. Our goal is to show the possibility that a certain cooperating group of transmitters (coalition) exists to maximize energy efficiency. It is important to note that this study is to show the effectiveness of coalition formation and not to demonstrate how it can be implemented in a distributed fashion. First, feedback operation is performed as explained in Section 5.3.1, where receivers provide the CSI to the K transmitters. In order to minimize the energy consumed in the cooperation phase, the transmitter furthest away from all receivers is removed from the coalition. If this elimination operation improves energy efficiency of the transmission, the next furthest away transmitter is removed. Elimination stops when energy efficiency starts to deteriorate and the coalition is returned to the last step. This greedy transmitter selection operation is explained in Algorithm 4.

This operation results in a coalition of K or less transmitters. The effect of this enhancement on energy efficiency and energy consumption compared to both normal Glossy and Glossy with transmit beamforming will be demonstrated in Section 5.5.

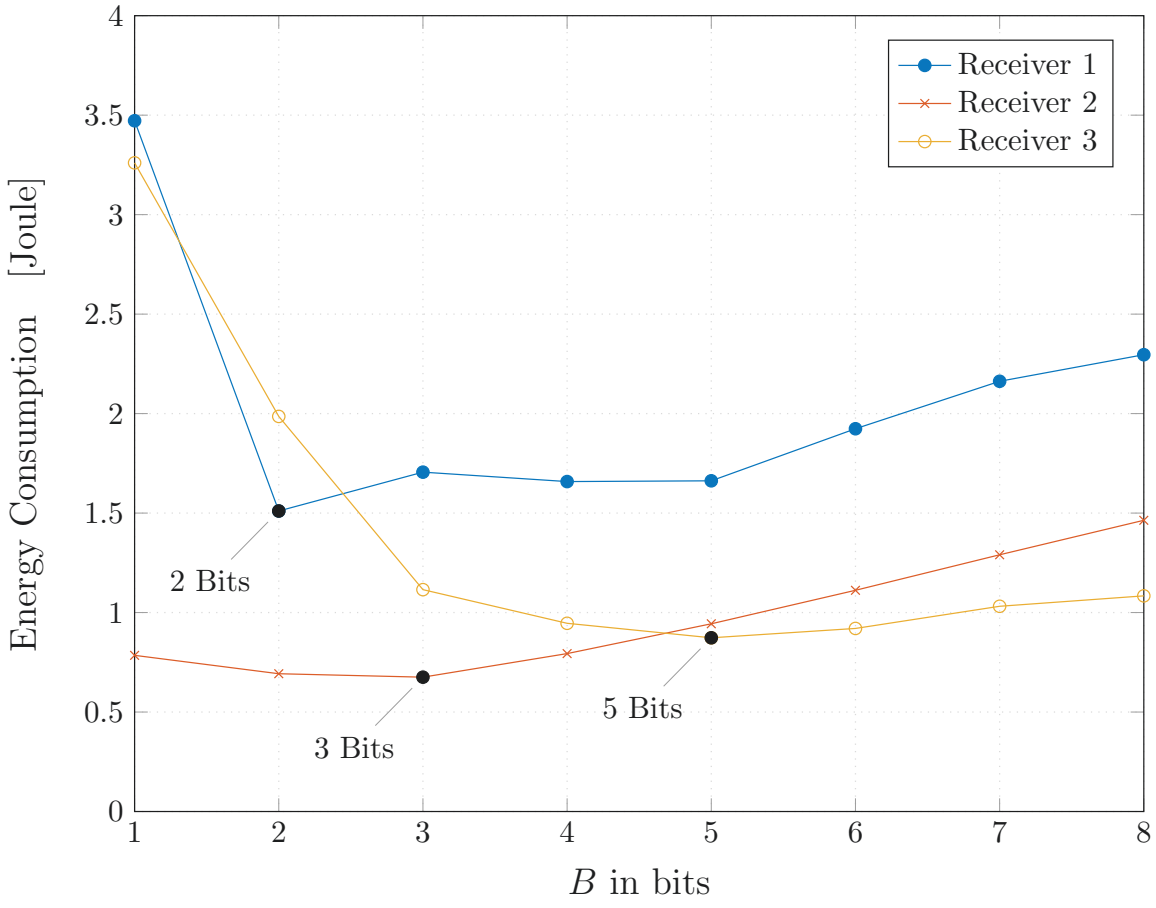

Figure 5.6: Energy consumption of feedback and multi-cast beamforming transmission of 4 transmitters calculated at 3 different receivers for different number of quantization bits B. Each receiver chooses B^* that minimizes energy consumption.

Algorithm 4 Greedy transmitter selection coalition formation algorithm based on minimizing energy consumption and maximizing energy efficiency

1: **loop**
2: **Calculate:** $\max_i \max_j |d_{ij}|$ Find the transmitter that is contributing the most to P_{coop}.
3: **Remove transmitter** i **from the coalition**.
4: **Calculate new energy efficiency**.
5: **if** Energy efficiency increases **then**
6: **Continue** Repeat from the beginning without transmitter j.
7: **else**
8: **Break** Transmitter j remains in the coalition.
9: **end if**
10: **end loop**

5.5 Results and Discussion

We evaluate the performance of the proposed approach in 2 different cases. First, we consider an intermediate stage in a Glossy flood with K transmitters and L receivers. This case is considered for Figure 5.7. Second, we consider a complete Glossy flood in a network of λ nodes, where a random node initiates the flood. Then, we apply standard Glossy and the robust multi-cast beamforming approach with and without coalition formation and evaluate the performance of each approach at the end of the flood, as in the case of Figure 5.8 and Figure 5.9.

We generate network topologies using a binomial point process with $\lambda = k + L$ nodes randomly and independently deployed in a square area. We then evaluate energy efficiency using robust multi-cast beamforming for different values of network side length in meters. Our results are averaged over 100 independent realizations of the network for the same λ. Irrespective of the topology, all transmitting nodes have a source rate $R = 250\,\text{kbps}$ which corresponds to the default setting as prescribed by the IEEE 802.15.4 standard. The first step to optimize the system is solving the programming problem in (5.23) for each receiver independently. After that, each receiver chooses the number of feedback bits B that minimizes energy consumption. This is shown together with the algorithm steps in Section 5.4.

5.5.1 Tightness of bounds

The programming problem in (5.23) is designed to minimize transmit power under QoS constraints in the worst case where the quantization error is at its maximum ϵ. However, minimizing transmit power does not always mean an increase in energy efficiency. Other factors affect energy efficiency such as outage probability and feedback overhead P_{coop} which can be seen in (5.32). Modifying the optimization problem depends on the reliability requirements of the application. For example, in critical applications, an upper bound on the outage is needed. Therefore, we use the CDF of $||\delta||^2$ acquired by empirical means where outage probability is upper bounded as such $\Pr_o \leq \Pr(||\delta||^2 > \epsilon^2)$ and we solve for $\epsilon(B, K)$. This bound is not a tight bound because of the random direction of the error δ, which can result in a better or worse quantized channel $\tilde{\boldsymbol{h}}_l$ than the real channel $\mathbf{h}_l$, depending on the direction of the error. Using this approach of accounting for worst case performance, results sometimes in over satisfying the reliability requirements, hence a loss in terms of energy efficiency. However, the system can be solved for different number of feedback bits B and ultimately find the optimum B^* that maximizes energy efficiency,

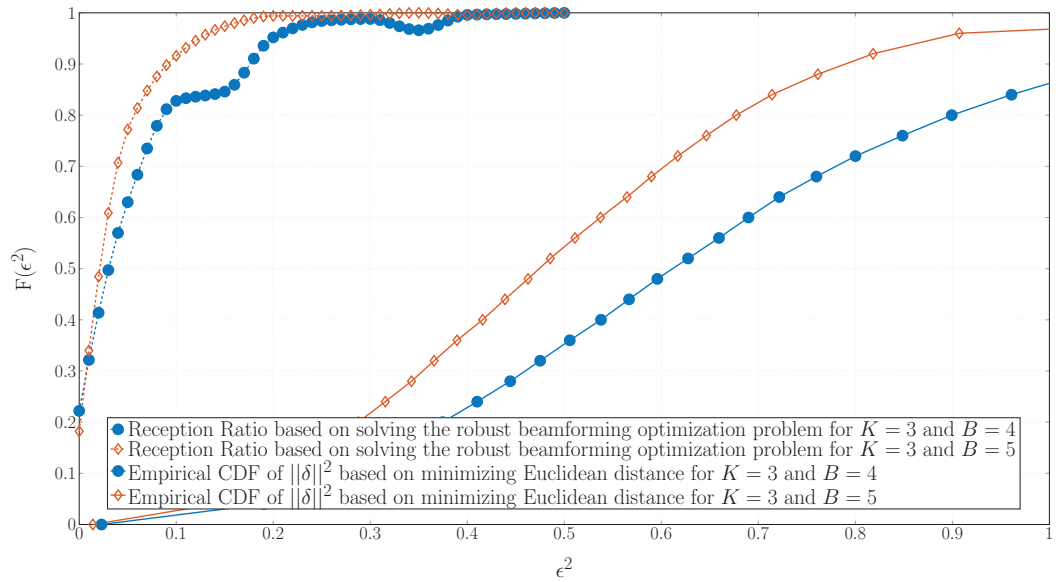

Figure 5.7: Expected reception ratio based on empirical CDF of $||\delta||^2$ and actual reception ratio after solving the robust beamforming optimization problem.

while maintaining a maximum outage probability Pr_o. The tightness of our bound can be seen in Figure 5.7, where the reception ratio resulting from solving our robust optimization problem in (5.23) is calculated for different values of ϵ^2. This is compared in the same plot with the empirical CDF of $||\delta||^2$ for the simulation scenario of $K = 3$ and $B = 4$.

It is critical here to emphasize the relationship between the CDF of ϵ^2 and the reception ratio. Assuming we use an ϵ^2 corresponding to a 90% in the CDF, this means that 90% of the square of the quantization error norm is indeed below this value, in turn, resulting in a successful reception 90% of the time. However, It is easy to notice from Figure 5.7 that achieving 90% reception ratio requires a smaller ϵ^2 than the one retrieved from the CDF information available at the transmitter. This bound can be tightened further by means of iterated optimization, where instead of minimizing $||\delta||^2$ we minimize $\delta^H \boldsymbol{G} \delta$. This results in recursively choosing a quantized channel $\tilde{\boldsymbol{h}}_l$ and a beamformer $\boldsymbol{G}$ that further maximizes energy efficiency under rate constraints, without over satisfying them. We leave this approach for future works, and we focus on optimizing the number of feedback bits B using offline databases stored at each node as explained in Section 5.4.

5.5.2 System level performance

We now test the performance of our proposed algorithm against state-of-the art Glossy. We consider a network consisting of 9 sensor nodes randomly deployed in a square area

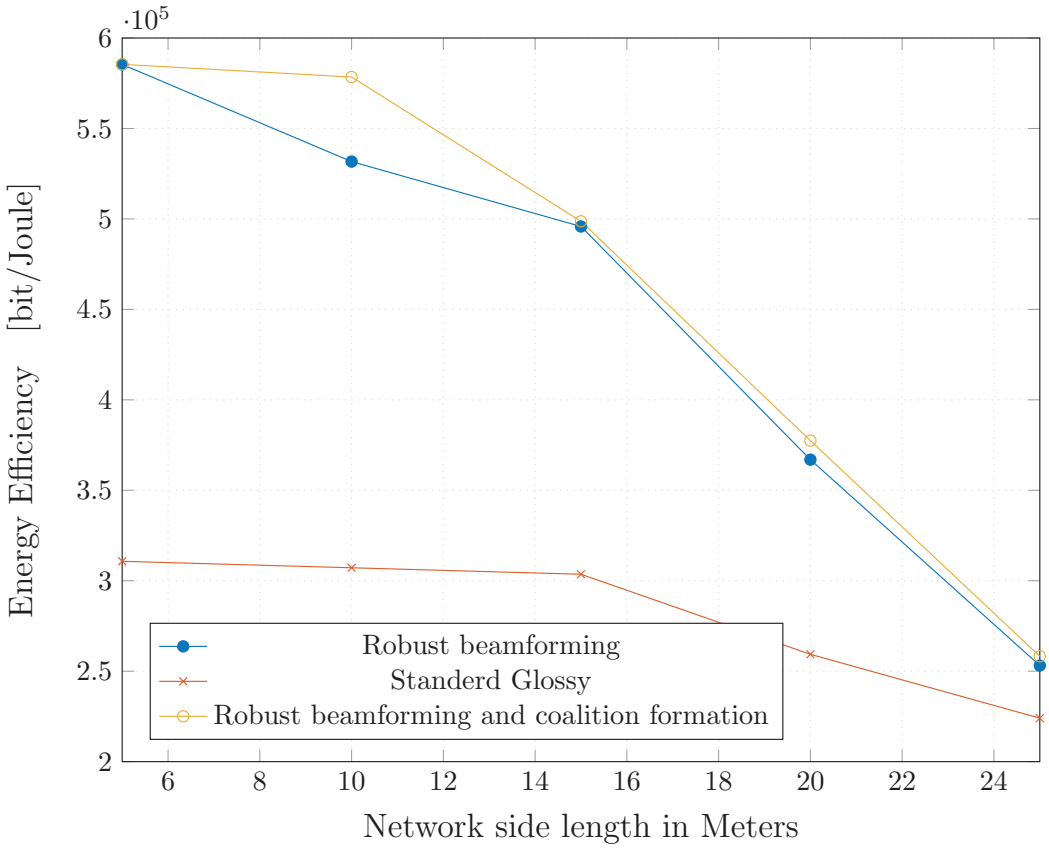

Figure 5.8: Energy efficiency in bit/Joule evaluated at different network side lengths for standard Glossy, robust beamforming and robust beamforming with coalition formation

with varying side length. One randomly chosen node initiates a flood with a required minimum reception ratio of 95% ($Pr_o = 5\%$), then energy consumption and energy efficiency are calculated at the end of the flood for both Glossy and the proposed algorithm. Both metrics are plotted in Figure 5.8 and Figure 5.9 against network side length in meters. Since the number of deployed nodes is fixed, varying the network side length can be seen as varying the network density.

At high network densities, we notice an increase in energy consumption and decrease in energy efficiency of the proposed approach as the network density decreases. This is due to the distances between sensor nodes increasing, resulting in higher feedback overhead and greater transmit powers. On the other hand, for Glossy, energy consumption and energy efficiency at high network densities do not change significantly. This reinforces our original motivation for this work, that the use of no power control in Glossy results in

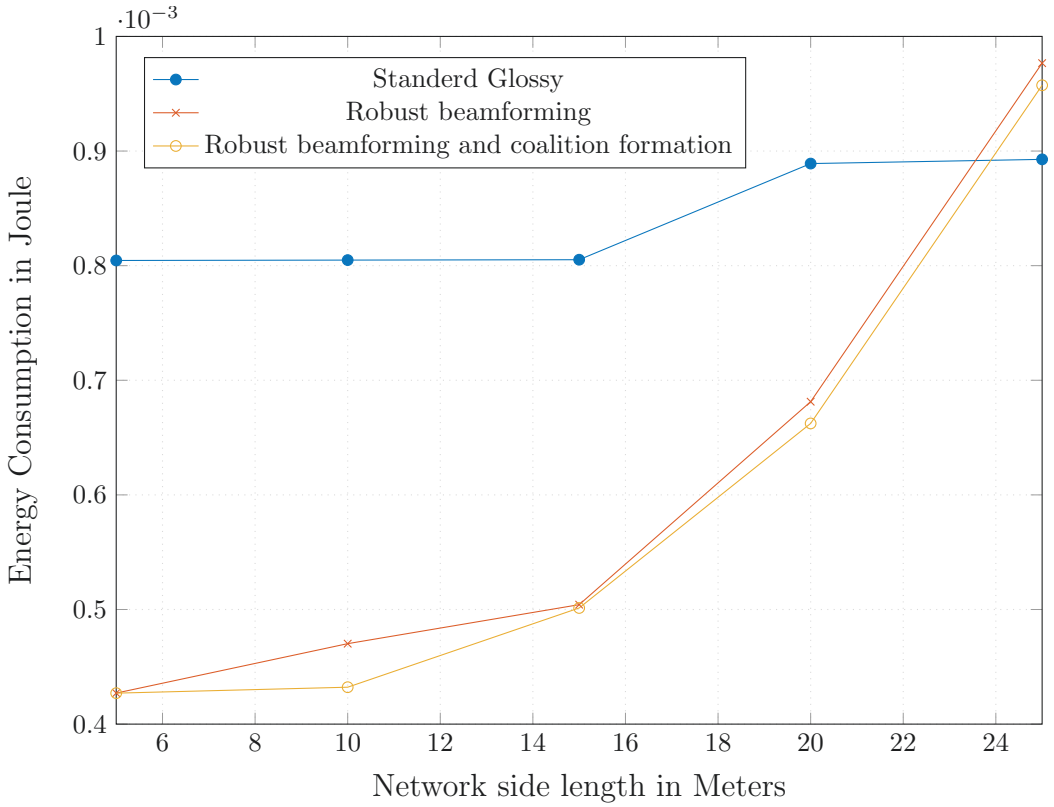

Figure 5.9: Energy consumption in Joule evaluated at different network side lengths for standard Glossy, robust beamforming and robust beamforming with coalition formation

some excess energy consumption for the same performance. Energy efficiency behavior in Figure 5.8 shows that our proposed algorithm greatly outperforms Glossy in dense networks, where nodes are close to each other and the cost of feedback (5.14) is not too high. This is expected since the feedback power needed for cooperation depends on the distance between nodes. Then, at lower network densities, the energy consumption and energy efficiency of the proposed approach significantly increase and decrease, respectively. The reason for this degradation in performance is the increase in feedback energy consumption. In Figure 5.9, we can notice that the total energy consumption of the proposed approach is more than that of Glossy for very low density networks. This is the extreme case where even though feedback is provided by the receivers, nodes need to operate at very high transmit powers in order to achieve successful reception. Hence, feedback overhead is a price payed for no actual profit in performance over Glossy. Resulting in excess energy consumption. This shows that the proposed algorithm is best suited for dense networks

scenarios where cooperation provides an edge in energy efficiency over Glossy.

Results also show that using greedy coalition formation provides a slight increase in energy efficiency and decrease in energy consumption of the proposed approach. This gap is biggest around high to medium network densities, where two or three transmitters can be dropped from the coalition in order to maximize energy efficiency. This performance can still be improved using better coalition formation approaches while keeping in mind the distributed nature of operation and importance of energy efficiency.

5.6 Conclusions

In this Chapter we studied the problem of robust multi-cast beamforming in Glossy under imperfect CSI due to limited feedback. It was shown that coherent multi-cast beamforming, can lead to significant gains in terms of energy efficiency. By studying the effect of number of feedback bits B on the performance, we show that there exists an optimal B that maximizes energy efficiency. Moreover, the problem was solved for a specific maximum allowed outage probability, which is set as an application-dependent QoS requirement. The results showed that stricter outage requirements result in higher values of optimal B^*. The upper bound used on the outage probability can be tightened using iterative beamforming, resulting in lower transmit power while still satisfying the rate constraints. However, we leave this for future investigations. Finally, a study was performed to examine the effect of selecting certain transmitting nodes for cooperation on energy efficiency. The simulation results showed that energy efficiency can be further improved by reducing the number of cooperating transmitters by means of greedy transmitter selection. The proposed robust multi-cast beamforming approach was shown to perform best in dense networks where it showed a significant performance edge over Glossy.

Chapter 6

Conclusion

Based on state of the art, low-power, network flooding protocol Glossy, this dissertation introduces two energy efficient, cooperative transmission schemes for low-power wireless communication in WSNs. With the aim of improving energy efficiency, latency and decreasing energy consumption, we used innovative cooperative transmission technologies such as physical layer network coding and multi-cast beamforming, as well as tools such as convex optimization and game theory in the analytical construction of the proposed approaches. Moreover, we depended on system level simulations to evaluate the proposed approaches and compare performance to standard Glossy based on different criteria.

We began by introducing MF-Glossy, a communication scheme that enables the simultaneous flooding of different packets from multiple sources to all nodes in the network. We analyzed the performance of MF-Glossy and Glossy from a communication theoretic point of view and provided, thus far unknown, upper bounds on their performance. Our simulation results showed that MF-Glossy can potentially achieve several-fold improvements in goodput and latency over Glossy across a wide spectrum of network configurations at lower energy costs and comparable packet reception rates. We also discussed the hardware implementation challenges that face the deployment of MF-Glossy in real WSNs.

Then, under the assumption of CSI availability at all nodes, we introduced a power control and beamforming scheme for Glossy. We described a centralized, as well as a distributed algorithm and evaluated their performance compared to Glossy. Numerical simulations demonstrated that a centralized power control scheme can achieve several-fold improvements in energy efficiency over Glossy across a wide spectrum of network configurations at comparable packet reception rates. After that, we introduce a robust beamforming algorithm to battle the unavailability of CSI at transmitting nodes and the limited nature of feedback channels from receive to transmit nodes. We showed that a two-level cooperation scheme is required such that; receiving nodes cooperate with transmitting

nodes providing them with quantized CSI, and transmitters cooperate through multi-cast beamforming. Our results showed that an optimal number of feedback bits B that maximizes energy efficiency exists, and how to calculate it by solving a programming problem that we formulated. Finally, we showed that choosing the optimal coalition of transmit nodes can improve performance, and we introduced a greedy transmitter selection algorithm to this end. System level simulations showed that coalition formation and robust multi-cast beamforming can achieve a 100% increase in energy efficiency over Glossy in very dense networks.

6.1 Open Research Questions

In this section, we discuss some open research questions regarding this dissertation. Hence, orienting new directions for future work.

6.1.1 MF-Glossy Hardware Implementation

In Section 3.7, we discussed the challenges facing the deployment of MF-Glossy in real WSNs. Based on recent implementations of the compute and forward framework, we see that it is difficult to harness the full advantage that MF-Glossy offers over Glossy due to two major challenges. First, lattice encoding/decoding time must be minimized in order to achieve the latency reduction promised by MF-Glossy. This can be done through specific optimization of the encoding/decoding operations. Second, synchronization of multiple concurrent transmitters must be guaranteed in MF-Glossy. Glossy guarantees microsecond synchronization of all nodes in the network. However, it achieves this by keeping the processing delays at every node as deterministic and fixed as possible. This must be the case in MF-Glossy, to assure correct alignment of concurrently transmitted packets.

6.1.2 Limited Feedback Optimization

In Section 5.5.1, we discussed the issue of over satisfying the QoS constraints in (5.32). Due to the random direction of the quantization error, the channel state can sometimes be better than the quantized channel state. This results in reducing energy efficiency. A possible solution for this issue is iterated optimization, where, instead of minimizing the norm of the quantization error, we minimize the quantization error in the direction of the beamfoming vector. However, this requires more analytical formulation as well as extra computational resources in such resource-limited sensor nodes.

6.2 Closing Remarks

The contributions of this dissertation provide a stepping stone towards highly intelligent transmission in low-power wireless communication. They also prove that, the use of co-operative transmission technologies promises huge performance gains when properly implemented in WSNs.

Appendix

A

S-Procedure

The S-Procedure gives conditions under which, a particular quadratic inequality is a consequence of another quadratic inequality [123]. Let $\boldsymbol{A_1}$ and $\boldsymbol{A_2}$ be symmetric matrices, $\mathbf{b_1}$ and $\mathbf{b_2}$ be vectors, and c_1 and c_2 are constants. Assuming there exists some $\mathbf{x}$ such that;

$$\mathbf{x}^H \boldsymbol{A_1} \mathbf{x} + 2\mathbf{b_1}\mathbf{x} + c_1 \geq 0\,. \tag{A.1}$$

Then, the following holds

$$\mathbf{x}^H \boldsymbol{A_2} \mathbf{x} + 2\mathbf{b_2}\mathbf{x} + c_2 \geq 0 \tag{A.2}$$

if and only if, there exists a $\mu \geq 0$, such that;

$$\begin{bmatrix} \boldsymbol{A_2} & \mathbf{b_2} \\ \mathbf{b_2}^H & c_2 \end{bmatrix} - \mu \begin{bmatrix} \boldsymbol{A_1} & \mathbf{b_1} \\ \mathbf{b_1}^H & c_1 \end{bmatrix} \succeq 0\,. \tag{A.3}$$

Appendix

B

Schur Complement

The Schur complement is defined as follows. Assume having

$$\boldsymbol{M} = \begin{bmatrix} \boldsymbol{A} & \boldsymbol{B} \\ \boldsymbol{C} & \boldsymbol{D} \end{bmatrix} \succeq 0\,, \tag{B.1}$$

where $\boldsymbol{A}, \boldsymbol{B}, \boldsymbol{C}$, and $\boldsymbol{D}$ are matrices, and $\boldsymbol{D}$ is invertible. Then, the Schur complement of $\boldsymbol{D}$ in $\boldsymbol{M}$ is

$$\boldsymbol{A} - \boldsymbol{B}\boldsymbol{D}^{-1}\boldsymbol{C} \succeq 0\,. \tag{B.2}$$

However, If $\boldsymbol{A}$ is invertible, then the Schur complement of $\boldsymbol{A}$ in $\boldsymbol{M}$ is

$$\boldsymbol{D} - \boldsymbol{C}\boldsymbol{A}^{-1}\boldsymbol{B} \succeq 0\,. \tag{B.3}$$

Bibliography

[1] M. Khan, B. N. Silva, and K. Han. "Internet of Things Based Energy Aware Smart Home Control System". In: *IEEE Access* 4 (Jan. 2016), pp. 7556–7566.

[2] H. F. Rashvand, A. Abedi, J. M. Alcaraz-Calero, P. D. Mitchell, and S. C. Mukhopadhyay. "Wireless Sensor Systems for Space and Extreme Environments: A Review". In: *IEEE Sensors Journal* 14.11 (Nov. 2014), pp. 3955–3970.

[3] M. Marzencki, P. Lin, T. Cho, J. Guo, B. Ngai, and B. Kaminska. "Remote health, activity, and asset monitoring with wireless sensor networks". In: *2011 IEEE 13th International Conference on e-Health Networking, Applications and Services*. June 2011, pp. 98–101.

[4] J. Chen, X. Cao, P. Cheng, Y. Xiao, and Y. Sun. "Distributed Collaborative Control for Industrial Automation With Wireless Sensor and Actuator Networks". In: *IEEE Transactions on Industrial Electronics* 57.12 (Dec. 2010), pp. 4219–4230.

[5] *IEEE Standard for Information technology– Local and metropolitan area networks– Specific requirements– Part 15.4: Wireless (MAC) and (PHY) Specifications for Low Rate (WPANs)*.

[6] F. Ferrari, M. Zimmerling, L. Thiele, and O. Saukh. "Efficient Network Flooding and Time Synchronization with Glossy". In: *Proc. of the ACM/IEEE IPSN*. 2011.

[7] F. Ferrari, M. Zimmerling, L. Mottola, and L. Thiele. "Low-Power Wireless Bus". In: *Proc. of the 10th ACM SenSys*. 2012.

[8] M. Wilhelm, V. Lenders, and J. B. Schmitt. "On the Reception of Concurrent Transmissions in Wireless Sensor Networks". In: *IEEE Transactions on Wireless Communications* 13.12 (Dec. 2014), pp. 6756–6767.

[9] M. Zimmerling, F. Ferrari, L. Mottola, and L. Thiele. "On Modeling Low-Power Wireless Protocols Based on Synchronous Packet Transmissions". In: *2013 IEEE 21st International Symposium on Modelling, Analysis and Simulation of Computer and Telecommunication Systems*. Aug. 2013, pp. 546–555.

[10] H. Rahul, H. Hassanieh, and D. Katabi. “SourceSync: A Distributed Wireless Architecture for Exploiting Sender Diversity”. In: *SIGCOMM Comput. Commun. Rev.* 40.4 (Aug. 2010).

[11] Moteiv. *Tmote Sky Datasheet*. 2006. URL: `https://www.advanticsys.com/`.

[12] J. Åkerberg, M. Gidlund, and M. Björkman. “Future Research Challenges in Wireless Sensor and Actuator Networks Targeting Industrial Automation”. In: *Proc. of the IEEE INDIN*. 2011.

[13] J. Lu and K. Whitehouse. “Flash flooding: Exploiting the capture effect for rapid flooding in wireless sensor networks”. In: *INFOCOM 2009, IEEE*. IEEE. 2009, pp. 2491–2499.

[14] D. Gislason. *Zigbee Wireless Networking*. Pap/Onl. Newton, MA, USA: Newnes, 2008. URL: `https://zigbee.org`.

[15] A. N. Kim, F. Hekland, S. Petersen, and P. Doyle. “When HART goes wireless: Understanding and implementing the WirelessHART standard”. In: *2008 IEEE International Conference on Emerging Technologies and Factory Automation*. Sept. 2008, pp. 899–907.

[16] J. Beutel, B. Buchli, F. Ferrari, M. Keller, and M. Zimmerling. “X-SENSE: Sensing in Extreme Environments”. In: *Proc. of DATE*. 2011.

[17] M. Ceriotti et al. “Is There Light at the Ends of the Tunnel? Wireless Sensor Networks for Adaptive Lighting in Road Tunnels”. In: *ACM/IEEE IPSN*. 2011.

[18] M. Maróti, B. Kusy, G. Simon, and Á. Lédeczi. “The flooding time synchronization protocol”. English. In: *SenSys’04 - Proceedings of the Second International Conference on Embedded Networked Sensor Systems*. 2004, pp. 39–49.

[19] K. S. Yıldırım, R. Carli, and L. Schenato. “Adaptive Proportional–Integral Clock Synchronization in Wireless Sensor Networks”. In: *IEEE Transactions on Control Systems Technology* 26.2 (Mar. 2018), pp. 610–623.

[20] K. Whitehouse et al. “Marionette: using RPC for interactive development and debugging of wireless embedded networks”. In: *2006 5th International Conference on Information Processing in Sensor Networks*. Apr. 2006, pp. 416–423.

[21] M. Brachmann, O. Landsiedel, and S. Santini. “Concurrent Transmissions for Communication Protocols in the Internet of Things”. In: *2016 IEEE 41st Conference on Local Computer Networks (LCN)*. Nov. 2016, pp. 406–414.

[22] Y.-C. Tseng, S.-Y. Ni, Y.-S. Chen, and J.-P. Sheu. "The Broadcast Storm Problem in a Mobile Ad Hoc Network". In: *Wireless Networks* 8.2 (Mar. 2002), pp. 153–167. URL: https://doi.org/10.1023/A:1013763825347.

[23] S. Ahn, Y. Lim, and H. Yu. "Energy-Efficient Flooding Mechanisms for the Wireless Sensor Networks". In: *2008 International Conference on Information Networking*. Jan. 2008, pp. 1–5.

[24] P. Levis, N. Patel, D. Culler, and S. Shenker. "Trickle: A Self-Regulating Algorithm for Code Propagation and Maintenance in Wireless Sensor Networks". In: *In Proceedings of the First USENIX/ACM Symposium on Networked Systems Design and Implementation (NSDI*. 2004, pp. 15–28.

[25] O. Landsiedel, F. Ferrari, and M. Zimmerling. "Chaos: Versatile and Efficient All-to-all Data Sharing and In-network Processing at Scale". In: *Proceedings of the 11th ACM SenSys*. NY, USA, 2013, 1:1–1:14.

[26] W. Du, J. C. Liando, H. Zhang, and M. Li. "When Pipelines Meet Fountain: Fast Data Dissemination in Wireless Sensor Networks". In: *Proc. of ACM SenSys*. 2015.

[27] M. Zimmerling, L. Mottola, P. Kumar, F. Ferrari, and L. Thiele. "Adaptive Real-time Communication for Wireless Cyber-physical Systems". In: *ACM Transactions on Cyber-Physical Systems* 1.2 (2017).

[28] J. N. Laneman, D. N. C. Tse, and G. W. Wornell. "Cooperative diversity in wireless networks: Efficient protocols and outage behavior". In: *IEEE Trans. on Information Theory* 50.12 (2004).

[29] D. Son, B. Krishnamachari, and J. Heidemann. "Experimental Study of Concurrent Transmission in Wireless Sensor Networks". In: *Proceedings of the 4th International Conference on Embedded Networked Sensor Systems*. SenSys '06. Boulder, Colorado, USA: ACM, 2006, pp. 237–250. URL: http://doi.acm.org/10.1145/1182807.1182831.

[30] D. Son, B. Krishnamachari, and J. Heidemann. *Evaluating the Importance of Concurrent Packet Communication in Wireless Networks*. 2007.

[31] P. Dutta, R. Musăloiu-E., I. Stoica, and A. Terzis. "Wireless ACK Collisions Not Considered Harmful". In: *ACM HotNets*. 2008.

[32] P. Dutta, S. Dawson-Haggerty, Y. Chen, C.-J. M. Liang, and A. Terzis. "Design and Evaluation of a Versatile and Efficient Receiver-initiated Link Layer for Low-power Wireless". In: *Proceedings of the 8th ACM Conference on Embedded Networked Sensor Systems*. SenSys '10. Zürich, Switzerland: ACM, 2010, pp. 1–14. URL: http://doi.acm.org/10.1145/1869983.1869985.

[33] D. Carlson and A. Terzis. "Flip-MAC: A density-adaptive contention-reduction protocol for efficient any-to-one communication". In: *2011 International Conference on Distributed Computing in Sensor Systems and Workshops (DCOSS)*. June 2011, pp. 1–8.

[34] K. Leentvaar and J. Flint. "The Capture Effect in FM Receivers". In: *IEEE Trans. Commun.* 24.5 (1976).

[35] D. Yuan and M. Hollick. "Let's talk together: Understanding concurrent transmission in wireless sensor networks". In: *38th Annual IEEE Conference on Local Computer Networks*. Oct. 2013, pp. 219–227.

[36] V. S. Rao, M. Koppal, R. V. Prasad, T. V. Prabhakar, C. Sarkar, and I. Niemegeers. "Murphy loves CI: Unfolding and improving constructive interference in WSNs". In: *IEEE INFOCOM 2016 - The 35th Annual IEEE International Conference on Computer Communications*. Apr. 2016, pp. 1–9.

[37] H. A. H. Alhalabi, T. Wan, L. Missif, and M. Ehalabi. "Performance analysis of the constructive interference flooding in wireless sensor networks". In: *2017 8th International Conference on Information Technology (ICIT)*. May 2017, pp. 75–81.

[38] C.-H. LIAO, M. SUZUKI, and H. MORIKAWA. "Receiver Performance Evaluation and Fading Duration Analysis for Concurrent Transmission". In: *IEICE Transactions on Communications* advpub (2017).

[39] M. Suzuki, Y. Yamashita, and H. Morikawa. "Low-Power, End-to-End Reliable Collection Using Glossy for Wireless Sensor Networks". In: *2013 IEEE 77th Vehicular Technology Conference (VTC Spring)*. June 2013, pp. 1–5.

[40] C. Sarkar, R. V. Prasad, and K. Langendoen. "FLEET: When Time-Bounded Communication Meets High Energy-Efficiency". In: *IEEE Access* 7 (Jan. 2019), pp. 77555–77568.

[41] T. Istomin, A. L. Murphy, G. P. Picco, and U. Raza. "Data Prediction + Synchronous Transmissions = Ultra-low Power Wireless Sensor Networks". In: *Proceedings of the 14th ACM Conference on Embedded Network Sensor Systems CD-ROM*. SenSys '16. Stanford, CA, USA: ACM, 2016, pp. 83–95. URL: http://doi.acm.org/10.1145/2994551.2994558.

[42] M. Brachmann, O. Landsiedel, D. Göhringer, and S. Santini. *Whisper: Fast Flooding for Low-Power Wireless Networks*. 2018. arXiv: 1809.03699 [cs.NI].

[43] D. Yuan, M. Riecker, and M. Hollick. "Making 'Glossy' Networks Sparkle: Exploiting Concurrent Transmissions for Energy Efficient, Reliable, Ultra-Low Latency Communication in Wireless Control Networks". In: *Proceedings of the 11th European Conference on Wireless Sensor Networks - Volume 8354*. EWSN 2014. Oxford, UK: Springer-Verlag New York, Inc., 2014, pp. 133–149. URL: http://dx.doi.org/10.1007/978-3-319-04651-8_9.

[44] B. Al Nahas and O. Landsiedel. "Competition: Towards Low-Power Wireless Networking That Survives Interference with Minimal Latency". In: *Proceedings of the 2017 International Conference on Embedded Wireless Systems and Networks*. EWSN ’17. Uppsala, Sweden: Junction Publishing, 2017, pp. 268–269. URL: http://dl.acm.org/citation.cfm?id=3108009.3108075.

[45] M. Luvisotto, Z. Pang, and D. Dzung. "Ultra High Performance Wireless Control for Critical Applications: Challenges and Directions". In: *IEEE Trans. on Industrial Informatics* PP.99 (2016).

[46] S. Hayat, E. Yanmaz, and R. Muzaffar. "Survey on Unmanned Aerial Vehicle Networks for Civil Applications: A Communications Viewpoint". In: *IEEE Communications Surveys Tutorials* 18.4 (2016).

[47] B. Sinopoli, L. Schenato, M. Franceschetti, K. Poolla, M. I. Jordan, and S. S. Sastry. "Kalman filtering with intermittent observations". In: *IEEE Trans. on Automatic Control* 49.9 (2004), pp. 1453–1464.

[48] BBC News. *US military tests swarm of mini-drones launched from jets*. URL: http://www.bbc.com/news/technology-38569027.

[49] RCR Wireless News. *5 connectivity challenges for drones*. URL: http://www.rcrwireless.com/20160802/europe/five-challenges-drones-tag28.

[50] B. Nazer and M. Gastpar. “Compute-and-Forward: Harnessing Interference Through Structured Codes”. In: *IEEE Trans. on Information Theory* 57.10 (Oct. 2011), pp. 6463–6486.

[51] J. Richter. “Compute-and-Forward in Multi-User Relay Networks: Optimization, Implementation, and Secrecy”. PhD Thesis to be published. 2017.

[52] R. Ahlswede, N. Cai, S.-Y. R. Li, and R. W. Yeung. “Network information flow”. In: *IEEE Trans. on Information Theory* 46.4 (July 2000), pp. 1204–1216.

[53] M. Médard, F. H. P. Fitzek, M.-J. Montpetit, and C. Rosenberg. “Network coding mythbusting: Why it is not about butterflies anymore”. In: *IEEE Communications Magazine* 52.7 (July 2014), pp. 177–183.

[54] S. Zhang, S. C. Liew, and P. P. Lam. “Hot topic: Physical-Layer Network Coding”. In: *Proc. of the 12th annual international conference on Mobile computing and networking*. Vol. 1. Node 1. 2006, pp. 358–365.

[55] S. Katti, S. Gollakota, and D. Katabi. “Embracing Wireless Interference: Analog Network Coding”. In: *SIGCOMM*. Oct. 2007, pp. 397–408.

[56] I. Marić, A. Goldsmith, and M. Médard. “Analog Network Coding in the High-SNR Regime”. In: *IEEE WiNC*. June 2010, pp. 1–6.

[57] H.-M. Wang, X.-G. Xia, and Q. Yin. “A Linear Analog Network Coding for Asynchronous Two-Way Relay Networks”. In: *IEEE Trans. on Wireless Communications* 9.12 (Dec. 2010), pp. 3630–3637.

[58] D. Maduike, H. D. Pfister, and A. Sprintson. “Design and implementation of physical-layer network-coding protocols”. In: *Forty-Third Asilomar Conference on Signals, Systems and Computers (ASILOMAR)*. Nov. 2009, pp. 781–787.

[59] R. H. Y. Louie, Y. Li, and B. Vucetic. “Practical physical layer network coding for two-way relay channels: Performance analysis and comparison”. In: *IEEE Trans. on Wireless Communications* 9.2 (2010), pp. 764–777.

[60] L. Lu, T. Wang, S. C. Liew, and S. Zhang. “Implementation of physical-layer network coding”. In: *ICC*. June 2012, pp. 4734–4740.

[61] L. Lu et al. “Real-time Implementation of Physical-layer Network Coding”. In: *Second Workshop on Software Radio Implementation Forum (SRIF)*. 2013, pp. 71–76.

[62] U. Erez and R. Zamir. "Achieving 1/2 log (1+ SNR) on the AWGN channel with lattice encoding and decoding". In: *IEEE Trans. on Information Theory* 50.10 (2004), pp. 2293–2314.

[63] A. Mejri and G. R.-B. Othman. "Practical Physical Layer Network Coding in Multi-Sources Relay Channels via the Compute-and-Forward". In: *WCNCW*. 2013, pp. 166–171.

[64] Y. Wang and A. Burr. "Physical-layer network coding via low density lattice codes". In: *2014 European Conference on Networks and Communications (EuCNC)*. June 2014, pp. 1–5.

[65] Y. Wang, A. Burr, and D. Fang. "Complex Low Density Lattice Codes to Physical Layer Network Coding". In: *2015 IEEE International Conference on Communications (ICC)*. June 2015, pp. 2060–2065.

[66] N. Sommer, M. Feder, and O. Shalvi. "Low Density Lattice Codes". In: *2006 IEEE International Symposium on Information Theory*. July 2006, pp. 88–92.

[67] J. A. Sheppard and A. G. Burr. "The design and implementation of lattice codes using digital signal processing techniques". In: *Sixth Int. Conf. on Digital Processing of Signals in Communications*. 1991.

[68] N. Wang and J. D. Gibson. "Leech lattice coding and modulation for IEEE 802.11a WLAN". In: *IEEE Emerging Technologies Symposium on BroadBand Communications for the Internet Era*. 2001.

[69] L.-J. Hu, C. Duan, D.-F. Zhao, and X. Liao. "Study Status and Prospect of Lattice Codes in Wireless Communication". In: *Fifth IMCCC*. Sept. 2015.

[70] R. Zamir. *Lattice Coding for Signals and Networks*. Cambridge University Press, 2014.

[71] M. P. Wilson, K. Narayanan, H. D. Pfister, and A. Sprintson. "Joint Physical Layer Coding and Network Coding for Bidirectional Relaying". In: *IEEE Transactions on Information Theory* 56.11 (Nov. 2010), pp. 5641–5654.

[72] A. Gamal and Y. Kim. *Network Information Theory*. Cambridge University Press, 2011.

[73] D. Tse and P. Viswanath. *Fundamentals of Wireless Communication*. New York, NY, USA: Cambridge University Press, 2005.

[74] P. Marsch and G. P. Fettweis. *Coordinated Multi-Point in Mobile Communications: From Theory to Practice*. 1st. New York, NY, USA: Cambridge University Press, 2011.

[75] M. Ceriotti et al. "Monitoring Heritage Buildings with Wireless Sensor Networks: The Torre Aquila Deployment". In: *ACM/IEEE IPSN*. 2009.

[76] The GNU Radio Foundation, Inc. *GNU Radio Website*. 2016. URL: http://www.gnuradio.org (visited on 12/13/2016).

[77] The Sage Developers. *SageMath, the Sage Mathematics Software System (Version 7.4)*. 2016. URL: http://www.sagemath.org (visited on 12/13/2016).

[78] Steinwurf. *fifi – Optimized Finite Fields*. 2017. URL: http://steinwurf.com/_products/fifi.html (visited on 02/27/2017).

[79] Y. Tan, S. C. Liew, and T. Huang. "Mobile Lattice-Coded Physical-Layer Network Coding with Practical Channel Alignment". In: *IEEE Transactions on Mobile Computing* 17.8 (Aug. 2018), pp. 1908–1923.

[80] J. Richter, C. Scheunert, and E. A. Jorswieck. "An efficient branch-and-bound algorithm for compute-and-forward". In: *IEEE PIMRC*. 2012.

[81] A. Sakzad, J. Harshan, and E. Viterbo. "Integer-Forcing MIMO Linear Receivers Based on Lattice Reduction". In: *IEEE Trans. on Wireless Communications* 12.10 (Oct. 2013), pp. 4905–4915. URL: http://dx.doi.org/10.1109/TWC.2013.090513.121465.

[82] S. Stanczak, M. Wiczanowski, and H. Boche. *Fundamentals of Resource Allocation in Wireless Networks: Theory and Algorithms*. 2nd. New York City, US: Springer Publishing Company, Incorporated, 2009.

[83] M. Dohler, E. Lefranc, and H. Aghvami. "Virtual antenna arrays for future wireless mobile communication systems". In: 2002.

[84] J. Zander. "Performance of optimum transmitter power control in cellular radio systems". In: *IEEE Transactions on Vehicular Technology* 41.1 (Feb. 1992), pp. 57–62.

[85] S. Schwarz and M. Rupp. "Transmit Optimization for the MISO Multicast Interference Channel". In: *IEEE Transactions on Communications* 63.12 (Dec. 2015), pp. 4936–4949.

[86] N. D. Sidiropoulos, T. N. Davidson, and Z.-Q. Luo. "Transmit beamforming for physical-layer multicasting". In: *IEEE Transactions on Signal Processing* 54.6 (June 2006), pp. 2239–2251.

[87] Z. q. Luo, W. k. Ma, A. M. c. So, Y. Ye, and S. Zhang. "Semidefinite Relaxation of Quadratic Optimization Problems". In: *IEEE Signal Processing Magazine* 27.3 (May 2010), pp. 20–34.

[88] A. B. Gershman, N. D. Sidiropoulos, S. Shahbazpanahi, M. Bengtsson, and B. Ottersten. "Convex Optimization-Based Beamforming". In: *IEEE Signal Processing Magazine* 27.3 (May 2010), pp. 62–75.

[89] R. Mudumbai, D. R. B. Iii, U. Madhow, and H. V. Poor. "Distributed transmit beamforming: challenges and recent progress". In: *IEEE Communications Magazine* 47.2 (Feb. 2009), pp. 102–110.

[90] R. F. Schaefer and H. Boche. "Physical Layer Service Integration in Wireless Networks : Signal processing challenges". In: *IEEE Signal Processing Magazine* 31.3 (May 2014), pp. 147–156.

[91] M. Bengtsson and B. E. Ottersten. "Optimal Downlink Beamforming Using Semidefinite Optimization". In: 1999.

[92] D. G. Luenberger. *Optimization by Vector Space Methods*. 1st. New York, NY, USA: John Wiley & Sons, Inc., 1997.

[93] K. Anstreicher and H. Wolkowicz. "On Lagrangian Relaxation of Quadratic Matrix Constraints". In: *SIAM J. Matrix Anal. Appl.* 22.1 (Apr. 2000), pp. 41–55. URL: https://doi.org/10.1137/S0895479898340299.

[94] E. Jorswieck and H. Boche. "Optimal Transmission with Imperfect Channel State Information at the Transmit Antenna Array". In: *Wireless Personal Communications* 27.1 (Oct. 2003), pp. 33–56. URL: https://doi.org/10.1023/A:1026048118953.

[95] M. Grant and S. Boyd. *CVX: Matlab Software for Disciplined Convex Programming, version 2.1*. Mar. 2014. URL: http://cvxr.com/cvx.

[96] M. Grant and S. Boyd. "Graph implementations for nonsmooth convex programs". In: *Recent Advances in Learning and Control*. Ed. by V. Blondel, S. Boyd, and H. Kimura. Lecture Notes in Control and Information Sciences. New York City, US: Springer-Verlag Limited, 2008, pp. 95–110. URL: http://stanford.edu/~boyd/graph_dcp.html.

[97] P. de Kerret, S. Lasaulce, D. Gesbert, and U. Salim. "Best-response team power control for the interference channel with local CSI". In: *ICC 2015, IEEE*. June 2015. URL: http://dx.doi.org/10.1109/ICC.2015.7248971.

[98] E. Koyuncu, C. Remling, X. Liu, and H. Jafarkhani. "Outage-Optimized Multicast Beamforming With Distributed Limited Feedback". In: *IEEE Transactions on Wireless Communications* 16.4 (Apr. 2017), pp. 2069–2082.

[99] H. Yetgin, K. T. K. Cheung, M. El-Hajjar, and L. H. Hanzo. "A Survey of Network Lifetime Maximization Techniques in Wireless Sensor Networks". In: *IEEE Communications Surveys Tutorials* 19.2 (May 2017), pp. 828–854.

[100] A. B. Noel, A. Abdaoui, T. Elfouly, M. H. Ahmed, A. Badawy, and M. S. Shehata. "Structural Health Monitoring Using Wireless Sensor Networks: A Comprehensive Survey". In: *IEEE Communications Surveys Tutorials* 19.3 (Aug. 2017), pp. 1403–1423.

[101] S. Buzzi, C. L. I, T. E. Klein, H. V. Poor, C. Yang, and A. Zappone. "A Survey of Energy-Efficient Techniques for 5G Networks and Challenges Ahead". In: *IEEE Journal on Selected Areas in Communications* 34.4 (Apr. 2016), pp. 697–709.

[102] M. Simsek, A. Aijaz, M. Dohler, J. Sachs, and G. Fettweis. "5G-Enabled Tactile Internet". In: *IEEE Journal on Selected Areas in Communications* 34.3 (Mar. 2016), pp. 460–473. URL: http://dx.doi.org/10.1109/JSAC.2016.2525398.

[103] A. Nosratinia, T. Hunter, and A. Hedayat. "Cooperative communication in wireless networks". In: *Communications Magazine, IEEE* 42 (Nov. 2004), pp. 74–80.

[104] J. Valenzuela-Valdés, F. Luna, R. M. Luque-Baena, and P. Padilla. "Saving energy in WSNs with beamforming". In: *2014 IEEE 3rd International Conference on Cloud Networking (CloudNet)*. Oct. 2014, pp. 255–260.

[105] H. Ochiai, P. Mitran, H. V. Poor, and V. Tarokh. "Collaborative beamforming for distributed wireless ad hoc sensor networks". In: *IEEE Transactions on Signal Processing* 53.11 (Nov. 2005), pp. 4110–4124.

[106] H. Ochiai, P. Mitran, H. V. Poor, and V. Tarokh. "Collaborative beamforming in ad hoc networks". In: *Information Theory Workshop*. Oct. 2004, pp. 396–401.

[107] G. Barriac, R. Mudumbai, and U. Madhow. "Distributed beamforming for information transfer in sensor networks". In: *Third International Symposium on Information Processing in Sensor Networks, 2004. IPSN 2004.* Apr. 2004, pp. 81–88.

[108] X. Zhang and K. G. Shin. "Cooperation without Synchronization: Practical Cooperative Relaying for Wireless Networks". In: *IEEE Transactions on Mobile Computing* 14.5 (May 2015), pp. 937–950. URL: https://doi.org/10.1109/TMC.2014.2341611.

[109] B. B. Haro, S. Zazo, and D. P. Palomar. "Energy Efficient Collaborative Beamforming in Wireless Sensor Networks". In: *IEEE Transactions on Signal Processing* 62.2 (Jan. 2014), pp. 496–510.

[110] S. Schedler and V. Kuehn. "Resource allocation for distributed beamforming with multiple relays and individual power constraints". In: *2014 11th International Symposium on Wireless Communications Systems (ISWCS).* Aug. 2014, pp. 1–5.

[111] J. Ding, E. Dutkiewicz, X. Huang, and G. Fang. "Energy-Efficient Distributed Beamforming in UWB Based Implant Body Area Networks". In: *2015 IEEE 81st Vehicular Technology Conference (VTC Spring).* May 2015, pp. 1–5.

[112] P. Ubaidulla and A. Chockalingam. "Robust distributed beamforming for wireless relay networks". In: *2009 IEEE 20th International Symposium on Personal, Indoor and Mobile Radio Communications.* Sept. 2009, pp. 2345–2349.

[113] S. A. Vorobyov, A. B. Gershman, and Z.-Q. Luo. "Robust adaptive beamforming using worst-case performance optimization: a solution to the signal mismatch problem". In: *IEEE Transactions on Signal Processing* 51.2 (Feb. 2003), pp. 313–324.

[114] W. Santipach and M. L. Honig. "Asymptotic capacity of beamforming with limited feedback". In: *International Symposium onInformation Theory, 2004. ISIT 2004. Proceedings.* June 2004, pp. 290–.

[115] R. Mochaourab and E. A. Jorswieck. "Robust Beamforming in Interference Channels with Imperfect Transmitter Channel Information". In: *Signal Process.* 92.10 (Oct. 2012), pp. 2509–2518. URL: http://dx.doi.org/10.1016/j.sigpro.2012.03.014.

[116] L. Wang, C. Zhang, J. Zhang, and G. Wei. "Distributed Beamforming with Limited Feedback in Regenerative Cooperative Networks". In: *Proceedings of the 5th International Conference on Wireless Communications, Networking and Mobile Computing*. WiCOM'09. Beijing, China: IEEE Press, 2009, pp. 1301–1304. URL: http://dl.acm.org/citation.cfm?id=1736862.1737177.

[117] D. Tse and P. Viswanath. *Fundamentals of Wireless Communication*. New York, NY, USA: Cambridge University Press, 2005.

[118] K. Y. Wang, T. H. Chang, W. K. Ma, and C. Y. Chi. "Optimal transmission strategy for outage rate maximization in MISO fading channels with training". In: *2012 IEEE International Conference on Acoustics, Speech and Signal Processing (ICASSP)*. Mar. 2012, pp. 2945–2948.

[119] A. Alkhateeb, O. E. Ayach, G. Leus, and R. W. Heath. "Channel Estimation and Hybrid Precoding for Millimeter Wave Cellular Systems". In: *IEEE Journal of Selected Topics in Signal Processing* 8.5 (Oct. 2014), pp. 831–846.

[120] J. Wang and D. P. Palomar. "Worst-Case Robust MIMO Transmission With Imperfect Channel Knowledge". In: *IEEE Transactions on Signal Processing* 57.8 (Aug. 2009), pp. 3086–3100.

[121] D. Goodman and N. Mandayam. "Power control for wireless data". In: *IEEE Personal Communications* 7.2 (Apr. 2000), pp. 48–54.

[122] F. Meshkati, H. V. Poor, S. C. Schwartz, and N. B. Mandayam. "An energy-efficient approach to power control and receiver design in wireless data networks". In: *IEEE Transactions on Communications* 53.11 (Nov. 2005), pp. 1885–1894.

[123] F. Uhlig. "A recurring theorem about pairs of quadratic forms and extensions: a survey". In: *Linear Algebra and its Applications* 25 (1979), pp. 219–237. URL: http://www.sciencedirect.com/science/article/pii/002437957990020X.